DOI 10.1007/s10778-016-0770-6
International Applied Mechanics, Vol. 52, No. 5, September, 2016

DYNAMICS OF ELASTIC BODIES, SOLID PARTICLES, AND FLUID PARCELS IN A COMPRESSIBLE VISCOUS FLUID (REVIEW)

A. N. Guz, A. P. Zhuk, and A. M. Bagno

The results of linearization of the basic equations describing a compressible viscous fluid in which low-amplitude oscillations occur or solids move or that interacts with elastic bodies in which small perturbations propagate are discussed. The general solutions of the linearized equations are presented. The results of studying wave processes in hydroelastic systems using the three-dimensional linearized theory of finite deformations and theory of compressible viscous fluid are discussed. The results of studying the propagation of acoustic waves of various types in waveguides with plane and circular cylindrical interfaces between elastic and liquid media and the influence of large (finite) initial deformations, viscosity and compressibility of the fluid on acoustic waves are presented. Studies of the motion of objects in compressible ideal and viscous fluids under the action of radiation forces due to the acoustic field are reviewed. The emphasis is placed on the studies that use a method involving the solution of hydrodynamic problems for a compressible fluid with solid particles and the evaluation of the forces acting on these particles. The radiation force is determined as the constant component of the hydrodynamic force. The numerical results are presented in the form of plots, which are then analyzed

Keywords: three-dimensional linearized theory, viscous compressible fluid, compressible and incompressible elastic body, prestress, radiation force, acoustic field, particle, harmonic wave

Introduction. The dynamics of a fluid interacting with rigid and deformable bodies is one of the fundamental and classical problems of mechanics, physics, and applied mathematics. The results obtained in studying this problem are of applied importance for various problems of natural sciences and engineering, including newest technologies.

So far, the dynamic behavior of rigid and elastic bodies in a viscous fluid has mainly been studied assuming that the fluid is incompressible and viscous. There are few publications where the fluid is considered to be viscous and compressible (see [31, 76, 78, 91, 95, 171] for reviews of such studies). An analysis of the results shows that, despite the importance of the dynamic problem, the low-amplitude vibrations of and the motion/interaction of rigid and elastic bodies in/with a compressible viscous fluid have been studied inadequately.

The present paper is a review of the results obtained in studying, using the three-dimensional linearized theory, the motion and interaction of solid particles in a fluid and the propagation of low-amplitude waves in elastic bodies interacting with a compressible viscous fluid.

Section 1 deals with the linearized equations for a resting compressible viscous fluid undergoing nonstationary and harmonic low-amplitude motions (oscillations). The exact expression for the total derivative of the velocity vector will be used. The linearized theory for a resting compressible viscous fluid will be shown to be analogous to a specific rheological model of a solid. The general solutions of the basic equations of the linearized theory for a compressible viscous fluid will be expressed in terms of scalar and vector potentials. The equations from which these potentials are derived will be presented as well. It will be

S. P. Timoshenko Institute of Mechanics, National Academy of Sciences of Ukraine, 3 Nesterova St., Kyiv, Ukraine 03057, e-mail: zhuk@inmech.kiev.ua. Translated from Prikladnaya Mekhanika, Vol. 52, No. 5, pp. 3–77, September–October, 2016. Original article submitted June 8, 2015.

shown that by passing to the limit, these general solutions can be reduced to general solutions for simpler fluid models (incompressible viscous fluid; compressible or incompressible ideal fluid).

The development of engineering and industry requires using theories that more adequately describe the properties of real elastic and liquid media. In this connection, it is important to use prestressed body and compressible viscous fluid models to study wave processes. Using such an approach is reasonable because neglecting the prestresses of the body and the viscosity of the fluid changes the structure of the differential equations so much that many real phenomena cannot be studied even qualitatively and the quantitative results obtained with approximate models do not meet the ever toughening accuracy requirements. It is, therefore, of theoretical and applied interest to study wave processes in hydroelastic systems using the equations of the three-dimensional linearized theory of elasticity with the assumption of finite deformation for the body and the three-dimensional linearized Navier–Stokes equations for the compressible viscous fluid. These issues are covered in Sec. 2.

Section 2 addresses the results of studying wave processes in hydroelastic waveguides with plane and curved interfaces. We will discuss statements of and problem-solving methods for the basic classes of aerohydroelastic problems for compressible and incompressible elastic bodies subjected to large (finite) initial deformation and interacting with a compressible viscous fluid. We will analyze the graphs of numerical solutions of the dispersion equations for some specific problems. They show how the viscosity of the compressible fluid and the prestresses of the body affect the phase velocities, damping factors, and dispersion of normal waves.

Section 3 analyzes the results of studying the interaction of an acoustic wave with rigid and elastic particles in a compressible (viscous or ideal) fluid, the measure of this interaction being radiation (period-average) forces. Radiation forces are caused by the time-independent radiation stresses occurring in an acoustic field. Unlike pressure, they are tensor quantities [162, 163]; hence, the components of the force vector acting on a unit area of the body can be determined as the inner product of the stress tensor and the unit normal vector to the area. This is not so with scalar pressure. The acoustic literature, however, uses the term "radiation pressure" for this vector quantity [48, 137, 145]. A change in the time-average momentum flux within some volume of a fluid is responsible for the occurrence of radiation stresses during the propagation of an acoustic wave (there were controversies in the literature over the momentum and flux of momentum of various waves [48, 137, 145]). Such changes are due to second-order effects such as scattering of sound by an obstacle, absorption of sound by a propagation medium, etc. Therefore, radiation pressure is a quadratic function of the acoustic-field variables. In Lagrangian coordinates, acoustic radiation pressure is the time-average acoustic pressure on the surface of an obstacle.

In this connection, linear approximation is insufficient to calculate the acoustic pressure exerted by a harmonic wave because the pressure is a periodic function of time in this approximation [136] and its average over the wave period is equal to zero. Therefore, to determine the acoustic pressure in a fluid, it is necessary to take into account the second-order effects due to the inharmonicity of the wave profile near the obstacle. Radiation pressure strongly affects the motion of a solid particle in the fluid and imparts a unidirectional displacement to it. If there are several particles in a fluid, the interference of the incident and reflected (from the particles) waves creates a complex acoustic field in which radiation forces different in magnitude and direction act on the particles, causing their relative drift. This circumstance is widely used to intensify many acoustically assisted processes [147, 152].

There are two types of acoustic radiation pressure [48, 49, 137, 141]: Rayleigh and Langevin, or Langevin–Brillouin. Rayleigh pressure occurs when waves propagate without interaction between the acoustic field and the unperturbed medium. These cases are characteristic of closed volumes where the mass of the oscillating medium remains constant. An example is the case, studied by Rayleigh, of plane standing waves between two fixed flat solid surfaces. The expression for Rayleigh acoustic pressure depends on a coefficient that describes the nonlinear properties of the medium.

Langevin pressure occurs when an acoustic field interacts with an unperturbed medium that affects the time-average pressure. An example is waves damped at infinity. Langevin acoustic pressure in one-dimensional acoustic fields was studied in [48, 144, 161, 179, etc.].

Here we will discuss studies on the interaction of acoustic waves with rigid and elastic particles in a bounded or unbounded viscous or ideal fluid conducted at the S. P. Timoshenko Institute of Mechanics.

1. Basic Equations of the Linearized Theory of Compressible Viscous Fluid. To adequately describe the dynamics of rigid and elastic bodies in a fluid, it is necessary to devise suitable fluid models, because rigid or elastic solid models are predetermined by a specific problem statement. The compressible viscous fluid model is the most general of the classical fluid models, because it combines the property of compressibility, which allows describing the propagation of waves in a compressible ideal fluid, and the property of viscosity, which allows describing the damping of dynamical processes in an

incompressible viscous fluid. When the viscous fluid model is used to describe the dynamics of rigid and elastic bodies in a fluid, the most complete information can be obtained using the Navier–Stokes equations. This, however, involves severe mathematical difficulties, which are overcome in each specific situation with the help of modern numerical methods and computers. There is a class of viscous fluid problems for which the Navier–Stokes equations can be greatly simplified. This class encompasses dynamic processes in which the disturbances are small, and the Navier–Stokes equations can be consistently linearized using the exact expression for the total derivative of the velocity vector. These processes are also fully consistent with the theory of low-amplitude vibrations of mechanical systems in the customary terminology used in mechanics. In [144], this situation is interpreted as the oscillation of an object in a fluid with an amplitude much smaller than its dimensions. Thus, the above-mentioned class includes problems of the dynamics (low-amplitude vibrations or motions) of rigid bodies in a compressible viscous fluid and the propagation of small disturbances (low-amplitude waves) in elastic bodies interacting with a compressible viscous fluid.

To derive the basic equations in the simplest and most compact form for the description of the motion of a continuum, different coordinates are used, depending on how it is modeled. Eulerian coordinates and the Eulerian description of motion are used in fluid mechanics and Lagrangian coordinates and the Lagrangian description of motion are used in solid mechanics. Accordingly, a major issue in studying combined motions of a fluid, a gas, and elastic and rigid bodies is to choose coordinates so as to simplify the basic equations of the coupled (general) problem. This issue is resolved most successfully if it is possible to introduce general coordinates that are Eulerian coordinates for a fluid or a gas and Lagrangian coordinates for an elastic body.

Aspects of identifying specially chosen Lagrangian and Eulerian coordinates for fluids (including compressible viscous fluids) and elastic bodies were analyzed in [75, 76, 78] using a linearized problem setting for the following classes of problems: (i) a fluid at rest and a prestressed elastic body, (ii) a moving fluid with uniform flow at infinity and an elastic body without prestresses, (iii) a fluid at rest and a prestressed elastic body, (iv) a moving fluid with uniform flow at infinity and a prestressed elastic body.

Viscous fluid mechanics assumes, based on the statistical mechanics of irreversible processes, that the stress tensor can be represented as the sum of a conservative stress tensor and a viscous (dissipative) stress tensor. Usually, these two terms are pressure and viscous stress tensor. In deriving constitutive equations for fluids, it is assumed that the viscous-stress tensor is a function of the strain-rate tensor. We will assume that viscous stresses and strain rates are in a linear relationship (i.e., the Navier–Stokes law holds true). The constitutive equation for such fluids is as follows [75, 171]:

$$\hat{\sigma} = (-p' + \lambda^* \nabla \cdot \mathbf{v})\hat{E} + 2\mu^* \hat{e}, \tag{1.1}$$

where p' is the pressure in the fluid; $\mathbf{v}$ is the velocity of a fluid parcel; $\hat{E}$ is a unit tensor; $\hat{\sigma}$ and $\hat{e}$ are the stress and strain-rate tensors; λ^* and μ^* are the kinematic and dynamic viscosity coefficients.

It is also assumed that the fluid is non-heat-conductive and the processes in it are slow; therefore, the volume viscosity coefficient can be considered equal to zero [75]: $\zeta^* = \lambda^* + 1/3\mu^* = 0$. This amounts to defining the pressure p' as the average normal stress in a compressible viscous fluid at rest. The adiabatic motion of a compressible viscous fluid is desribed by the following equations [75, 144]:

$$\rho'\left[\frac{\partial \mathbf{v}}{\partial t} + (\mathbf{v}\cdot\nabla)\mathbf{v}\right] = -\nabla p' + \mu^* \Delta \mathbf{v} + (\lambda^* + \mu^*)\nabla(\nabla \cdot \mathbf{v}), \tag{1.2}$$

the continuity equation

$$\frac{\partial \rho'}{\partial t} + \nabla \cdot (\rho' \mathbf{v}) = 0, \tag{1.3}$$

and the constitutive equation for a non-heat-conductive fluid

$$p' = p'(\rho'), \tag{1.4}$$

where ρ' is the density of the fluid. These equations are nonlinear. For the problems addressed below, it is assumed that the motions and processes under consideration are small perturbations to some equilibrium states or primary motion, considered

known. Considering the unknown functions first-order terms and rejecting the terms of the second order and higher, we linearized Eqs. (1.2)–(1.4) [64, 75]:

$$\rho_0 \frac{\partial \mathbf{v}}{\partial t} - \mu^* \Delta \mathbf{v} + \nabla p - (\lambda^* + \mu^*) \nabla (\nabla \cdot \mathbf{v}) = 0, \tag{1.5}$$

$$\frac{\partial \rho}{\partial t} + \rho_0 \nabla \cdot \mathbf{v} = 0, \tag{1.6}$$

$$p = p(\rho). \tag{1.7}$$

After simplification, the constitutive equation (1.1) takes the following form [75]:

$$\hat{\sigma} = (-p + \lambda^* \nabla \cdot \mathbf{v}) \hat{E} + 2\mu^* \hat{e}, \qquad 2\hat{e} = \nabla \mathbf{v} + (\nabla \mathbf{v})^T. \tag{1.8}$$

If the oscillations of the fluid about the equilibrium position are small, the following equation can be used to close the system:

$$\frac{\partial p}{\partial \rho} = a_0^2. \tag{1.9}$$

Equations (1.5)–(1.9) represent the linearized theory of non-heat-conductive compressible viscous fluid, where ρ_0 and a_0 are the density of and the speed of sound in the fluid in equilibrium; p and ρ are the perturbations of the pressure and density of the fluid; $p' = p_0 + p, \rho' = \rho_0 + \rho$.

The following general solutions of the equations of a compressible viscous liquid were first derived in [64]:

$$v = \nabla \Phi + \nabla \times \boldsymbol{\Psi}, \qquad \nabla \cdot \boldsymbol{\Psi} = \operatorname{div} \boldsymbol{\Psi} = 0, \tag{1.10}$$

$$p = \left[(\lambda^* + 2\mu^*) \Delta - \rho_0 \frac{\partial}{\partial t} \right] \Phi, \tag{1.11}$$

$$\rho = \left(\frac{\lambda^* + 2\mu^*}{a_0^2} \Delta - \frac{\rho_0}{a_0^2} \frac{\partial}{\partial t} \right) \Phi, \tag{1.12}$$

where Φ and $\boldsymbol{\Psi}$ are scalar and vector potentials,

$$\left[\left(1 + \frac{\lambda^* + 2\mu^*}{a_0^2 \rho_o} \frac{\partial}{\partial t} \right) \Delta - \frac{1}{a_0^2} \frac{\partial^2}{\partial t^2} \right] \Phi = 0, \tag{1.13}$$

$$\left(\nu^* \Delta - \frac{\partial}{\partial t} \right) \boldsymbol{\Psi} = 0, \tag{1.14}$$

where $\nu^* = \mu^* / \rho_0$ is the kinematic viscosity coefficient.

The boundary conditions are linearized as well. This is possible if the motion of a rigid body in a fluid is small displacements about some position. In this case, the boundary conditions on the surface of the moving body are carried over along the normal to the same surface at rest. If the body moves in a compressible viscous fluid, then no-slip conditions must be satisfied on its surface S. This means that the velocity vector (1.10) is equal to zero if the body is at rest. A free body will move under hydrodynamic forces [67, 77]. In this case, the no-slip conditions are

$$\mathbf{v} = \mathbf{v}_S, \qquad \mathbf{v}_S = \dot{\mathbf{u}} + \boldsymbol{\omega} \times \mathbf{r}, \tag{1.15}$$

where $\dot{\mathbf{u}}$ and $\mathbf{v}_S$ are the velocity vectors of the center of inertia and an arbitrary point of the surface S; $\boldsymbol{\omega}$ is the instantaneous rate of rotation of the body; $\mathbf{r}$ is the position vector the center of inertia to an arbitrary point of the surface S. The quantities $\mathbf{u}$ and $\boldsymbol{\omega}$ are determined from the equations of motion of a rigid body under hydrodynamic forces and moments:

$$\mathbf{F}_r = \int_S \hat{\sigma}\cdot\mathbf{N}dS, \qquad \mathbf{M}_r = \int_S \mathbf{r}_S \times (\hat{\sigma}\cdot\mathbf{N})\,dS. \tag{1.16}$$

To derive the equations of motion of a rigid body in a fluid, use is made of the center-of-mass and momentum theorems:

$$\rho_1 V \frac{d^2\mathbf{u}}{dt^2} = \mathbf{F}_r, \qquad \frac{d\mathbf{L}}{dt} = \mathbf{M}_r, \tag{1.17}$$

where V and ρ_1 are the volume and density of the body; $\mathbf{L} = \rho_1 \int_V \mathbf{r}\times(\boldsymbol{\omega}\times\mathbf{r})\,dV$ is the kinematic moment of the rigid body in the moving frame of reference.

2. Waves in Prestressed Elastic Bodies Interacting with a Compressible Viscous Fluid. Most studies on prestrained elastic bodies interacting with a fluid used simplified applied two-dimensional theories for prestressed bodies and assumed the fluid to be ideal or incompressible viscous.

However, this approach has significant shortcomings which are manifested in dynamic problems. Additional simplifying hypotheses strongly reduce the applicability of the results.

An approach free from these shortcomings and based on the linearized three-dimensional theory of finite deformations for solids bodies and the linearized three-dimensional Navier–Stokes equations for a compressible viscous fluid was first proposed in [57–59, 62–68, 71–79, 168, 170, 171]. This approach is more general and allows a more adequate description of wave processes in real hydroelastic systems.

In this connection, we will only focus on the studies conducted at the S. P. Timoshenko Institute of Mechanics using this approach.

2.1. Statement of Three-Dimensional Problems of Hydroelasticity for Prestressed Bodies and Compressible Viscous Fluid. The general problem of the interaction of compressible and incompressible elastic bodies with high (finite) prestrains with a compressible viscous fluid at rest was formulated in [55–73, 75, 76, 78, 79], where a method of study was proposed and the basic equations of the linearized theory of aerohydroelasticity for prestressed bodies and compressible viscous fluid were derived.

Following this method, we can assume that elastic bodies can be described by isotropic hyperelastic materials with an arbitrary elastic potential function. The elastic potential function of a nonlinear elastic body can be an arbitrary twice continuously differentiable function of the components of the Green strain tensor. Also, let the fluid at rest be Newtonian and have arbitrary viscosity. Thermal effects can be neglected, according to Mises. Such dynamic processes in hydroelastic systems are considered that the additional strains induced, i.e., strain perturbations, are much lower than the prestrains.

The assumptions made allow applying the linearized theory of elasticity to elastic bodies, and the smallness of the perturbations allow applying the linearized Navier–Stokes equations to the compressible viscous fluid. This problem statement makes it possible to analyze the effect of prestresses of the elastic body and the viscosity of the fluid on the following parameters of the wave process: phase velocity of perturbations, damping factor of modes, critcal frequencies, dispersion of waves, etc. The general case is considered where the initial state is described by the theory of large (finite) deformations. Models based on various theories of small initial deformations, approximate applied two-dimensional theories for bodies with or without prestresses, the classical theory of elasticity, and approximate fluid models are special cases of the model considered in the cited publications and can be arrived at by making additional simplifying assumptions.

With these assumptions, the system of linearized equations of aerohydroelasticity for prestressed bodies interacting with a viscous compressible fluid takes the following form [55–73, 75, 76, 78, 79, 168, 170, 171]:

(i) compressible elastic bodies:

$$\left(\tilde{\omega}_{ij\alpha\beta}\frac{\partial^2}{\partial z_i \partial z_\beta} - \delta_{j\alpha}\tilde{\rho}\frac{\partial^2}{\partial t^2}\right)u_\alpha = 0, \qquad z_k \in V_1,$$

$$\tilde{Q}_j \equiv N_i^0 \tilde{\omega}_{ij\alpha\beta}\frac{\partial u_\alpha}{\partial z_\beta}, \qquad \tilde{\omega}_{ij\alpha\beta} = \frac{\lambda_i\lambda_\beta}{\lambda_1\lambda_2\lambda_3}\omega_{ij\alpha\beta}, \qquad \tilde{\rho} = \frac{\rho}{\lambda_1\lambda_2\lambda_3},$$

(ii) incompressible elastic bodies:

$$\left(\widetilde{\kappa}_{ij\alpha\beta}\,\frac{\partial^2}{\partial z_i\partial z_\beta}-\delta_{j\alpha}\rho\,\frac{\partial^2}{\partial t^2}\right)u_\alpha+\widetilde{q}\,\frac{\partial f}{\partial z_i}=0,\qquad z_k\in V_1,$$

$$\widetilde{q}_{ij}\,\frac{\partial u_j}{\partial z_i}=0,\qquad z_k\in V_1,\qquad \widetilde{Q}_j\equiv N_i^0\left(\widetilde{\kappa}_{ij\alpha\beta}\,\frac{\partial u_\alpha}{\partial z_\beta}+\widetilde{q}_{ij}f\right),$$

$$\widetilde{\kappa}_{ij\alpha\beta}=\lambda_i\lambda_\beta\kappa_{ij\alpha\beta},\qquad \widetilde{q}_{ij}=\lambda_i q_{ij},\qquad \lambda_1\lambda_2\lambda_3=1,$$

(iii) compressible viscous fluid:

$$\frac{\partial\mathbf{v}}{\partial t}-\nu^*\Delta\mathbf{v}+\frac{1}{\rho_0}\nabla p-\frac{1}{3}\nu^*\nabla(\nabla\cdot\mathbf{v})=0,\qquad z_k\in V_2,$$

$$\frac{1}{\rho_0}\frac{\partial\rho}{\partial t}+\nabla\cdot\mathbf{v}=0,\qquad \frac{\partial p}{\partial\rho}=a_0^2,\qquad a_0=\text{const},\qquad z_k\in V_2,$$

$$p_{ij}=-\delta_{ij}p-\frac{2}{3}\delta_{ij}\mu^*\nabla\cdot\mathbf{v}+\mu^*\left(\frac{\partial v_i}{\partial z_j}+\frac{\partial v_j}{\partial z_i}\right).$$

Specific features in the interaction between an elastic body and a fluid are described by the dynamic conditions

$$\widetilde{Q}_j=p_{ij}N_i^0,\qquad z_k\in S$$

and the kinematic conditions

$$\frac{\partial\mathbf{u}}{\partial t}=\mathbf{v},\qquad z_k\in S$$

specified at the body–fluid interface.

The tensors $\widetilde{\omega}_{ij\alpha\beta}$, $\widetilde{\kappa}_{ij\alpha\beta}$, and $\widetilde{q}_{ij}$ depend on the type of the initial state and the elastic potential of the body. The expressions for the components of these tensors can be found in [61] where simplifications for various theories of small initial deformations were proposed.

The equations for elastic bodies are expressed in terms of the Lagrangian coordinates z_i of the initial state and are valid for both homogeneous and inhomogeneous strains.

Harmonic wave processes of small amplitude in elastic bodies in initial state are further studied. Unlike solid bodies, the equations for the fluid are expressed in terms of Eulerian coordinates of its natural state. In the hydroelastic problem, the initial state of the elastic body is a natural state relative to the fluid and to the system as a whole. Since we are considering the propagation of small perturbations, the Eulerian and Lagrangian approaches to the description of the behavior of the media coincide, as indicated in Sec. 1. Therefore, the differences between the Lagrangian and Eulerian coordinates is ignored, which eliminates the difficulties associated with the formulation of boundary conditions typical for nonlinear problems. Wave processes in compressible and incompressible prestrained elastic bodies interacting with a compressible viscous fluid whose initial state is homogeneous are further studied. The displacements to the initial state are defined by

$$u_j^0=\lambda_j^{-1}(\lambda_j-1)z_j,\qquad \lambda_j=\text{const},$$

where λ_j are the elongations along the coordinate axes. The following general solutions for compressible and incompressible elastic bodies in homogeneous initial stress–strain state were obtained in [57–59, 71, 72, 75, 79, 168, 170]:

$$u_1 = \frac{\partial \psi_1}{\partial z_2} - \frac{\partial^2 \psi_2}{\partial z_1 \partial z_3}, \qquad u_2 = -\frac{\partial \psi_1}{\partial z_1} - \frac{\partial^2 \psi_2}{\partial z_2 \partial z_3}, \qquad z_k \in V_1,$$

$$u_3 = (\tilde{\omega}_{1133} + \tilde{\omega}_{1313})^{-1} \left(\tilde{\omega}_{1111} \Delta_1 + \tilde{\omega}_{3113} \frac{\partial^2}{\partial z_3^2} - \rho \frac{\partial^2}{\partial t^2} \right) \psi_2$$

$$\left\{ \left(\Delta_1 + \xi_1^2 \frac{\partial^2}{\partial z_3^2} - \frac{\rho}{\tilde{\omega}_{1221}} \frac{\partial^2}{\partial t^2} \right) \psi_1 = 0, \ z_k \in V_1, \right.$$

$$\left[\left(\Delta_1 + \xi_2^2 \frac{\partial^2}{\partial z_3^2} \right) \left(\Delta_1 + \xi_3^2 \frac{\partial^2}{\partial z_3^2} \right) - \rho \left(\frac{\tilde{\omega}_{1111} + \tilde{\omega}_{1331}}{\tilde{\omega}_{1111} \tilde{\omega}_{1331}} \Delta_1 + \frac{\tilde{\omega}_{3333} + \tilde{\omega}_{3113}}{\tilde{\omega}_{1111} \tilde{\omega}_{1331}} \frac{\partial^2}{\partial z_3^2} \right) \frac{\partial^2}{\partial t^2} \right.$$

$$\left. + \frac{\rho^2}{\tilde{\omega}_{1111} \tilde{\omega}_{1331}} \frac{\partial^4}{\partial t^4} \right] \psi_2 = 0, \qquad z_k \in V_1, \qquad \tilde{\omega}_{ij\alpha\beta} = \text{const},$$

$$\tilde{\omega}_{ij\alpha\beta} = \frac{\lambda_i \lambda_j \lambda_\alpha \lambda_\beta}{\lambda_1 \lambda_2 \lambda_3} \left[\delta_{ij} \delta_{\alpha\beta} a_{i\beta} + (1 - \delta_{ij})(\delta_{i\alpha} \delta_{j\beta} + \delta_{j\alpha} \delta_{i\beta}) \mu_{ij} + \frac{\delta_{i\beta} \delta_{j\alpha}}{\lambda_j \lambda_\alpha} s^0_{\beta\beta} \right],$$

$$\xi_1^2 = \frac{\tilde{\omega}_{3113}}{\tilde{\omega}_{1221}}, \qquad \xi_{2,3}^2 = g \pm \left(g^2 - \frac{\tilde{\omega}_{3333} \tilde{\omega}_{3113}}{\tilde{\omega}_{1111} \tilde{\omega}_{1331}} \right)^{1/2},$$

$$\left. 2\tilde{\omega}_{1111} \tilde{\omega}_{1331} g = \tilde{\omega}_{1111} \tilde{\omega}_{3333} + \tilde{\omega}_{1331} \tilde{\omega}_{3113} - (\tilde{\omega}_{1133} + \tilde{\omega}_{1313})^2 \right\}$$

for prestrained compressible bodies and

$$u_1 = \frac{\partial x_1}{\partial z_2} - \frac{\partial^2 x_2}{\partial z_2 \partial z_3}, \qquad u_2 = -\frac{\partial x_1}{\partial z_1} - \frac{\partial^2 x_2}{\partial z_2 \partial z_3}, \qquad u_3 = \Delta_1 x_2, \qquad z_k \in V_1$$

$$\left\{ \left(\Delta_1 + \eta_1^2 \frac{\partial^2}{\partial z_3^2} - \frac{\rho}{\tilde{\kappa}_{1221}} \frac{\partial^2}{\partial t^2} \right) x_1 = 0, \qquad \tilde{\kappa}_{ij\alpha\beta} = \text{const}, \qquad z_k \in V_1, \right.$$

$$\left[\left(\Delta_1 + \eta_2^2 \frac{\partial^2}{\partial z_3^2} \right) \left(\Delta_1 + \eta_3^2 \frac{\partial^2}{\partial z_3^2} \right) - \frac{\rho}{\tilde{\kappa}_{1331}} \left(\Delta_1 + \frac{\partial^2}{\partial z_3^2} \right) \frac{\partial^2}{\partial t^2} \right] x_2 = 0, \qquad z_k \in V_1,$$

$$\tilde{\kappa}_{ij\alpha\beta} = \lambda_i \lambda_j \lambda_\alpha \lambda_\beta \left[\delta_{ij} \delta_{\alpha\beta} a_{i\beta} + (1 - \delta_{ij})(\delta_{i\alpha} \delta_{j\beta} + \delta_{j\alpha} \delta_{i\beta}) \mu_{ij} + \frac{\delta_{i\beta} \delta_{j\alpha}}{\lambda_j \lambda_\alpha} s^0_{\beta\beta} \right],$$

$$\eta_1^2 = \frac{\tilde{\kappa}_{3113}}{\tilde{\kappa}_{1221}}, \qquad \eta_{2,3}^2 = m \pm \left(m^2 - \frac{\tilde{\kappa}_{3113}}{\tilde{\kappa}_{1331}} \right)^{1/2},$$

$$\left. 2\tilde{\kappa}_{1331} m = \tilde{\kappa}_{3333} + \tilde{\kappa}_{1111} - 2(\tilde{\kappa}_{1133} + \tilde{\kappa}_{1313}), \qquad \Delta_1 = \frac{\partial^2}{\partial z_1^2} + \frac{\partial^2}{\partial z_2^2} \right\}$$

for incompressible elastic bodies.

The general solutions of the linearized equations of hydrodynamics of a Newtonian compressible viscous fluid at rest expressed in terms of scalar and vector potentials in Sec. 1 are as follows [62–65, 71, 72, 75, 76, 78, 171]:

$$\mathbf{v} = \frac{\partial}{\partial t}(\nabla\Phi + \nabla\times\boldsymbol{\Psi}), \qquad z_k \in V_2, \qquad p^* = \rho_0\left(\frac{4}{3}\nu^*\Delta - \frac{\partial}{\partial t}\right)\Phi, \qquad z_k \in V_2,$$

$$\rho^* = \frac{\rho_0}{a_0^2}\left(\frac{\lambda^* + 2\mu^*}{\rho_0}\Delta - \frac{\partial}{\partial t}\right)\Phi, \qquad z_k \in V_2$$

$$\left\{\left[\left(1 + \frac{4\nu^*}{3a_0^2}\frac{\partial}{\partial t}\right)\Delta - \frac{1}{a_0^2}\frac{\partial^2}{\partial t^2}\right]\Phi = 0, \qquad z_k \in V_2, \qquad \left(\frac{\partial}{\partial t} - \nu^*\Delta\right)\boldsymbol{\Psi} = 0, \qquad z_k \in V_2,\right.$$

$$\Delta = \nabla\cdot\nabla = \frac{\partial^2}{\partial z_1^2} + \frac{\partial^2}{\partial z_2^2} + \frac{\partial^2}{\partial z_3^2}, \qquad \nu^* = \frac{\mu^*}{\rho_0}, \qquad \lambda^* = -\frac{2}{3}\mu^*, \qquad \delta_{ij} = \begin{cases} 1, & i = j, \\ 0, & i \neq j \end{cases},$$

where **u** is the displacement vector in the elastic body; ρ is the density of the elastic body; a_{ij} and μ_{ij} are the coefficients of the constitutive equations of the elastic bodies; $s^0_{\beta\beta}$ are the prestresses; v is the velocity perturbation vector in the fluid; p^* and ρ^* are the perturbations of the density and pressure in the fluid; ρ_0 and a_0 are the density of and the speed of sound in the fluid at rest; μ^* and ν^* are the dynamic and kinematic viscosity coefficients of the fluid; V_1 is the volume of the elastic body; V_2 is the volume occupied by the fluid; S is the interface between the media.

Note that these solutions are the most general and can be reduced, by making additional simplifying assumptions, to special-case solutions for simpler models of elastic bodies and fluids.

The above system of equations of the three-dimensional linearized theory completes the statement of hydroelastic problems for elastic bodies with homogeneous initial strains and a Newtonian compressible viscous fluid at rest, the thermal effects being neglected. There are, as special cases, simpler models of fluid (incompressible viscous, compressible ideal, incompressible ideal) and elastic body (various theories of small initial deformations, classical theory of elasticity, applied two-dimensional theories for bodies with or without prestresses).

Note that the equations for perturbations are linear, but the initial stress–strain state is determined from the general nonlinear equations. In this connection, despite the fact that the basic equations are written for the coordinates z_i of the initial stress–strain state and all quantities are referred to the dimensions of the body in this state (therefore, the general statement of hydroelastic problems for prestressed bodies in coordinates z_i is similar to the statement of linear problems of classical hydroelasticity), there are, however, substantial differences in the equations and the boundary conditions in these problem statements.

The above models helped to find solutions to some specific problems.

2.2. Wave Processes in Hydroelastic Systems with Flat Interfaces between the Media.

2.2.1. Stoneley Waves in the Interface between Prestressed Elastic and Compressible Viscous Liquid Half-Spaces. The propagation of surface waves along the interface between prestrained compressible and incompressible elastic and compressible viscous liquid half-spaces was studied in [9, 12, 28, 30, 31, 71, 72, 75, 79, 80, 171, 190, etc.].

The interest in these problems is due to the resonant effects that can occur in such hydroelastic systems and generate waves localized near the interface. The effect of initial strains on the phase velocities of Stoneley waves in the interface between an elastic body and an ideal fluid was studied in [3, 11, 31, 71, 72, 75, 79, 106, 107, etc.]. The prestresses in the body and the viscosity of the fluid were taken into account in [9, 12, 28, 30, 31, 71, 72, 75, 79, 80, 171, 190, etc.].

2.2.1.1. Compressible Elastic Body and Compressible Viscous Fluid. The problem for compressible elastic and viscous compressible liquid half-spaces is characterized by the following dynamic and kinematic boundary conditions:

$$\widetilde{Q}_1|_{z_2=0} = \widetilde{P}_1|_{z_2=0}, \qquad \widetilde{Q}_2|_{z_2=0} = \widetilde{P}_2|_{z_2=0}, \tag{2.1}$$

$$v_1|_{z_2=0} = \left.\frac{\partial u_1}{\partial t}\right|_{z_2=0}, \qquad v_2|_{z_2=0} = \left.\frac{\partial u_2}{\partial t}\right|_{z_2=0}. \tag{2.2}$$

We will now use the following general solutions for the plane case under consideration [57, 62–65, 71, 72, 75, 79]:

$$u_1 = -\frac{\partial^2 x_1}{\partial z_1 \partial z_2},$$

$$u_2 = \frac{(\lambda_1^2 a_{11} + s_{11}^0)}{\lambda_2^2 (a_{12} + \mu_{12})}\left[\frac{\partial^2}{\partial z_1^2} + \frac{\lambda_2^2 (\lambda_1^2 \mu_{12} + s_{22}^0)}{\lambda_1^2 (\lambda_1^2 a_{11} + s_{11}^0)}\frac{\partial^2}{\partial z_2^2} - \frac{\rho}{\lambda_1^2 (\lambda_1^2 a_{11} + s_{11}^0)}\frac{\partial^2}{\partial t^2}\right] x_1,$$

$$v_1 = \frac{\partial^2 x_2}{\partial z_1 \partial t} + \frac{\partial^2 x_3}{\partial z_2 \partial t}, \qquad v_2 = \frac{\partial^2 x_2}{\partial z_2 \partial t} - \frac{\partial^2 x_3}{\partial z_1 \partial t},$$

where x_i are potentials determined from the following equations [57, 62–65, 71, 72, 75, 79]:

$$\left[\left(\frac{\partial^2}{\partial z_1^2} + \frac{\lambda_2^2 (\lambda_1^2 \mu_{12} + s_{22}^0)}{\lambda_1^2 (\lambda_1^2 a_{11} + s_{11}^0)}\frac{\partial^2}{\partial z_2^2} - \frac{\rho}{\lambda_1^2 (\lambda_1^2 a_{11} + s_{11}^0)}\frac{\partial^2}{\partial t^2}\right)\left(\frac{\partial^2}{\partial z_1^2} + \frac{\lambda_2^2 (\lambda_2^2 a_{22} + s_{22}^0)}{\lambda_1^2 (\lambda_2^2 \mu_{12} + s_{11}^0)}\frac{\partial^2}{\partial z_2^2}\right.\right.$$

$$\left.\left. - \frac{\rho}{\lambda_1^2 (\lambda_2^2 \mu_{12} + s_{11}^0)}\frac{\partial^2}{\partial t^2}\right) - \frac{\lambda_2^4 (a_{12} + \mu_{12})^2}{(\lambda_1^2 a_{11} + s_{11}^0)(\lambda_2^2 \mu_{12} + s_{11}^0)}\frac{\partial^4}{\partial z_1^2 \partial z_2^2}\right] x_1,$$

$$\left[\left(1 + \frac{4\nu^*}{3a_0^2}\frac{\partial}{\partial t}\right)\left(\frac{\partial^2}{\partial z_1^2} + \frac{\partial^2}{\partial z_2^2}\right) - \frac{1}{a_0^2}\frac{\partial^2}{\partial t^2}\right] x_2 = 0, \qquad \left[\frac{\partial}{\partial t} - \nu^*\left(\frac{\partial^2}{\partial z_1^2} + \frac{\partial^2}{\partial z_2^2}\right)\right] x_3 = 0.$$

The parameters characterizing the propagation of surface waves are defined in the class of traveling waves in the form: $x_j = X_j(z_2)\exp[i(kz_1 - \omega t)]$, $j = \overline{1,3}$, where k ($k = \beta + i\gamma$) is the wave number, γ is the damping factor, and ω is the circular frequency ($i^2 = -1$).

Note that despite the fact that the class of harmonic waves selected above is the most simple and convenient for theoretical studies, it does not reduce the generality of the results obtained because a linear wave of arbitrary profile can be represented by harmonic components.

We will now discuss the solutions to two Sturm–Liouville eigenvalue problems for the equations of motion of the fluid and the elastic body and the corresponding eigenfunctions. Substituting the solutions into the boundary conditions (2.1) and (2.2), we obtain a system of linear homogeneous algebraic equations for arbitrary constants. From the condition for the existence of a nontrivial solution, we derive the dispersion equation

$$\det||e_{lm}(c, a_{ij}, \mu_{ij}, s_{ii}^0, \rho_0, \mu^*, \omega)|| = 0 \qquad (l, m = \overline{1,4}). \tag{2.3}$$

Note that the dispersion equation (2.3) is the most general and can be reduced, by making additional assumptions, to equations for special cases of wave processes and simpler models of elastic bodies and fluids, some of which were used in [43, 45, 46].

Passing to the limit in (2.3) yielded characteristic expressions for incompressible viscous, compressible ideal, and incompressible ideal fluids and both bodies with and without prestresses. Note that in deriving Eq. (2.3), the only constraint imposed on the elastic potential function was its continuous bidifferentiability. Therefore, Eq. (2.3) is general and valid for prestressed compressible elastic bodies described by arbitrary elastic potential functions. It was shown that if the coefficient of viscosity μ^* of the fluid and the prestresses s_{ii}^0 tend to zero, then the dispersion equation (2.3) goes over into the well-known Stoneley characteristic equation [43, 45, 46, 197]. If, additionally, the density of the fluid is assumed zero, then Eq. (2.3) goes over into the equation first derived by Rayleigh [41, 43, 45, 151, 193]. Note that both characteristic equations have been thoroughly analyzed in seismology within the framework of the classical theory of elasticity and the hydrodynamics of ideal fluid.

The general dispersion equation (2.3) was solved numerically. It was assumed that the elastic half-plane is loaded along the oz_1-axis. With such a load, there is no analogy between linearized and linear problems. Hence, solutions for prestrained bodies cannot be obtained from the linear solutions [68, 169]. For compressible stiff materials (organic glass) described by the three-invariant Murnaghan potential function, expressions for the phase velocities and the damping factors of surface waves as functions of the prestresses were derived. Numerical results were obtained for fluids (water and glycerin) in contact with organic glass. An analysis of the resulting graphs shows that the prestresses $\overline{\sigma}_{11}^0$ ($\overline{\sigma}_{11}^0 = \lambda_1 \overline{s}_{11}^0 / (\lambda_2 \lambda_3 \mu)$, where μ is the shear modulus in the elastic body without prestresses) increase the phase velocities $\overline{c}$ ($\overline{c} = c / c_s$, $c_s = \sqrt{\mu / \rho}$) and decrease the damping factors $\overline{\gamma}$ ($\overline{\gamma} = \gamma / k_s$, where k_s is the wave number of a shear wave in the elastic body) of surface waves and that the viscosity of the fluid has the inverse effect on these quantities.

Graphs of the phase velocity $\overline{c}$ and damping factor $\overline{\gamma}$ of Stoneley waves versus the dimensionless speed of sound $\overline{a}_0$ in fluid were plotted numerically in [9, 12, 72, 75, 79].

Note that $\overline{a}_0$ equal to the ratio of the velocity of acoustic wave in the fluid to the velocity of shear wave in the infinite elastic body ($\overline{a}_0 = a_0 / c_s$) characterizes the compressibility of the fluid. Therefore, these graphs illustrate the effect of the compressibility of the fluid on surface waves.

Both the velocity and damping factor of Stoneley waves in water and glycerin change substantially with increasing $\overline{a}_0$. If $\overline{a}_0$ tends to infinity, we have the case of an incompressible viscous fluid. Thus, we may conclude that assuming the incompressibility of the fluid in analyzing wave processes in hydroelastic systems consisting of compressible elastic bodies and a fluid can lead to inaccurate quantitative results.

2.2.1.2. Incompressible Elastic Body and Compressible Viscous Fluid. Unlike compressible rigid bodies, highly elastic incompressible materials such as rubber can be subjected to large initial deformations without failure. An analysis of the effect of finite initial strains on wave process is of importance and interest. This problem was addressed in [11, 30, 31, 38, 72, 75, 79, 190].

We will now use the following general solutions of the linearized equations for incompressible bodies interacting with a incompressible viscous fluid in the plane case under consideration [58, 62–65, 71, 72, 75, 79]:

$$u_1 = -\frac{\partial^2 \psi_1}{\partial z_1 \partial z_2}, \qquad u_2 = \lambda_1 q_1 \lambda_2^{-1} q_2^{-1} \frac{\partial^2}{\partial z_1^2} \psi_1,$$

$$p = \lambda_1^{-1} q_1^{-1} \left\{ \lambda_1^2 \left[\lambda_1^2 a_{11} + s_{11}^0 - \lambda_1 \lambda_2 q_1 q_2^{-1} (a_{12} + \mu_{12}) \right] \frac{\partial^2}{\partial z_1^2} + \lambda_2^2 (\lambda_1^2 \mu_{12} + s_{22}^0) \frac{\partial^2}{\partial z_2^2} - \rho \frac{\partial^2}{\partial t^2} \right\} \frac{\partial}{\partial z_2} \psi_1,$$

$$\nu_1 = \frac{\partial^2 x_2}{\partial z_1 \partial t} + \frac{\partial^2 x_3}{\partial z_2 \partial t}, \qquad \nu_2 = \frac{\partial^2 x_2}{\partial z_2 \partial t} - \frac{\partial^2 x_3}{\partial z_1 \partial t},$$

where ψ_1, x_2, and x_3 are potential functions determined from the following equations [58, 62–65, 71, 72, 75, 79]:

$$\left[\frac{\partial^4}{\partial z_1^4} + \frac{\lambda_2^4 q_2^2 (\lambda_1^2 \mu_{12} + s_{22}^0)}{\lambda_1^4 q_1^2 (\lambda_2^2 \mu_{12} + s_{11}^0)} \frac{\partial^4}{\partial z_2^4} - \frac{\rho}{\lambda_1^2 (\lambda_2^2 \mu_{12} + s_{11}^0)} \frac{\partial^4}{\partial z_1^2 \partial t^2} \right.$$

$$+ \frac{q_1 q_2^{-1} (\lambda^2{}_2 a_{22} + s_{22}^0) + q_1^{-1} q_2 (\lambda_1^2 a_{11} + s_{11}^0) - 2\lambda_1 \lambda_2 (a_{12} + \mu_{12})}{\lambda_1^2 \lambda_2^{-2} (\lambda_2^2 \mu_{12} + s_{11}^0) q_1 q_2^{-1}} \frac{\partial^4}{\partial z_1^2 \partial z_2^2}$$

$$\left. - \frac{\lambda^2{}_2 q_2^2 \rho}{\lambda^4{}_1 q_1^2 (\lambda^2{}_2 \mu_{12} + s_{11}^0)} \frac{\partial^4}{\partial z_2^2 \partial t^2} \right] \psi_1 = 0,$$

$$\left[\left(1 + \frac{4\nu^*}{3a_0^2} \frac{\partial}{\partial t} \right) \left(\frac{\partial^2}{\partial z_1^2} + \frac{\partial^2}{\partial z_2^2} \right) - \frac{1}{a_0^2} \frac{\partial^2}{\partial t^2} \right] x_2 = 0, \qquad \left[\frac{\partial}{\partial t} - \nu^* \left(\frac{\partial^2}{\partial z_1^2} + \frac{\partial^2}{\partial z_2^2} \right) \right] x_3 = 0.$$

The following dispersion equation was derived for a highly elastic incompressible prestressed half-space interacting with a compressible viscous fluid by a method similar to that for compressible materials:

$$\det||\widetilde{e}_{lm}(c, \gamma, a_{ij}, \mu_{ij}, \lambda_i, \rho_0, a_0, \mu^*, \omega)||=0 \qquad (l,m=\overline{1,4}). \tag{2.4}$$

Note that the dispersion equation (2.4) is the most general and can be reduced, by making additional assumptions, to characteristic equations for special cases of wave processes and simpler models of elastic bodies and fluids, some of which were used earlier by other researchers.

Equation (2.4) was solved numerically for highly elastic incompressible bodies described by the Treloar potential function [55, 56, 61, 69–72, 75, 79]. Graphs of the phase velocities of Rayleigh and Stoneley waves versus the prestrains were plotted for different densities of and speeds of sound in the ideal fluid of the hydroelastic system. The influence of the viscosity of the fluid and the finite prestrains on the phase velocities and damping factors of surface waves was analyzed as well.

It follows from the graphs that when the load is compressive and $\lambda_1 \approx 0.54$ (more precise value $\lambda_1 = 0.543694$), i.e., the length of the highly elastic incompressible body decreases by 46%, the phase velocity $\overline{c}_{\mathrm{R}}$ ($\overline{c}_{\mathrm{R}} = c_{\mathrm{R}} / c_{\mathrm{s}}$) of the Rayleigh wave drops to zero. This suggests that if the initial stress–strain state of the highly elastic incompressible neo-hookean body is plane, then surface instability occurs when $\lambda_1 \approx 0.54$. This value is equal to that obtained in the theory of stability [55, 56, 61, 69–72, 75, 79] and corresponds to the critical shortening λ_{cr}. An analysis of the numerical results also shows that the phase velocity $\overline{c}_{\mathrm{St}}$ ($\overline{c}_{\mathrm{St}} = c_{\mathrm{St}} / c_{\mathrm{s}}$) of the Stoneley wave vanishes when the elastic half-space is compressed by $\lambda_1 = 0.543695$, i.e., the surface instability of the hydroelastic system occurs somewhat earlier. Also, the viscous fluid, as well as the ideal fluid, promotes surface instability of the hydroelastic system at less compression of the elastic body. Thus, the linearized theory of waves in highly elastic incompressible bodies allows studying not only wave processes in the general case and some special cases, but also the conditions for the occurrence of surface instability of the elastic body and the hydroelastic system.

2.2.2. Wave Processes in Prestressed Elastic Half-Spaces Interacting with a Compressible Viscous Liquid Layer. The propagation of perturbations in an elastic half-space interacting with a liquid layer, which are also among the main types of surface waves, was studied in [13–16, 31, 33, 34]. A typical feature of such hydroelastic waveguides is that their wave field is affected by the interaction of waves not only with the interface between the elastic and liquid media, but also with the free surface.

In the cited publications, the propagation of such surface waves was studied taking into account the prestresses in the elastic medium and the viscosity of the fluid. For this problem with the boundary conditions

$$\widetilde{P}_1|_{z_2=h}=0, \qquad \widetilde{P}_2|_{z_2=h}=0, \qquad \widetilde{Q}_1|_{z_2=0}=\widetilde{P}_1|_{z_2=0},$$

$$\widetilde{Q}_2|_{z_2=0}=\widetilde{P}_2|_{z_2=0}, \qquad v_1|_{z_2=0}=\left.\frac{\partial u_1}{\partial t}\right|_{z_2=0}, \qquad v_2|_{z_2=0}=\left.\frac{\partial u_2}{\partial t}\right|_{z_2=0}$$

the following dispersion equations for compressible and incompressible bodies were derived:

$$\det||b_{lm}(c, \gamma, a_{ij}, \mu_{ij}, s_{ii}^0, \rho_0, a_0, \mu^*, \omega h / c_{\mathrm{s}})||=0 \qquad (l,m=\overline{1,6}),$$

$$\det||\widetilde{b}_{lm}(c, \gamma, a_{ij}, \mu_{ij}, \lambda_i, \rho_0, a_0, \mu^*, \omega h / c_{\mathrm{s}})||=0 \qquad (l,m=\overline{1,6}).$$

These dispersion equations are the most general and can be reduced, by making additional assumptions, to equations for special cases of wave processes and simpler models of elastic bodies and fluids, some of which were earlier used by other researchers.

The general dispersion equations were solved numerically for compressible and incompressible elastic half-spaces interacting with a compressible viscous liquid layer for different densities of and speeds of sound in it. It was assumed that the compressible elastic bodies are described by the three-invariant Murnaghan potential function, and the highly elastic incompressible bodies are described by the Treloar potential function.

2.2.2.1. Compressible Elastic Bodies and Compressible Viscous Fluid. Dispersion curves for fluids with different speeds of sound were plotted in [13–15, 31, 34]. An analysis of the curves shows that the compressibility of the fluid interacting

with a compressible elastic body has a strong effect on the dispersion properties of the wave process. The more compressible the fluid, the more there are propagating modes and the more their phase velocities change. This suggests that the fluid incompressibility assumption in designing hydroelastic waveguides consisting of compressible elastic materials and a liquid layer may lead to very inaccurate quantitative and qualitative results.

The effect of the pretension ($\overline{\sigma}_{11}^{0} = 0.004$) on the phase velocities of surface waves was studied as well. An analysis of the graphs plotted shows that despite the fact that the decomposition of the surface wave typical for a compressible elastic half-space into several modes is due to the presence of the liquid layer, the prestresses in the elastic body affect all the modes. The effect of the prestrains on the phase velocities of the modes is especially strong at their critical frequencies. The higher the frequency (the thicker the liquid layer), the weaker the effect of the prestresses. The phase velocities of the high-order modes beginning from the second order asymptotically tend to the speed of sound in the fluid, and the effect of the elastic body weakens.

The influence of the viscosity of the fluid, the thickness of the liquid layer, and the prestresses on the phase velocities and damping factors of surface waves was also analyzed for two materials: steel and organic glass. A comparative analysis of the results for steel and organic glass shows that, unlike Stoneley waves existing for each ratio between the parameters of the elastic and liquid media, the decomposition of the Rayleigh wave typical for an elastic half-space into several modes caused by the liquid layer occurs only when the velocity of the shear wave in the elastic half-space exceeds the velocity of the acoustic wave in the fluid [33, 34]. Otherwise, only one wave propagates in the system and its velocity monotonically decreases from the Rayleigh-wave velocity to the Stoneley-wave velocity. The numerical results show that the prestresses and the viscosity and density of and the speed of sound in the fluid affect the critical frequencies of waves and the phase velocities of the modes at these frequencies.

2.2.2.2. Incompressible Elastic Bodies and Compressible Viscous Fluid. The effect of large (finite) initial strains and the viscosity of the fluid on wave propagation was studied in [16]. The phase velocities $\overline{c}$ of the modes were plotted against the thickness $\overline{h}$ ($\overline{h} = \omega h / c_s$) of the viscous liquid layer contacting with a precompressed ($\lambda_1 = 0.8$) or prestretched ($\lambda_1 = 1.5$) incompressible half-space. Also, the function $\overline{\gamma} = f(\overline{h})$ was plotted to demonstrate the effect of the prestresses on the damping factor of waves.

2.2.3. Wave Processes in a Prestressed Elastic Layer on a Compressible Viscous Liquid Half-Space. The studies on this class of waves and the associated results obtained using the classical theory of elasticity and the assumption of ideal fluid are reviewed in [41, 43, 45, 53, 54]. As already mentioned, some factors inherent in real materials and affecting the wave process cannot be described by the classical theory of elasticity and the hydrodynamics of an ideal fluid.

The propagation of normal waves in an elastic layer interacting with a compressible viscous liquid half-space, which are also among the main types of acoustic waves, was studied in [31, 37, 39, 71, 72, 75, 79, 81]. A typical feature of such hydroelastic waveguides is that their wave field is affected by the interaction of waves not only with the interface between the elastic and liquid media, but also with the free surface of the elastic layer.

In the cited publications, the propagation of such surface waves was studied taking into account the prestresses in the elastic medium and the viscosity of the fluid.

For this problem with the dynamic boundary conditions $\widetilde{Q}_1|_{z_2=h} = 0$, $\widetilde{Q}_2|_{z_2=h} = 0$, $\widetilde{Q}_1|_{z_2=0} = \widetilde{P}_1|_{z_2=0}$, $\widetilde{Q}_2|_{z_2=0} = \widetilde{P}_2|_{z_2=0}$ and kinematic boundary conditions $v_1|_{z_2=0} = \left.\dfrac{\partial u_1}{\partial t}\right|_{z_2=0}$, $v_2|_{z_2=0} = \left.\dfrac{\partial u_2}{\partial t}\right|_{z_2=0}$, the following dispersion equations were derived for compressible and incompressible bodies, respectively:

$$\det||\Im_{lm}(c, \gamma, a_{ij}, \mu_{ij}, s_{ii}^{0}, \rho_0, a_0, \mu^*, \omega h / c_s)|| = 0 \quad (l, m = \overline{1,6}),$$

$$\det||\widetilde{\Im}_{lm} I(c, \gamma, a_{ij}, \mu_{ij}, \lambda_i, \rho_0, a_0, \mu^*, \omega h / c_s)|| = 0 \quad (l, m = \overline{1,6}).$$

Note that these dispersion equations are the most general and can be reduced, by making additional assumptions, to equations for special cases of wave processes and simpler models of elastic and liquid media, some of which were used in [41, 43, 45, 53, 54]. Both general dispersion equations were solved numerically. The influence of the speed of sound in the fluid, its density and viscosity, and the prestresses and the thickness of the elastic layer on the phase velocities and damping factors of quasi-Lamb waves was analyzed.

The phase velocities c_ε of the modes were plotted against the thickness $\bar{h}$ of the elastic layer (frequency) to illustrate the influences of pretension ($\bar{\sigma}_{11}^0 = 0.004$) on the phase velocities of normal waves. An analysis of the graphs shows that the effect of the prestress ($\bar{\sigma}_{11}^0 = 0.004$) is closely related to the compressibility of the fluid. For less compressible fluids ($a_0 = 2000$ m/sec), the prestresses reduce the phase velocities of the higher modes at the critical frequencies (thickness). With further increase in the thickness of the elastic layer (frequency), the prestrains increase the phase velocity. An analysis also shows that in such hydroelastic waveguides, there are certain modes whose phase velocities do not depend on the prestresses. Note that this qualitatively new phenomenon, which is absent in unbounded and semibounded bodies, was discovered and described in [98] for an elastic layer that does not interact with a fluid.

The influence of the viscous fluid on the wave process was analyzed as well. The dimensionless phase velocities $\bar{c}$ of waves were plotted against the dimensionless thickness $\bar{h}$ of the elastic layer. Comparing the dispersion curves for an elastic layer in vacuum [98] and the hydroelastic system shows that the compressible viscous fluid changes the critical frequencies of waves. It was shown that with increase in the thickness of the elastic layer, all the modes in it, beginning from the fourth one, go farther away from the surfaces into the layer. This is a major factor that weakens the effect of the viscosity of the fluid on the phase velocities and reduces the damping factors of these modes. Unlike the high-order modes, mode 1 tends to the interface between the media with increase in the thickness and becomes a quasisurface Stoneley-type wave. This explains why the viscosity of the fluid decreases the phase velocities and increases the damping factors of this mode. Quasisurface Rayleigh-type mode 2 in the elastic layer tends to the interface with increase in the thickness. This explains the effect of the viscosity of the fluid on the kinematic characteristics of this mode over the entire frequency range.

Graphs of the damping factors $\bar{\gamma}$ of the modes versus the thickness $\bar{h}$ of the layer were plotted as well. Their feature is strong damping of the first mode at its critical frequency. The damping factors of the high-order modes first increase after the origination of waves and then substantially decrease with increase in the layer thickness.

An analysis of the results obtained in the cited studies shows that the compressibility of the fluid has a strong effect on the wave properties of a hydroelastic waveguide consisting of compressible elastic bodies and a fluid. The damping factors of the high-order modes decrease with increase in the thickness of the elastic layer (frequency). The higher the viscosity of the fluid, the lower the phase velocities and the higher the damping factors of waves.

The effect of the viscosity of a liquid half-space on the phase velocities of waves interacting with a prestrained incompressible elastic layer was studied in [31, 39, 71, 72, 75, 79]. The relative change in the phase velocities c^* of modes ($c^* = (c_i - c_v)/c_i$, c_i is the velocity of waves in the elastic layer–ideal fluid system; c_v is the velocity of waves in the elastic layer–viscous fluid system) was plotted against the thickness $\bar{h}$ of the elastic layer (frequency). Also, graphs were drawn showing the influence of the frequency (the thickness of the elastic layer) $\bar{h}$, the viscosity $\bar{\mu}^*$ of the fluid, and the prestrains λ_1 on the damping factors of various modes.

An analysis of the graphs shows that the effect of the viscosity of the fluid on the damping factors and phase velocities of the high-order modes weakens with increase in the frequency.

For a highly elastic incompressible neo-hookean thin elastic layer interacting with a liquid half-space, the combined effect of the viscosity of the fluid and the prestresses is mainly exerted on the lower bending mode and becomes stronger with increase in the prestrains. The rate of this change is maximum near the bending buckling mode.

2.2.4. Wave Processes in the Prestressed Elastic Layer–Compressible Viscous Liquid Layer System. The specific behavior of propagating perturbations in such a hydroelastic waveguide is due to the presence of boundary surfaces in the elastic body and the fluid. This considerably complicates the wave field in it, which is because the wave field is strongly affected not only by the interaction of longitudinal and transverse waves with the surface of the elastic body contacting with the fluid, but also by the presence and interaction of free boundaries. The interaction of waves on the boundary surfaces results in wave dispersion.

Waves propagating in such a hydroelastic system are a generalization of the well-studied Rayleigh, Stoneley, Love, and Lamb waves. Studies on and results obtained using the classical theory of elasticity and the assumption that compressible fluid is ideal are reviewed in [41, 43, 45]. For wide application of surface waves, it is necessary to allow for the characteristics of real media. This is also because these properties affecting the wave process cannot be described by the classical theory of hydroelasticity. Among such properties are the prestresses in the elastic body and the viscosity and compressibility of the fluid. Relevant problems and results obtained with allowance for these properties are discussed in [17–25].

For this problem with the dynamic and kinematic boundary conditions

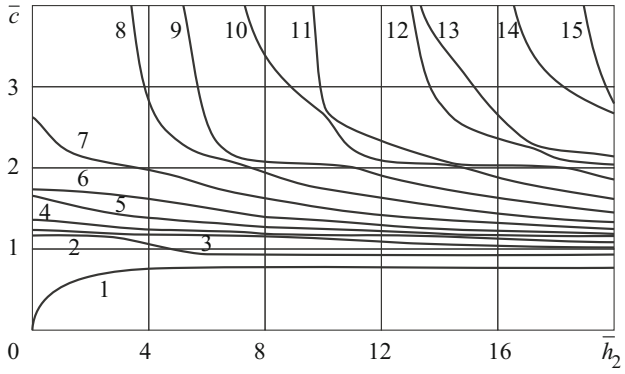

Fig. 2.1

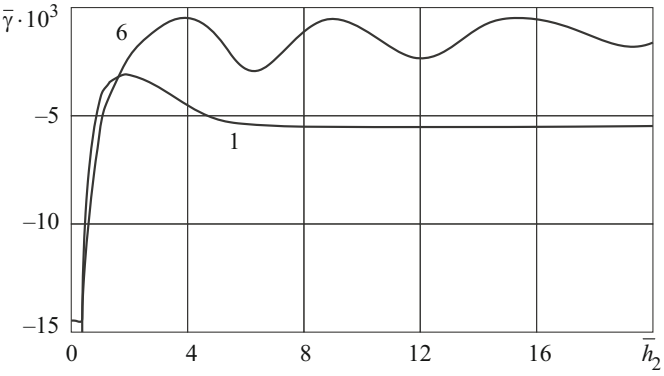

Fig. 2.2

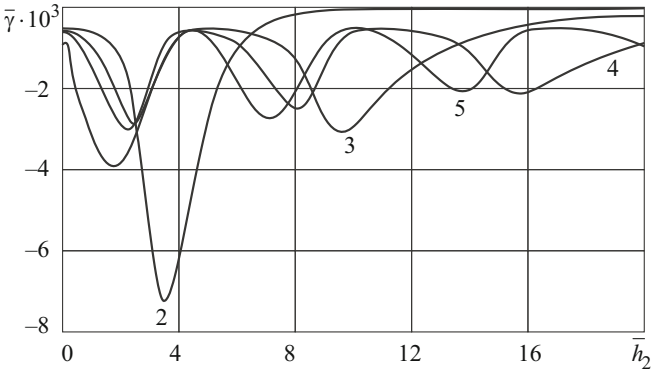

Fig. 2.3

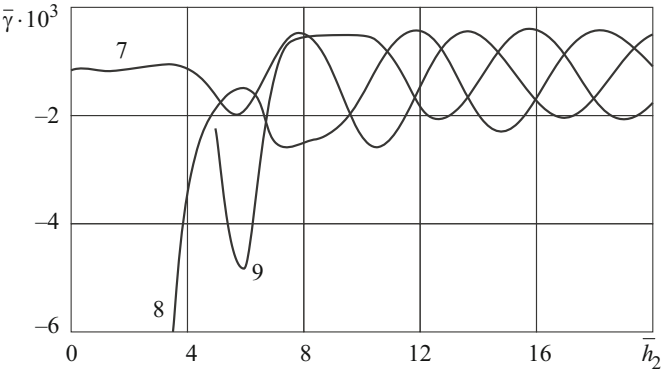

Fig. 2.4

$$\widetilde{Q}_1|_{z_2=0} = \widetilde{P}_1|_{z_2=0}, \quad \widetilde{Q}_2|_{z_2=0} = \widetilde{P}_2|_{z_2=0}, \quad \widetilde{Q}_1|_{z_2=-h_2} = 0, \quad \widetilde{Q}_2|_{z_2=-h_2} = 0,$$

$$\widetilde{P}_1|_{z_2=h_1} = 0, \quad \widetilde{P}_2|_{z_2=h_1} = 0, \quad v_1|_{z_2=0} = \left.\frac{\partial u_1}{\partial t}\right|_{z_2=0}, \quad v_2|_{z_2=0} = \left.\frac{\partial u_2}{\partial t}\right|_{z_2=0},$$

the following dispersion equation was derived:

$$\det||r_{lm}(c, \gamma, a_{ij}, \mu_{ij}, s_{ii}^0, \rho_0, a_0, \mu^*, \omega h_1 / c_s, \omega h_2 / c_s)|| = 0 \qquad (l, m = \overline{1,8}).$$

Note that this dispersion equation is the most general and can be reduced, by making additional assumptions, to equations for special cases of wave processes and simpler models of elastic and liquid media, some of which were used in [41, 43, 45, 143, 182, 198]. This general dispersion equation was solved numerically using the three-invariant Murnaghan potential function for the elastic body [71, 72, 74, 100, 101, 170, 172, 173]. The influence of the viscosity of the fluid, the prestresses, and the thicknesses of the elastic and liquid layers on the phase velocities and damping factors of quasi-Lamb waves was numerically analyzed for two hydroelastic systems: (i) organic glass–water with the following parameters for the elastic and liquid layers, respectively: $\rho = 1160$ kg/m^3, $\lambda = 3.96\cdot 10^9$ Pa, $\mu = 1.86\cdot 10^9$ Pa, $a = -3.91\cdot 10^9$ Pa, $b = -7.02\cdot 10^9$ Pa, $c = -1.41\cdot 10^9$ Pa [98, 100, 101, 172, 173] and $\rho_0 = 1000$ kg/m^3, $a_0 = 1459.5$ m/sec, $\bar{\mu}^* = 0.001$, $\bar{a}_0 = a_0 / c_s = 1.152595$; (ii) 09G2S steel–water waveguide with the following parameters for the elastic and liquid layers, respectively: $\rho = 7800$ m/sec, $\lambda = 9.26\cdot 10^{10}$ Pa, $\mu = 7.75\cdot 10^{10}$ Pa, $a = -319\cdot 10^9$ Pa, $b = -303\cdot 10^9$ Pa, $c = -78.4\cdot 10^9$ Pa [98, 100, 101, 172, 173] and ρ_0 = 1000 kg/m^3, a_0 = 1459.5 m/sec, $\bar{a}_0 = a_0 / c_s = 0.463021$. The calculated results are presented in Figs. 2.1–2.30.

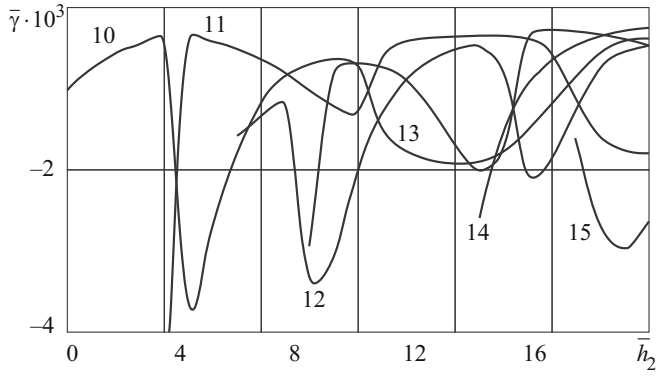

Fig. 2.5

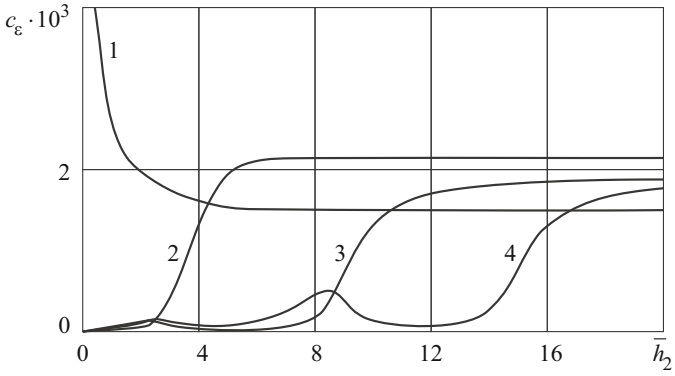

Fig. 2.6

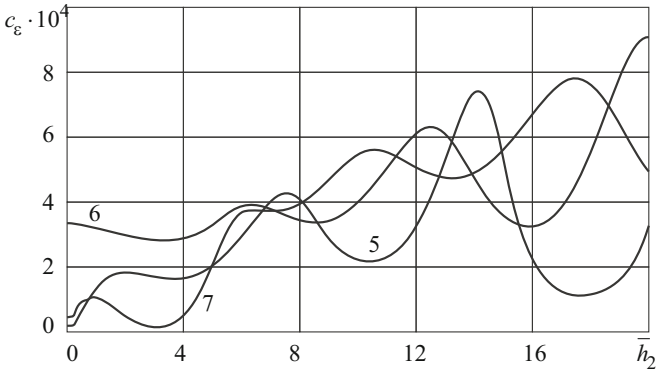

Fig. 2.7

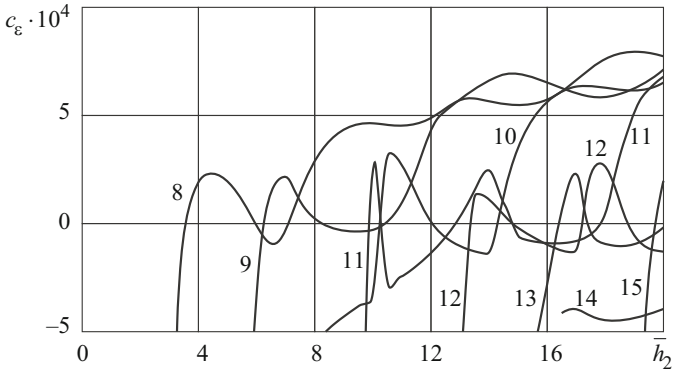

Fig. 2.8

Figures 2.1–2.14 represent the organic glass–water system. Figure 2.1 shows dispersion curves for the hydroelastic waveguide (the dimensionless phase velocities $\bar{c}$ ($\bar{c} = c / c_s$) of modes versus the dimensionless thickness $\bar{h}_2$ ($\bar{h}_2 = \omega h_2 / c_s$) of the elastic layer without prestrains in contact with the thick compressible viscous liquid layer of thickness $\bar{h}_1 = 20$ ($\bar{h}_1 = \omega h_1 / c_s$) and $\bar{\mu}^* = 0.001$.

Figures 2.2–2.5 show the dimensionless damping factors $\bar{\gamma}$ ($\bar{\gamma} = \gamma / k_s, k_s$ is the wave number of the shear wave in the elastic layer) versus the dimensionless thickness $\bar{h}_1$ of the elastic layer of thickness $\bar{h}_2$ without prestrains in contact with the viscous liquid layer of thickness $\bar{h}_1 = 20$ and $\bar{\mu}^* = 0.001$.

The effect of pretension ($\bar{\sigma}_{11}^0 = 0.004$) on the velocities of normal waves in the hydroelastic system is demonstrated by Figs. 2.6–2.8, which show the relative changes in the phase velocities c_ε ($c_\varepsilon = (c_\sigma - c)/c$, c_σ is the phase velocity of modes in the prestressed layer, c is the phase velocity of normal waves in the elastic layer without prestrains) versus the thickness $\bar{h}_2$ of the elastic layer in contact with the viscous liquid layer of thickness $\bar{h}_1 = 20$ and $\bar{\mu}^* = 0.001$.

The effect of pretension ($\bar{\sigma}_{11}^0 = 0.004$) on the damping factors of modes in the elastic layer interacting with the viscous liquid layer is demonstrated by Figs. 2.9–2.11, which show the relative changes in the damping factors γ_ε ($\gamma_\varepsilon = (\gamma_\sigma - \gamma)/\gamma$, γ_σ are the damping factors of modes in the hydroelastic system with prestrained elastic layer, γ are the damping factors of modes in the hydroelastic system without prestrains) versus the thickness $\bar{h}_2$ of the elastic layer in contact with the liquid layer of thickness $\bar{h}_1 = 20$ and $\bar{\mu}^* = 0.001$.

The effect of the viscosity ($\bar{\mu}^* = 0.001$) of the fluid on the velocities of modes in the hydroelastic system is demonstrated by Figs. 2.12–2.14, which show the relative changes in the phase velocities c^* ($c^* = (c_i - c_v)/c_i$, c_i is the phase velocity of normal waves in the hydroelastic system with an ideal fluid, c_v is the phase velocity of modes in the system with a viscous fluid) versus the thickness $\bar{h}_2$ of the elastic layer in contact with the viscous liquid layer of thickness $\bar{h}_1 = 20$ and $\bar{\mu}^* = 0.001$.

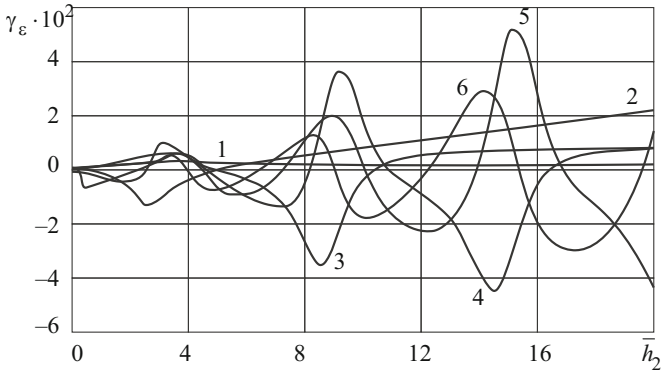

Fig. 2.9

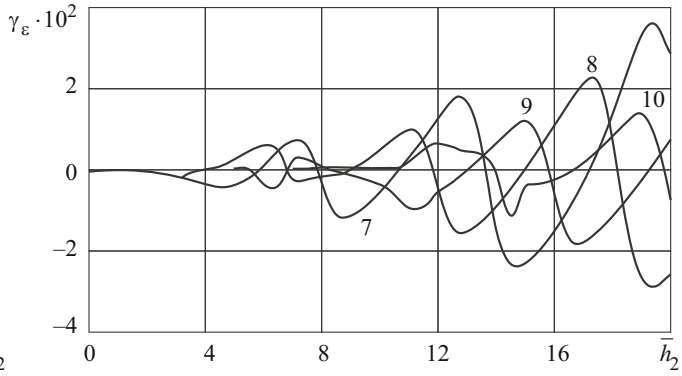

Fig. 2.10

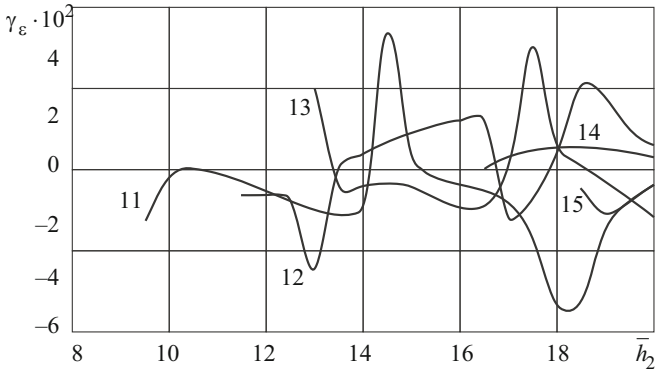

Fig. 2.11

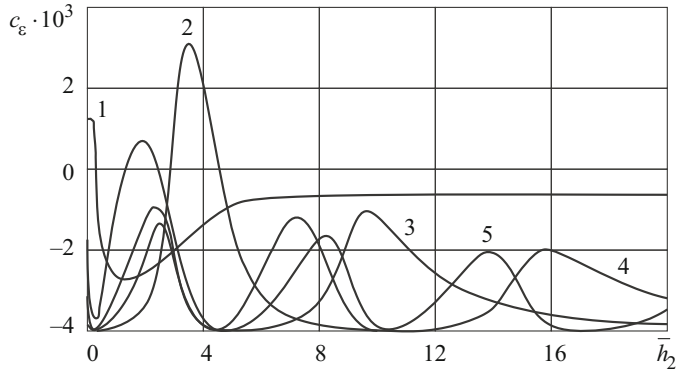

Fig. 2.12

It can be seen from Fig. 2.1 that with increase in the thickness $\bar{h}_2$ of the elastic layer, the velocity of the first mode tends to the Stoneley-wave velocity $\bar{c}_{\mathrm{St}}$ ($\bar{c}_{\mathrm{St}} = c_{\mathrm{St}} / c_{\mathrm{s}} = 0.769121$) from below and the velocity of the second mode tends to the Rayleigh-wave velocity $\bar{c}_{\mathrm{R}}$ ($\bar{c}_{\mathrm{R}} = c_{\mathrm{R}} / c_{\mathrm{s}} = 0.933558$) from above. Note that quasisurface mode 1 propagating along the interface in the hydroelastic system with $\bar{a}_0 = 1.152595 > \bar{c}_{\mathrm{R}} = 0.933558$ is localized near the surface of the elastic body [46] and quasi-Rayleigh mode 2 propagates along the free surface of the elastic layer. The phase velocities of all the high-order modes tend to the shear-wave velocity $\bar{c}_{\mathrm{s}}$ in the elastic body. With increase in the thickness, these modes are localized in the elastic layer [45]. The fluid increases the number of normal quasi-Lamb waves in the hydroelastic system. The low-order modes have zero cutoff frequencies.

Figures 2.2–2.5 indicate that there are thicknesses of the elastic layer for which the damping factor of each mode is maximum or minimum. With increase in the thickness of the elastic layer, the damping factors of the quasi-Lamp modes (except for the first one) decrease and the effect of the viscous fluid on them weakens.

It can be seen from Figs. 2.6–2.8 that the pretension ($\bar{\sigma}_{11}^0 = 0.004$) of the elastic layer increases the phase velocities of modes 1–7. At the critical frequencies, the velocities of modes 8–15 are lower than those in the elastic layer without prestresses. It can easily be seen that there are certain values of the thickness of the elastic layer at which the prestrains do not affect the phase velocities of all the modes beginning from the eighth. In the hydroelastic system with a thick liquid layer, there are three such thicknesses of the elastic layer for each of modes 8, 9, and 10 and five thicknesses for the next high-order modes.

It follows from Figs. 2.9–2.11 that there are certain thicknesses of the elastic layer at which the pretension ($\bar{\sigma}_{11}^0 = 0.004$) does not affect the damping factors of all the modes beginning from the second.

It follows from Figs. 2.12–2.14 that there are certain thicknesses of the elastic layer at which the effect of the viscosity of the fluid on the phase velocities of all the modes is the weakest. If the elastic layer is thick, there are thicknesses of the elastic layer at which the effect of the viscosity of the fluid on the phase velocities of a number of modes is substantial. With increase in the thickness of the elastic layer, the effect of the viscosity of the fluid on the phase velocities of all the modes beginning from the second weakens.

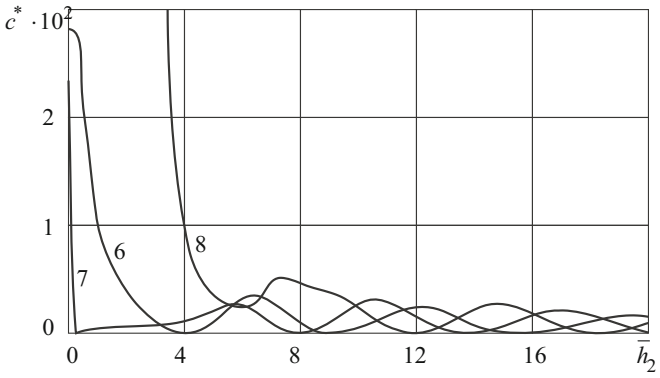

Fig. 2.13

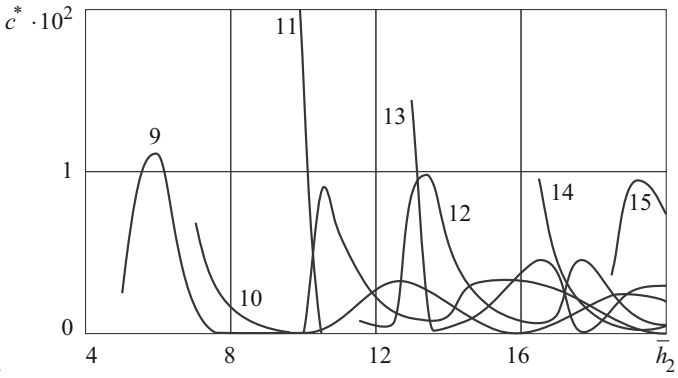

Fig. 2.14

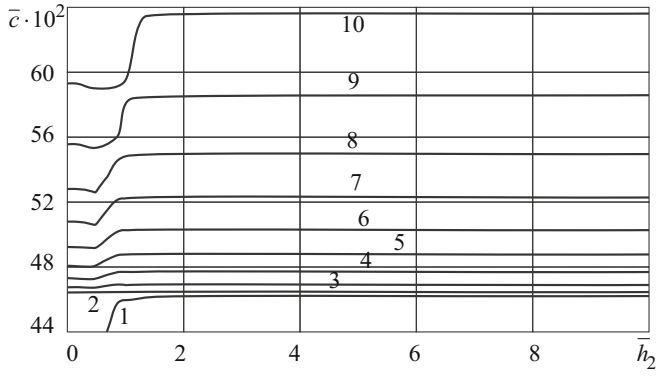

Fig. 2.15

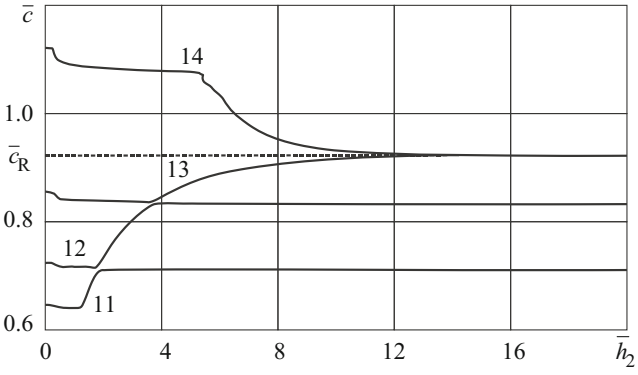

Fig. 2.16

Figures 2.15–2.17 show dispersion curves for the hydroelastic waveguide (the dimensionless phase velocities $\bar{c}$ of modes versus the dimensionless thickness $\bar{h}_2$ of the elastic layer without prestrains in contact with the thick viscous liquid layer of thickness $\bar{h}_1 = 20$ and $\bar{\mu}^* = 0.001$). Figure 2.15 represents the first ten modes and Figs. 2.16 and 2.17 represent modes 11 to 23.

Figures 2.18–2.22 show the dimensionless damping factors $\bar{\gamma}$ of modes versus the dimensionless thickness $\bar{h}_2$ of the elastic layer without prestrains in contact with the viscous liquid layer of thickness $\bar{h}_1 = 20$ and $\bar{\mu}^* = 0.001$.

The effect of pretension ($\bar{\sigma}_{11}^0 = 0.004$) on the velocities of normal waves in the hydroelastic system is demonstrated by Figs. 2.23–2.26, which show the relative changes in the phase velocities c_ε versus the thickness $\bar{h}_2$ of the elastic layer in contact with the liquid layer of thickness $\bar{h}_1 = 20$ and $\bar{\mu}^* = 0.001$.

Figure 2.23 represents modes 1, 7–10, Fig. 2.24 represents modes 2–6, and Figs. 2.25 and 2.26 modes 11–24.

The effect of pretension ($\bar{\sigma}_{11}^0 = 0.004$) on the damping factors of modes in the hydroelastic waveguide is demonstrated by Figs. 2.27–2.30, which show relative changes in the damping factors γ_ε versus the dimensionless thickness $\bar{h}_2$ of the elastic layer in contact with the compressible viscous liquid layer of thickness $\bar{h}_1 = 20$ and $\bar{\mu}^* = 0.001$.

Figure 2.15 shows that as the thickness $\bar{h}_2$ of the elastic layer increases, the velocity of the first mode tends to the Stoneley-wave velocity $\bar{c}_{St}$ ($\bar{c}_{St} = 0.461819$) from below, which is slightly lower than the velocity $\bar{a}_0$ ($\bar{a}_0 = 0.463021$) of acoustic waves in the fluid. The phase velocities of modes 2–10 tend to the velocities of waves that are higher than the acoustic-wave velocity $\bar{a}_0$ ($\bar{a}_0 = 0.463021$) in the fluid, but lower than the quasi-Rayleigh-wave velocity $\bar{c}_R$ ($\bar{c}_R = 0.923008$). The dispersion curves of these normal waves are characterized by zero cutoff frequencies. Moreover, they become almost dispersionless as their length decreases and frequency increasingly differs from the cutoff frequencies.

Figure 2.16 demonstrates that with increase in the thickness of the elastic layer, the velocity of mode 13 tends to the Rayleigh-wave velocity $\bar{c}_R$ ($\bar{c}_R = 0.923008$) from below, the phase velocity of mode 14 tends to the Rayleigh-wave velocity $\bar{c}_R$ from above, and the phase velocities of all the subsequent high-order modes tend to the shear-wave velocity $\bar{c}_s$ (Figs. 2.16 and 2.17).

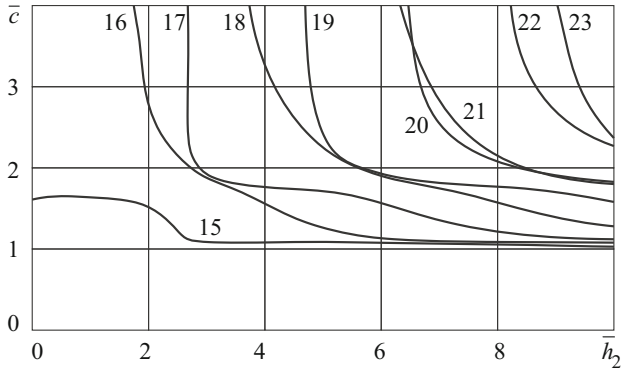

Fig. 2.17

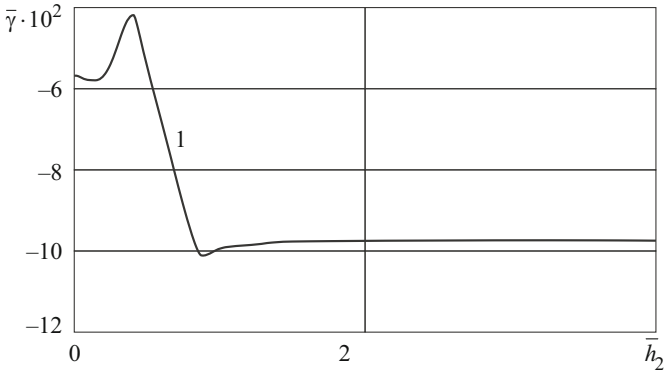

Fig. 2.18

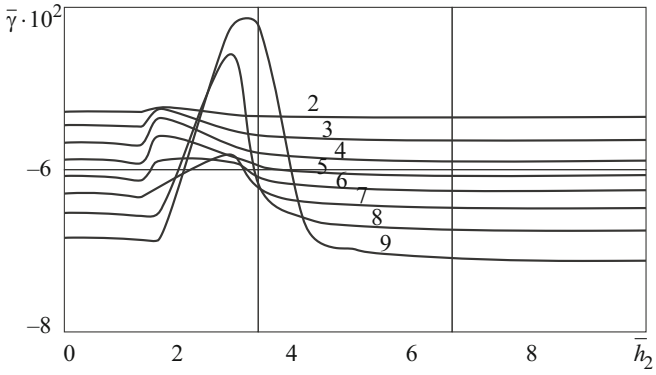

Fig. 2.19

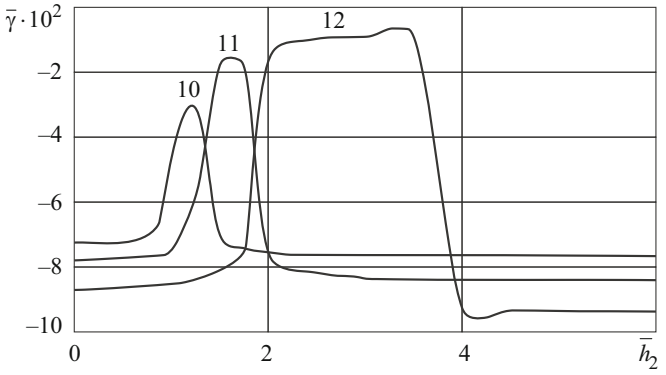

Fig. 2.20

Figures 2.18–2.22 indicate that there are thicknesses of the elastic layer for which the damping factor of each mode is maximum or minimum. With increase in the thickness of the elastic layer, the damping factors of the quasi-Lamp modes (beginning from the 13th) decrease and the effect of the viscous fluid on them weakens.

It can be seen from Figs. 2.23–2.26 that the pretension ($\bar{\sigma}_{11}^0 = 0.004$) of the elastic layer increases the phase velocities of modes 1–10. At the critical frequencies, the velocities of modes 11–24 are lower than those in the elastic layer without prestresses. It can easily be seen that there are certain values of the thickness of the elastic layer at which the prestrains do not affect the phase velocities of the second mode and all the modes beginning from the 11th. In the hydroelastic system with a thick liquid layer ($\bar{h}_1 = 20$), there is one such thicknesses for the second mode and for each of modes 11–24.

It follows from Figs. 2.27–2.30 that there are certain thicknesses of the elastic layer at which the pretension ($\bar{\sigma}_{11}^0 = 0.004$) does not affect the damping factors of all the modes.

2.2.4.1. Influence of the Viscosity of the Fluid on the Dispersion of Quasi-Lamb Waves in Hydroelastic Waveguides. In a hydroelastic waveguide, the fluid changes the critical frequencies, shifts the dispersion curves to the long-wave part of the spectrum, and changes their configuration for some modes and gives rise to new modes. As a result, the effect of the fluid on the phase velocities of modes at their critical frequencies becomes substantial.

The effect of the viscosity of the fluid is due to its interaction with the displacements occurring in the hydroelastic system during the propagation of waves. At those points of the modes where the shear displacements at the interface between the media are predominant, the effect of viscosity is the strongest and the damping factors and relative changes in the velocities are maximum. At points of waves with small surface shear displacements, the effect of viscosity is the weakest. As indicated above, with increase in the thickness, the phase velocities of high-order modes tend to the shear-wave velocity in the elastic body. With increase in the thickness [45], those transverse displacements dominate whose amplitude on the layer surfaces tends to zero compared with the amplitudes inside the layer, i.e., the displacements in high-order modes shift from the surface into the layer. As a result, the effect of the viscosity of the fluid on the phase velocities and damping factors of these modes weakens with increase in the thickness of the elastic layer in the short-wave part of the spectrum.

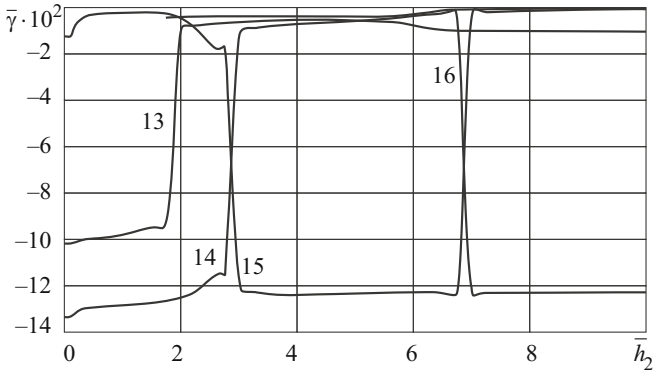

Fig. 2.21

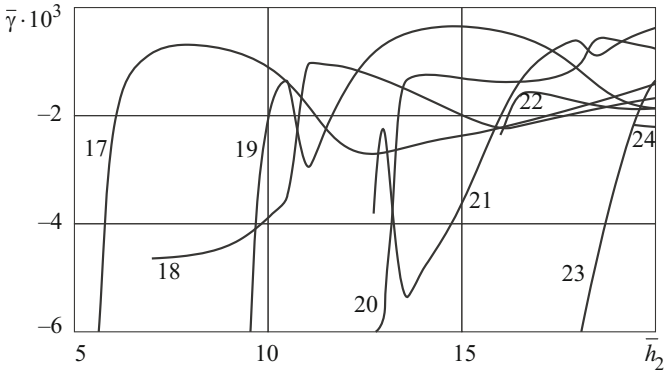

Fig. 2.22

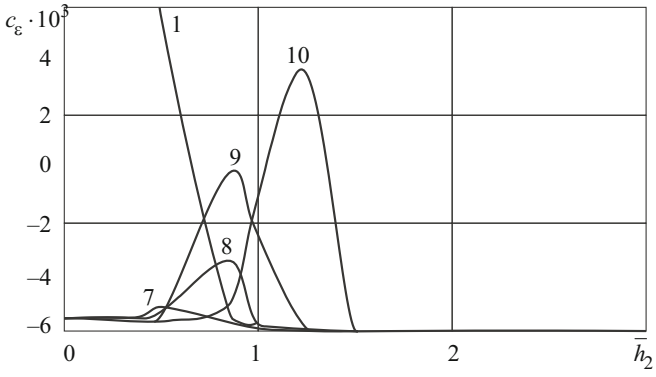

Fig. 2.23

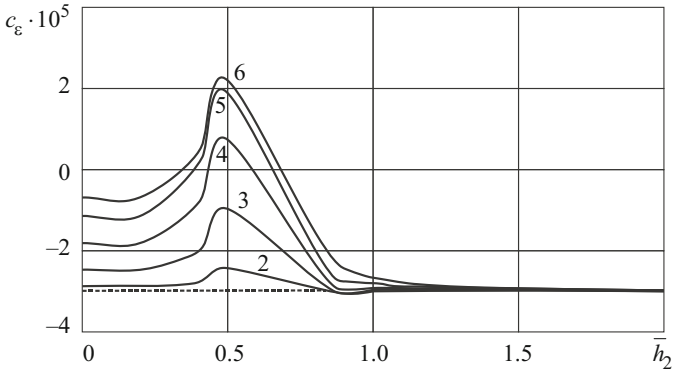

Fig. 2.24

2.2.4.2. Influence of the Prestresses on the Dispersion of Quasi-Lamb Waves in Hydroelastic Waveguides. As shown in [98], the pretension of an elastic waveguide without fluid changes the critical frequencies of the modes and shifts their dispersion curves. As a result, at the critical frequencies, the phase velocities of the modes in a prestrained layer can be either lower or higher than those in the absence of prestresses. This is also why there are frequencies (thicknesses) at which the prestresses do not affect the phase velocities of some normal Lamb waves.

The pretension in hydroelastic waveguides changes the critical frequencies and shifts the dispersion curves to the long-wave part of the spectrum. Because of this, there are certain thicknesses of the elastic layer at which the prestresses do not affect the phase velocities of some quasi-Lamb modes.

In the organic glass–water system, the pretension ($\bar{\sigma}_{11}^0 = 0.004$) shifts the dispersion curves of the modes to the long-wave part of the spectrum and changes their configuration. The scale of these changes depends on the mode number. The higher the order of modes, the stronger these changes. Because of this, there is one frequency of the elastic layer at which the phase velocity of each of the lower modes does not depend on the pretension. There are more such thicknesses for modes of higher order.

In the steel–water system, the pretension also shifts the dispersion curves to the long-wave part of the spectrum and changes their configuration. Unlike the organic glass–water system, the pretension ($\bar{\sigma}_{11}^0 = 0.004$) stretches the dispersion curves of the modes. Therefore, there is one thickness of the elastic layer at which the phase velocity of each of the modes beginning from the 16th does not depend on the pretension.

2.2.4.3. Localization Properties of the Lower-Order Modes in Hydroelastic Waveguides. Figure 2.1 demonstrates that as the thickness $\bar{h}_2$ of the elastic layer in the organic glass–water system increases, the velocity of mode 1 propagating along the interface between the media tends to the Stoneley-wave velocity $\bar{c}_{\mathrm{St}}$ ($\bar{c}_{\mathrm{St}} = 0.769121$) from below. Regarding the behavior of this mode in the short-wave part of the spectrum, the following is noteworthy. The phase velocity and profile of a Stoneley wave in the interface between solid and liquid half-spaces is known [46] to depend on the mechanical parameters of the hydroelastic

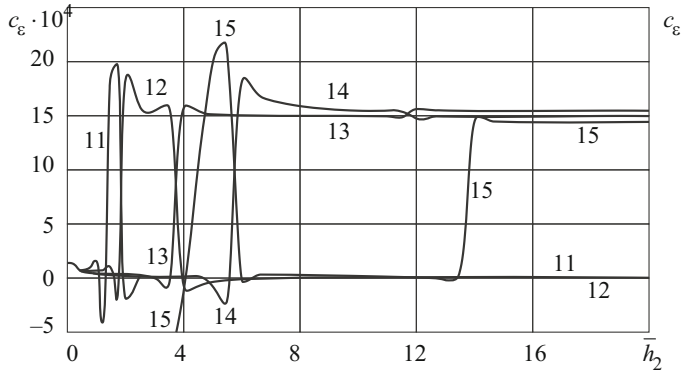

Fig. 2.25

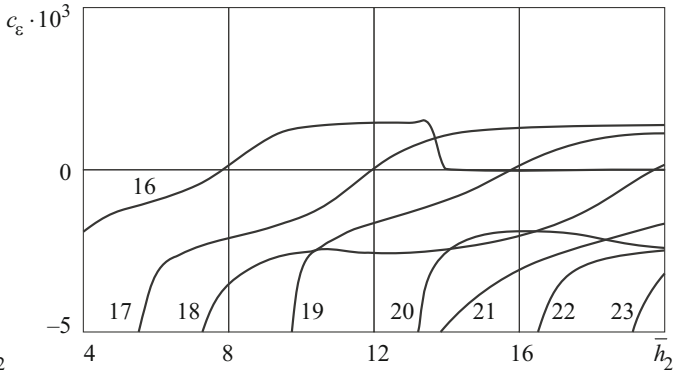

Fig. 2.26

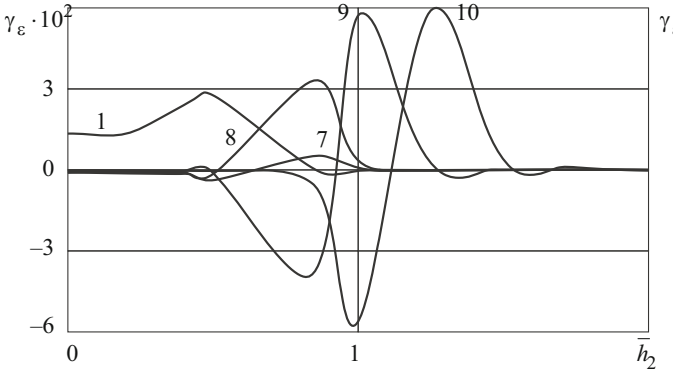

Fig. 2.27

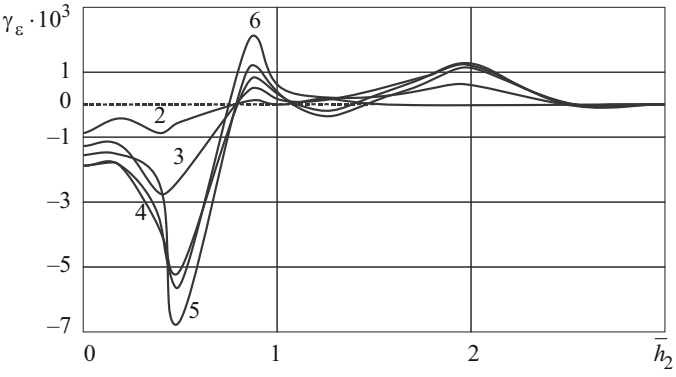

Fig. 2.28

system and are determined by the ratio between the acoustic-wave velocity in the fluid and the Rayleigh-wave velocity in the solid half-space. The mechanical parameters of the organic glass–water system are such that the speed of sound $\bar{a}_0$ in the fluid ($\bar{a}_0 = 1.152595$) is higher than the quasi-Rayleigh-wave velocity $\bar{c}_R$ ($\bar{c}_R = 0.933558$). According to [46], in the short-wave part of the spectrum, quasisurface mode 1 penetrates deeper into the elastic body than into the fluid. Therefore, mode 1 propagating along the interface of the media is mainly localized near the surface of the elastic layer. The velocity of mode 2 propagating in the elastic layer along its free boundary tends to the Rayleigh-wave velocity $\bar{c}_R$ ($\bar{c}_R = 0.933558$) from above. The velocities of all the high-order modes tend to the shear-wave velocity $\bar{c}_s$ in the elastic body. With increase in the thickness of the elastic layer, these modes tend to localize in it [45].

Thus, in this hydroelastic system, the low-order modes get into the solid body and, as well as the high-order modes, propagate in the elastic layer. This explains the influence of the prestresses on the phase velocities of all modes. The elastic layer makes the major contribution to the formation of the wave field and to the transfer of the wave energy.

Figures 2.15–2.17 demonstrate that as the thickness $\bar{h}_2$ of the elastic layer in the steel–water system increases, the velocity of mode 1 propagating along the interface between the media tends to the Stoneley-wave velocity $\bar{c}_{St}$ ($\bar{c}_{St} = 0.461819$) from below. The mechanical parameters of the steel–water system are such that the speed of sound $\bar{a}_0$ in the fluid ($\bar{a}_0 =$ 0.463021) is lower than the quasi-Rayleigh-wave velocity $\bar{c}_R$ ($\bar{c}_R = 0.923008$). According to [46], in the short-wave part of the spectrum, quasisurface mode 1 penetrates deeper into the fluid than into the elastic body. Therefore, mode 1 propagating along the interface of the media is mainly localized near the surface of the liquid layer. This also applies to modes 2–12 which propagate in the fluid. Since no low-order mode penetrates into the elastic body, the surface of the elastic layer adjoining the fluid remains free of them. This region is occupied by mode 13. The velocity of this mode propagating in the elastic layer along the interface tends to the Rayleigh-wave velocity $\bar{c}_R$ ($\bar{c}_R = 0.923008$) from below, as in an elastic layer that interacts with no fluid. The velocity of mode 14 propagating in the elastic layer along its free boundary tends to the Rayleigh-wave velocity $\bar{c}_R$ ($\bar{c}_R =$ 0.923008) from above. The velocities of all the high-order modes tend to the shear-wave velocity $\bar{c}_s$ in the elastic body, and, as mentioned above, these modes are localized in the elastic layer.

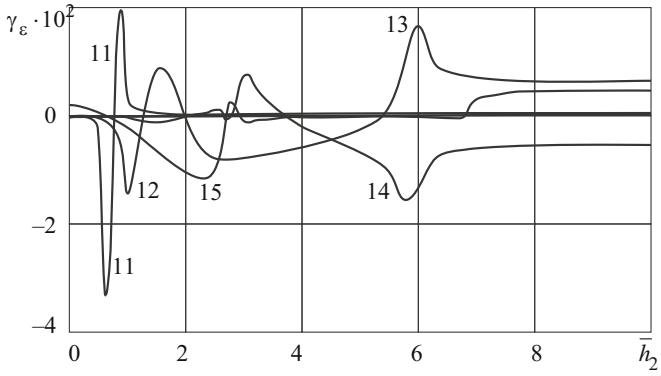

Fig. 2.29

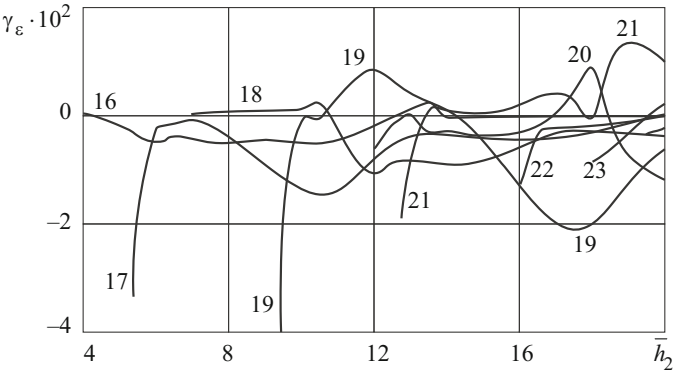

Fig. 2.30

Thus, in this hydroelastic system, not only the first mode, but also modes 2–12 resulting from the interaction between the elastic and liquid layers do not penetrate into the elastic body and propagate in the fluid near the interface. This explains the weak effect of the elastic layer and its prestresses on the phase velocities and dispersion of these modes. All the other high-order modes propagate in the elastic layer. In this case, both elastic and liquid layers transfer the energy of normal waves.

The liquid layer gives rise to new normal waves with zero cutoff frequencies. The fluid changes the critical frequencies and the configuration of the dispersion curves and shifts them to the long-wave part of the spectrum. The fluid affects the distribution of the modes between the media. The localization of the low-order modes in the liquid layer–elastic layer system depends on the mechanical parameters of the hydroelastic system. The basic criterion of distribution of the normal low-order waves between the media is the ratio between the acoustic velocity in the fluid and the velocity of the quasi-Rayleigh wave propagating in the elastic layer near its free surface.

2.3. Wave Processes in Hydroelastic Waveguides with Cylindrical Interfaces between Elastic and Compressible Viscous Liquid Media. The interest to such hydroelastic waveguides is due to their wide use. In this connection, it is necessary to theoretically study the effect of such factors as the geometry, curvature, and wall thickness of the hollow cylinder, prestresses, the presence of fluid and its properties, and the type of symmetry of motions on the parameters of wave processes. The three-dimensional linearized theory of aerohydroelasticity of prestressed bodies and compressible viscous fluid can be used for this purpose.

The linearized theory of aerohydroelasticity for prestressed bodies developed in [55–66, 69–79, 168–171] to solve spatial dynamic problems of the propagation of small perturbations in prestrained compressible and incompressible hollow cylinders containing a compressible viscous fluid at rest has been further developed in [5–8, 10, 26, 27, 29, 31, 32, 35, 62, 63, 66, 71, 72, 75, 82, 99, 155, 171].

For this problem with the dynamic and kinematic boundary conditions

$$\widetilde{Q}_r|_{r=R+h}=0, \quad \widetilde{Q}_\theta|_{r=R+h}=0, \quad \widetilde{Q}_z|_{r=R+h}=0,$$

$$\widetilde{Q}_r|_{r=R-h}=P_{rr}|_{r=R-h}, \quad \widetilde{Q}_\theta|_{r=R-h}=P_{r\theta}|_{r=R-h}, \quad \widetilde{Q}_z|_{r=R-h}=P_{rz}|_{r=R-h},$$

$$\left.\frac{\partial u_r}{\partial t}\right|_{r=R-h}=v_r|_{r=R-h}, \quad \left.\frac{\partial u_\theta}{\partial t}\right|_{r=R-h}=v_\theta|_{r=R-h}, \quad \left.\frac{\partial u_z}{\partial t}\right|_{r=R-h}=v_z|_{r=R-h}$$

the following dispersion equations were derived for compressible [8, 29, 71, 72, 75] and incompressible [26, 27, 71, 72, 75, 79] materials, respectively:

$$\det||T_{lm}(c,\gamma,a_{ij},\mu_{ij},s_{ii}^0,\rho_0,a_0,\mu^*,\omega,h)||=0 \qquad (l,m=\overline{1,9}),$$

$$\det||\widetilde{T}_{lm}(c,\gamma,a_{ij},\mu_{ij},\lambda_i,\rho_0,a_0,\mu^*,\omega,h)||=0 \qquad (l,m=\overline{1,9}).$$

These dispersion equations are the most general and can be reduced, by making additional assumptions, to equations for special cases of wave processes and simpler models of elastic bodies and fluids, some of which were earlier used by other researchers.

2.3.1. Special Cases.

2.3.1.1. Waves in an Isotropic Shell Filled with a Compressible Viscous Fluid (Kirchhoff–Love Model). A special case of the general problem is the propagation of normal waves in an isotropic cylindrical shell filled with a compressible viscous fluid. Such a problem was solved in [66, 71, 72, 75, 99] using the two-dimensional Kirchhoff–Love shell model. The following dispersion equation was derived:

$$\det||\alpha_{lm}||=0 \quad (l, m=\overline{1,3}), \tag{2.5}$$

where the elements of the determinant α_{ij} are expressed as

$$\alpha_{11}=\frac{h^2}{12}\left(k^2-\frac{n^2}{R^2}\right)^2+\frac{1}{R^2}-\frac{1-\nu^2}{Eh}\rho h\omega^2-\frac{i\omega(1-\nu^2)}{Eh}\beta_{1m}\gamma_{m1},$$

$$\alpha_{12}=\frac{n}{R^2}-\frac{i\omega(1-\nu^2)}{Eh}\beta_{1m}\gamma_{m2}, \qquad \alpha_{13}=\frac{ik\nu}{R}-\frac{i\omega(1-\nu^2)}{Eh}\beta_{1m}\gamma_{m3},$$

$$\alpha_{21}=-\frac{n}{R^2}+\frac{i\omega(1-\nu^2)}{Eh}\beta_{2m}\gamma_{m1}, \qquad \alpha_{22}=-\frac{k^2(1-\nu)}{2}-\frac{n^2}{R^2}+\frac{1-\nu^2}{Eh}\rho h\omega^2$$

$$+\frac{i\omega(1-\nu^2)}{Eh}\beta_{2m}\gamma_{m2}, \qquad \alpha_{23}=-\frac{(1+\nu)nik}{2R}+\frac{i\omega(1-\nu^2)}{Eh}\beta_{2m}\gamma_{m3},$$

$$\alpha_{31}=\frac{ik\nu}{R}+\frac{i\omega(1-\nu^2)}{Eh}\beta_{3m}\gamma_{m1}, \qquad \alpha_{32}=\frac{(1+\nu)nik}{2R}+\frac{i\omega(1-\nu^2)}{Eh}\beta_{3m}\gamma_{m2},$$

$$\alpha_{33}=-k^2-\frac{(1-\nu)n^2}{R^2}+\frac{(1-\nu^2)\rho h\omega^2}{Eh}+\frac{i\omega(1-\nu^2)}{Eh}\beta_{3m}\gamma_{m3} \qquad (m=\overline{1,3}),$$

where ν and E are Poisson's ratio and Young's modulus of the material the shell is made of; R and h are the radius of curvature of the midsurface and the thickness of the shell.

The dispersion equation (2.5) describes the propagation of nonaxisymmetric waves in a circular cylindrical shell filled with a compressible viscous fluid at rest. Special cases can be derived from this equation some of which have been examined earlier and some have not.

By passing to the limit in the dispersion equations, the following special cases were obtained and analyzed in [66, 71, 72, 75, 99]: incompressible viscous fluid, compressible ideal fluid, incompressible ideal fluid, torsional oscillations, axisymmetric waves.

It was shown that if the viscosity of the fluid is low ($\varepsilon=\sqrt{\nu^*/(\omega R^2)}<<1$), the phase velocity and damping factor of torsional waves can be expressed analytically up to ε: $c_1\approx\sqrt{\mu/\rho}(1-\varepsilon(\rho_0 R)/(2\sqrt{2}\rho h))$, $\gamma\approx\dfrac{\varepsilon\omega\rho_0 R}{2\sqrt{2}\rho h}\sqrt{\rho/\mu}$.

Note that in studying torsional waves in systems elastic bodies interacting with a viscous fluid, the results do not depend on whether the fluid is compressible or incompressible because torsional waves do not compress the viscous fluid and the parameters characterizing its compressibility do not appear in the equations.

The axisymmetric problem was addressed in [160] where only the long-wave approximation was discussed in detail.

2.3.1.2. Waves in an Orthotropic Shell Filled with a Compressible Viscous Fluid (Timoshenko Model). A special case of the general problem is the propagation of normal waves in an orthotropic cylindrical shell filled with a compressible viscous fluid. Such a problem was solved in [31, 35, 71, 72, 75, 82, 99, 153] using the two-dimensional Timoshenko shell model (with shear strains allowed for).

The following dispersion equation was derived:

$$\det||\tilde{\alpha}_{ij}||=0 \qquad (i,j=\overline{1,5}), \tag{2.6}$$

where the elements of the determinant $\tilde{\alpha}_{ij}$ are expressed as follows [99]:

$$\tilde{\alpha}_{11}=\frac{b_1\omega^2}{\varepsilon_1 c^2}+b_2+\frac{b_2 n^2}{\varepsilon_2}-b_1\omega^2-\frac{b_1 i\omega}{k_0}\beta_{1m}\gamma_{m1}, \qquad \tilde{\alpha}_{12}=b_2 n\left(1+\frac{1}{\varepsilon_2}\right)-\frac{b_1 i\omega}{k_0}\beta_{1m}\gamma_{m2},$$

$$\tilde{\alpha}_{13}=\frac{b_{12} i\omega}{c}-\frac{b_1 i\omega}{k_0}\beta_{1m}\gamma_{m3}, \qquad \tilde{\alpha}_{14}=-\frac{b_2 n}{\varepsilon_2}, \qquad \tilde{\alpha}_{15}=-\frac{ib_1\omega}{c\varepsilon_1},$$

$$\tilde{\alpha}_{21}=-b_2 n\left(1+\frac{1}{\varepsilon_2}\right)+\frac{b_1 i\omega}{k_0}\beta_{2m}\gamma_{m1}, \qquad \tilde{\alpha}_{22}=b_1\omega^2-\frac{b_2}{\varepsilon_2}-b_2 n^2-\frac{\omega^2}{c^2}+\frac{b_1 i\omega}{k_0}\beta_{2m}\gamma_{m2},$$

$$\tilde{\alpha}_{23}=-\frac{i\omega n}{c}(1+b_{12})+\frac{b_1 i\omega}{k_0}\beta_{2m}\gamma_{m3}, \qquad \tilde{\alpha}_{24}=\frac{b_2}{\varepsilon_2}, \qquad \tilde{\alpha}_{25}=\tilde{\alpha}_{34}=\tilde{\alpha}_{35}=\tilde{\alpha}_{42}=\tilde{\alpha}_{43}=\tilde{\alpha}_{53}=0,$$

$$\tilde{\alpha}_{31}=\frac{b_{12} i\omega}{c}+\frac{b_1 i\omega}{k_0}\beta_{3m}\gamma_{m1}, \qquad \tilde{\alpha}_{32}=\frac{i\omega n}{c}(1+b_{12})+\frac{b_1 i\omega}{k_0}\beta_{3m}\gamma_{m2},$$

$$\tilde{\alpha}_{33}=b_1\omega^2-n^2-\frac{b_1\omega^2}{c^2}+\frac{b_1 i\omega}{k_0}\beta_{3m}\gamma_{m3},$$

$$\tilde{\alpha}_{41}=-\frac{b_1 i\omega}{c\varepsilon_1}, \qquad \tilde{\alpha}_{44}=\frac{in\omega k_0^2}{12c}(1+b_{12}), \qquad \tilde{\alpha}_{45}=\frac{k_0^2}{12}\left(b_1\omega^2-n^2-\frac{b_1\omega^2}{c^2}\right)-\frac{b_1}{\varepsilon_1},$$

$$\tilde{\alpha}_{51}=\frac{b_2 n}{\varepsilon_2}, \qquad \tilde{\alpha}_{52}=\frac{b_2}{\varepsilon_2}, \qquad \tilde{\alpha}_{54}=\frac{k_0^2}{12}\left(b_1\omega^2-b_2 n^2-\frac{\omega^2}{c^2}\right)-\frac{b_2}{\varepsilon_2}, \qquad \tilde{\alpha}_{55}=-\frac{i\omega n k_0^2}{12c}(1+b_{12}),$$

where the summation is over m from 1 to 3; $b_n=E_n/G_{12}(1-\nu_{12}\nu_{21})$, $\varepsilon_n=E_n/k'G_{13}(1-\nu_{12}\nu_{21})$, $n=1,2$, $b_{12}=b_1\nu_{21}=b_2\nu_{12}$, $k_0=2h/a$; ν_{ij}, E_i, and G_{ij} are Poisson's ratios, Young's moduli, and shear moduli of the shell material; a and $2h$ is the mid-surface radius and the thickness of the shell; k' is the shear coefficient used in the Timoshenko theory of shells [99].

Note that this dispersion equation is the most general and can be reduced, by making additional assumptions, to equations for special cases of wave processes and simpler models of elastic bodies and fluids (incompressible viscous fluid, ideal fluid, empty shell, torsional modes, axisymmetric and nonaxisymmetric waves, isotropic shell, Kirchhoff–Love model). These special cases were obtained and examined in [71, 72, 75, 99] by passing to the limit, and the associated dispersion equations were derived.

The general dispersion equation (2.6) was solved numerically for isotropic and orthotropic boron-fiber-reinforced plastic shells filled with glycerin and water. The influence of the parameters and properties of shells (rotary inertia, shear strain, orthotropy, Poisson's ratio) and fluid (viscosity, compressibility, density) and the types of symmetry of motion (torsional, axisymmetric, nonaxisymmetric) on the dispersion, phase velocities, and damping factors of longitudinal waves was studied. Many numerical results were obtained and plotted in [35, 71, 72, 75, 82, 99, 153].

The results obtained with the former model, which neglects shear, are overestimated for the first mode, coincide for the second mode, and are absent for the third mode. This is consistent with the physics of the process because an increase in the shear modulus G_{13} is equivalent to an increase in the stiffness of the shell material, which leads to an increase in the velocities of the waves. The third mode can only be described with the Timoshenko theory of shells. For more adequate qualitative and quantitative study of wave processes in orthotropic and isotropic shells made of materials with low shear stiffness, it is necessary to use models that allow for transverse-shear strains and rotary inertia.

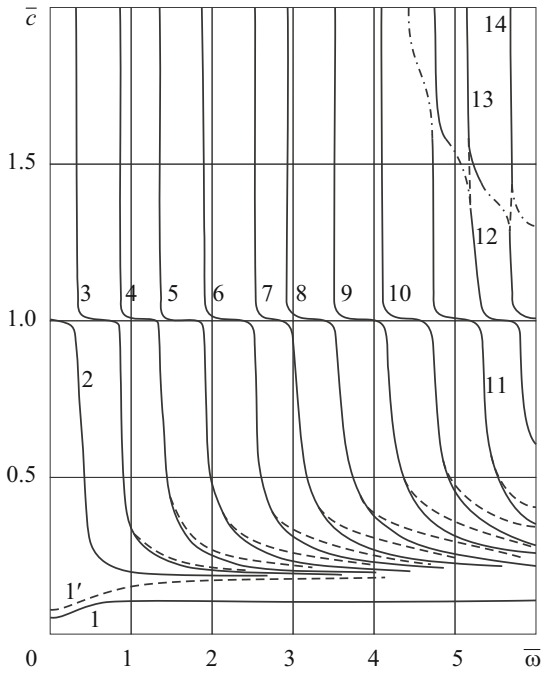

Fig. 2.31

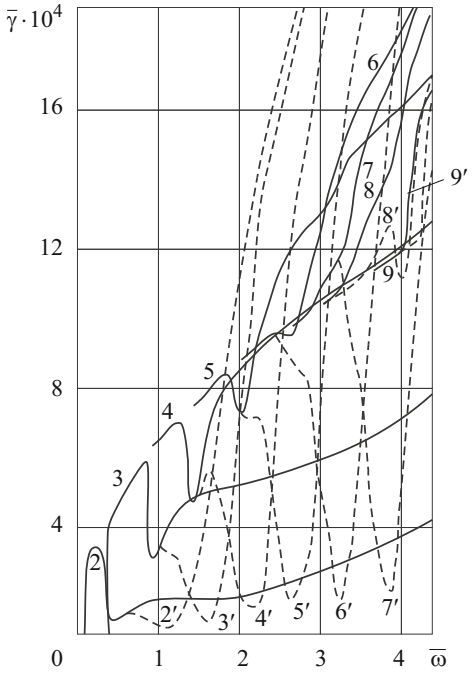

Fig. 2.32

Figures 2.31 and 2.32 show how the shear strain and rotary inertia influence the dispersion curves of the orthotropic shell–viscous fluid system. The former figure presents frequency–phase characteristics and the latter figure the frequency dependence of the damping factors. The dash-and-dot line in Fig. 2.31 represents the sections of the dispersion curves that in the absence of fluid merge into a third dispersion curve typical for empty shells. A numerical analysis of the effect of shear strain and rotary inertia on the characteristics of the hydroelastic waveguide shows that if these factors are neglected, the dash-and-dot sections of the dispersion curves will be absent in Fig. 2.31. The frequency–phase curves in this region will coincide with the solid lines (the junction sections being dashed). Moreover, if $G_{13} \to \infty$, then the phase velocities of the first mode and high-order modes are higher than those in the system with shear strains (the dashed lines in Fig. 2.31 correspond to $E_1 / G_{13} = 2.6$). For example, decreasing E_1 / G_{13} by 95% increases the phase velocities of the seventh and first modes at frequency $\bar{\omega} = 4$ by 20 and 45%, respectively. This result, apparently, confirms that it is desirable to use the equations of motion based on the Timoshenko hypothesis to study wave processes in shells made of a material with low shear stiffness and filled with a viscous fluid.

The fluid in the shell considerably affects the qualitative pattern of dispersion curves, no matter whether axisymmetric or nonaxisymmetric ($n \geq$ l) waves propagate in the shell–fluid system. Figure 2.33 shows graphs of $\bar{c} = f(\bar{\omega})$ for a shell with a fluid for $n = 2$ (the solid lines represent boron-fiber-reinforced plastic shell filled with glycerin). It can be seen that the viscous fluid greatly increases the number of modes, the first 14 modes being shown in this figure.

Figure 2.34 shows (solid lines) the damping factors $\bar{\gamma}$ versus frequency $\bar{\omega}$ for $n = 2$. For $n = 2$, unlike axisymmetric waves, the damping factors of the first mode alone monotonically increase with frequency. For all the other modes, there are a range of $\bar{\omega}$ in which $\bar{\gamma}$ monotonically increases or a range in which $\bar{\gamma}$ monotonically decreases.

Figures 2.33 and 2.34 show how Poisson's ratio influences the behavior of the frequency–phase curves. The dashed lines correspond to $\nu_{12} = 0.28$ and $\nu_{21} = 0.1$.

In the publications cited above, the effect of some other parameters of shells and fluid and the types of symmetry of motion on the wave processes in hydroelastic systems was numerically analyzed as well, and the results were presented in the form of graphs.

2.3.1.3. Waves in Prestrained Elastic Cylinders with a Compressible Ideal Fluid (Three-Dimensional Linearized Theory). Another special case is a wave process in prestressed compressible and incompressible hollow cylinders filled with an ideal fluid. Such a problem was solved in [5–7, 10, 26, 29, 31, 71, 72, 75, 99, 155] using the three-dimensional linearized theory.

Dispersion equations were derived for compressible and incompressible hollow elastic cylinders subjected to large (finite) prestrains and filled with a compressible ideal fluid.

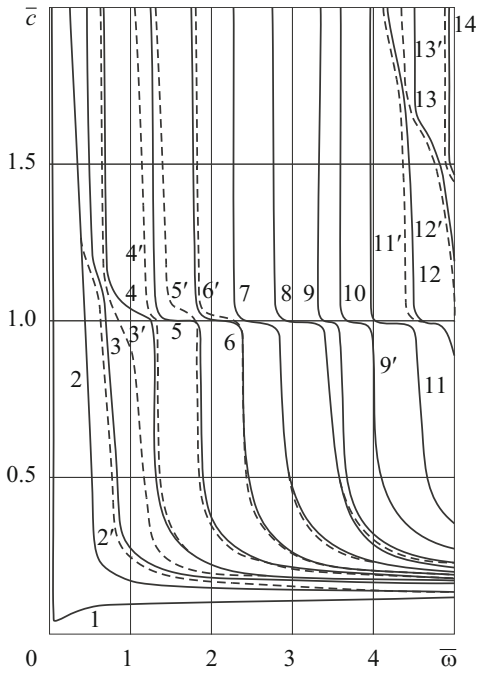

Fig. 2.33

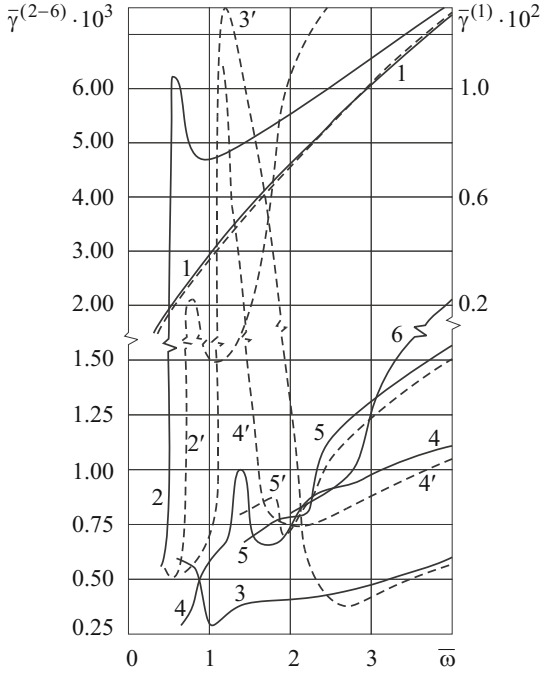

Fig. 2.34

2.3.1.3.1. Compressible Elastic Bodies and Compressible Ideal Fluid. A wave process in prestressed compressible hollow cylinders filled with a compressible ideal fluid was considered in [6, 7, 10, 29, 31, 71, 72, 75, 99, 155]. Wave propagation in either thin-walled ($\bar{h} = h / R = 0.05$) or thick-walled ($\bar{h} = 0.75$) hollow cylinders either containing or not a compressible ideal fluid was studied. The cylinders were considered to be made of compressible elastic materials, such as steel, described by the three-invariant Murnaghan potential function. It was shown that the fluid has a strong effect on the dispersion pattern, especially in thin-walled hollow cylinders. Figures 2.35 and 2.36 show the dimensionless phase velocities $\bar{c}$ ($\bar{c} = c / c_s$, $c_s^2 = \mu / \rho$ is the shear-wave velocity in the body without prestresses) versus the dimensionless frequency $\bar{\omega}$ ($\bar{\omega} = \omega R / c_s$) for thin-walled cylinders of thickness $\bar{h} = 0.05$, Fig. 2.35 representing a hollow cylinder without fluid. Comparing Figs. 2.35 and 2.36 shows that the fluid substantially increases the number of modes propagating in the hydroelastic system.

Unlike the fluid, the prestresses affect the phase velocities of the modes mainly at their critical frequency in both thin-walled and thick-walled cylinders.

Figures 2.37 and 2.38 show the relative velocities c_ε of various modes versus the frequency $\bar{\omega}$ in precompressed ($\bar{\sigma}_{33}^0 =$ –0.004) thick-walled hollow cylinders of thickness $\bar{h} = 0.75$ filled with a fluid. It can be seen that, as in cylinders without fluid, there are certain modes whose phase velocities do not depend on the prestresses.

The effect of the prestrains and fluid on the phenomenon of backward wave in a hollow compressible cylinder filled with an ideal fluid at rest was studied in [7, 31, 71, 72, 75, 79].

A backward wave in an elastic body is known [31, 54, 71, 72, 75, 148] to be a wave whose group and phase velocities are of opposite signs, like some modes existing in electromagnetic waveguides.

Note that Lamb was the first to predict such waves in some one-dimensional media [182]. Later, in studying waves in lattices, Mandel'shtam [146] noticed frequency ranges in which modes have negative group velocity. This phenomenon in elastic layers [198], plates and solid cylinders [186] was studied in detail. The propagation of normal waves with abnormal dispersion in a cylinder with a fluid was discussed in [7, 31, 72, 75, 140].

In [54, 146, 182, 186, 198], this phenomenon was studied using the classical theory of elasticity and disregarding the prestresses. However, quantitative data are necessary to continue the dispersion curves after the intersection of branches of various families in studying frequency spectra and unsteady wave processes in various waveguides subject to prestrains.

The phenomenon of backward waves in hydroelastic waveguides was studied in [7, 31, 72, 75] taking into account the presence of a fluid and prestresses.

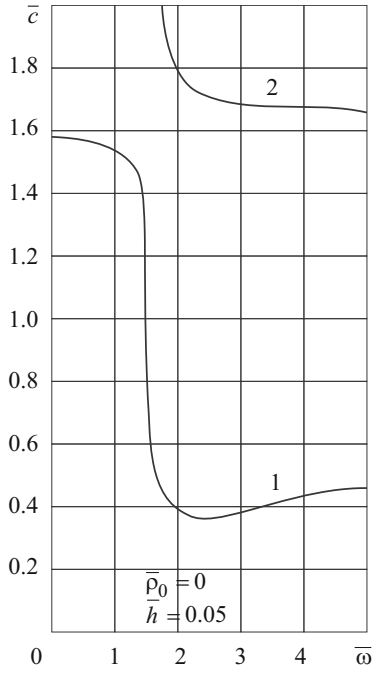

Fig. 2.35

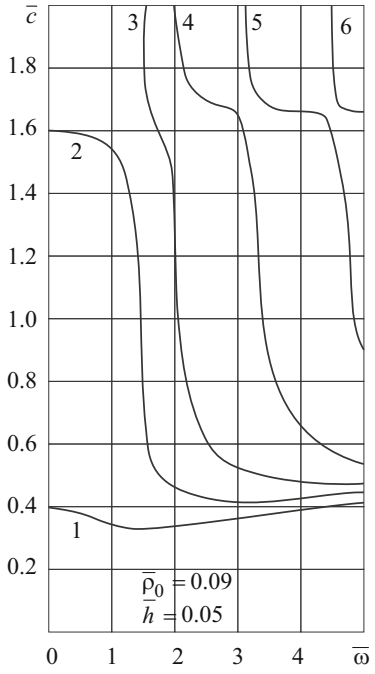

Fig. 2.36

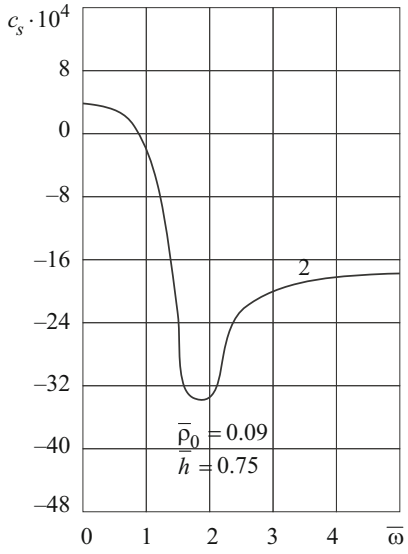

Fig. 2.37

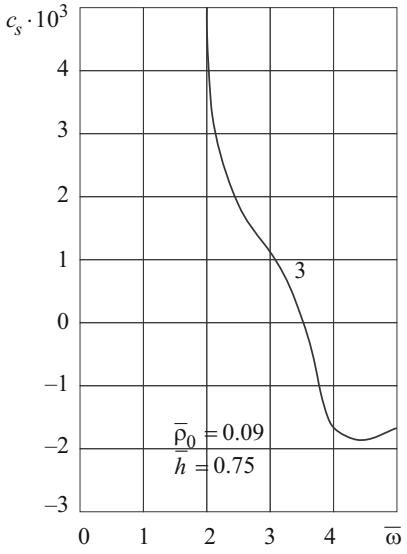

Fig. 2.38

A numerical solution of a transcendental dispersion equation is presented in Figs. 2.39 and 2.40, which show $\bar{\omega} = f(\bar{k})$ for a thick-walled hollow cylinder with dimensionless wall thickness $\bar{h} = 0.75$ filled with a compressible ideal fluid.

From the graphs presented in the cited publications and in Figs. 2.39 and 2.40, it follows that the phenomenon of backward wave (section *BA* of curve *3* in Fig. 2.39) is three-dimensional and exists only in thick-walled hollow cylinders either containing a fluid or not. It was established that in thin-walled hollow cylinders filled with a fluid, waves propagate without abnormal dispersion and the backward-wave phenomenon does not occur. It was shown (Fig. 2.40) that axial compression ($\bar{\sigma}_{33}^0 = -0.004$) and fluid increase the phase velocity of the backward wave in a compressible elastic hollow cylinder made of 09G2S low-alloyed steel described by the three-invariant Murnaghan potential function.

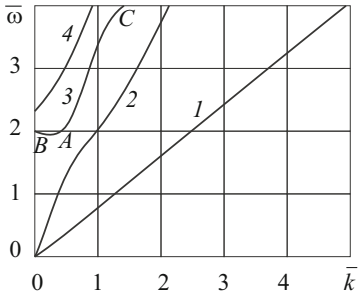

Fig. 2.39

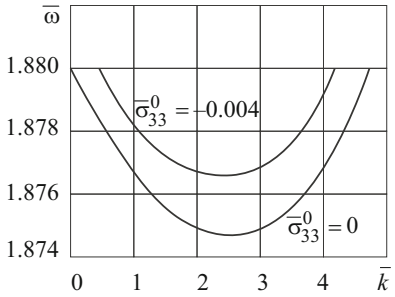

Fig. 2.40

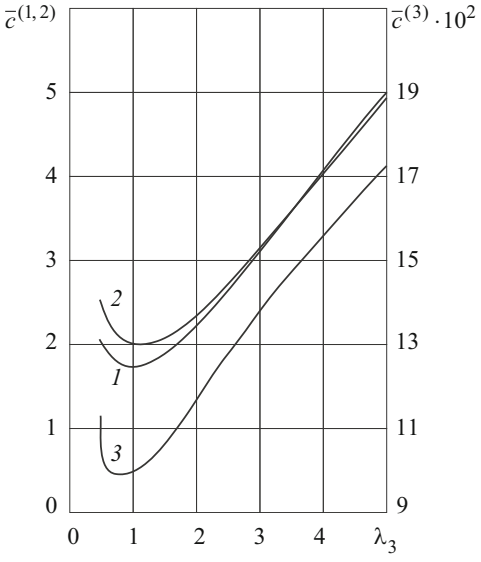

Fig. 2.41

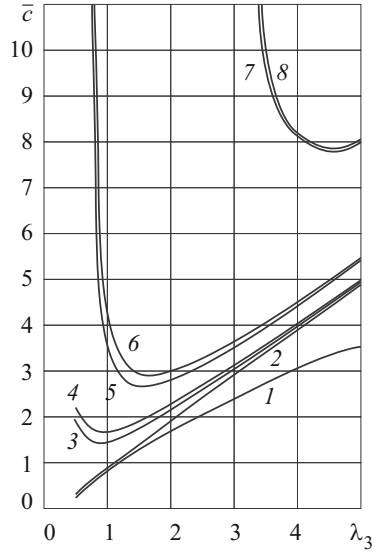

Fig. 2.42

2.3.1.3.2. Incompressible Elastic Bodies and Compressible Ideal Fluid. The influence of large (finite) prestrains on the phase velocities of axisymmetric longitudinal waves propagating in highly elastic rubber-like incompressible hollow cylinders filled with a compressible ideal fluid at rest was analyzed in [5, 26, 27, 31, 71, 72].

Figure 2.41 shows $\bar{c} = f(\lambda_3)$ for $\bar{h} = h/R = 0.002$ and $\bar{\omega} = \omega R / c_s = 0.01$. Curve *1* (first mode) represents a hollow cylinder without fluid, and curves *2* (second mode) and *3* (first mode) show how the prestrains influence the phase velocities of waves in the shell–fluid system. These curves represent low-frequency waves propagating in a thin-walled shell containing a fluid. Figure 2.42 corresponds to $\bar{\omega} = 18$ and $\bar{h} = 0.1$. Such behavior of the low-order modes (curves *1* and *2* in Fig. 2.42) is due to the increase in the compliance of the cylinder in compression ($\lambda_3 < 1$) and the decrease in its compliance in tension ($\lambda_3 > 1$). The phase velocities of the third, fourth, and all the higher modes so behave because an increase in λ_3 leads to a decrease in the cutoff frequencies and to some decrease in the velocities of axisymmetric longitudinal waves. Further increase in the velocities is due to the decrease in the compliance of the cylinder walls under tension.

From the curves presented in the cited publications and in Figs. 2.41 and 2.42, it follows that the prestrains have a strong effect on the critical frequencies of modes and on the phase velocities of waves at these frequencies.

2.3.1.4. Waves in Prestrained Elastic Media with Cylindrical Cavities with a Compressible Viscous Fluid (Three-Dimensional Linearized Theory). Special cases are also wave processes in prestrained compressible and incompressible unbounded bodies with cylindrical cavities filled with a viscous compressible fluid at rest.

Biot was the first to address this problem in a simpler statement (within the framework of the classical theory of elasticity and the hydrodynamics of ideal fluid) [159].

A three-dimensional problem was solved in [31, 72, 75] using the three-dimensional linearized theory and allowing for the prestresses in the elastic body and the viscosity and compressibility of the fluid. The following dispersion equations for compressible and incompressible materials were obtained:

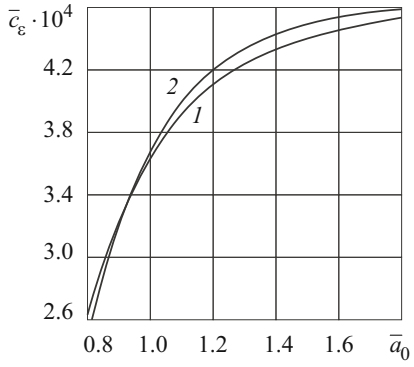

Fig. 2.43

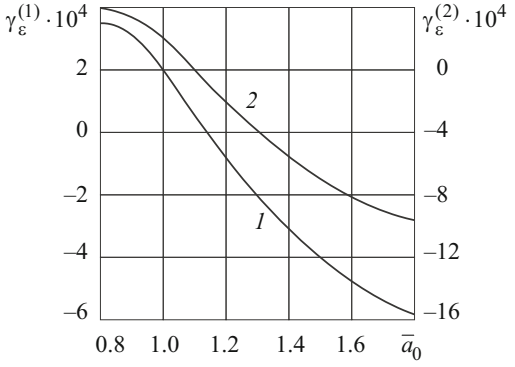

Fig. 2.44

$$\det||H_{lm}(c, \gamma, a_{ij}, \mu_{ij}, s_{ii}^0, \rho_0, a_0, \mu^*, \omega, R)|| = 0 \quad (l, m = \overline{1,6}), \tag{2.7}$$

$$\det||\tilde{H}_{lm}(c, \gamma, a_{ij}, \mu_{ij}, \lambda_i, \rho_0, a_0, \mu^*, \omega, R)|| = 0 \quad (l, m = \overline{1,6}). \tag{2.8}$$

These dispersion equations are the most general and can be reduced to characteristic equations for special cases of wave processes and simpler models of elastic bodies and fluids, some of which were earlier used by other researchers. The dispersion equations (2.7) and (2.8) were solved numerically for high-frequency waves.

Figures 2.43 and 2.44 show the effect of prestresses for fluids characterized by different compressibility and a compressible elastic body described by the three-invariant Murnaghan potential function and prestretched along the axis *oz* of the cylindrical cavity ($\bar{\sigma}_{33}^0 = \sigma_{33}^0 / \mu = 0.004$).

Figure 2.43 shows the relative change in the phase velocities c_ε versus the dimensionless speed of sound $\bar{a}_0$ in the fluid. Curve *1* corresponds to the organic glass–water system, and curve *2* to the organic glass–glycerin system.

Figure 2.44 shows the relative change in the damping factors γ_ε [$\gamma_\varepsilon = (\gamma_\sigma - \gamma)/\gamma$] versus the dimensionless speed of sound $\bar{a}_0$ in the fluid. The left ordinate axis corresponds to the organic glass–water system (curve *1*), and the right axis to the organic glass–glycerin system (curve *2*). It can be seen that the less compressible the fluid, the stronger the effect of the prestresses. This is physically consistent. For glycerin, this effect is stronger than for water. Moreover, the fact that the curves cross the abscissa axis (Fig. 2.44) indicates that in such hydroelastic waveguides, there are certain levels of the compressibility of the fluid at which the damping factors of waves do not depend on the prestresses.

The calculated results demonstrate how the compressibility and viscosity of the fluid influence the phase velocities and damping factors of high-frequency waves: the less compressible the fluid, the higher the phase velocity and the lower the damping factors of high-frequency waves.

The dispersion equation (2.8) was solved numerically for a highly elastic rubber-like body described by the Treloar potential function with $E = 2.5 \cdot 10^6$ Pa, $\rho = 1200\,\text{kg/m}^3$ and a fluid with $\rho_0 = 1000\,\text{kg/m}^3$, $a_0 = 1459.5$ m/sec, $\bar{\mu}^* = 0.00002$. The calculated results are presented in Figs. 2.45 and 2.46. Figure 2.45 shows how the precompression influences the phase velocity $\bar{c}$ of a high-frequency wave. For comparison, this figure represents a high-frequency quasi-Rayleigh wave $\bar{c}_R$ for a cavity without fluid.

The effect of large (finite) prestrains on the damping factors of high-frequency waves was analyzed as well. It follows from Fig. 2.46 that the damping factor abruptly increases as compression tends to the level of surface instability.

Figure 2.45 shows that if the prestress is compressive and $\lambda_3 = 0.44$, the phase velocities of high-frequency waves in both purely elastic and hydroelastic waveguides tend to zero. This suggests that in highly elastic incompressible neo-hookean bodies either interacting with a fluid or not and being in three-dimensional initial stress–strain state, surface instability occurs under axial compression and $\lambda_3 = 0.44$. Moreover, comparing the plane and spatial cases shows that surface instability in spatial waveguides occurs at lower initial uniaxial compressive strains ($\lambda_3 \approx 0.44$) than in flat bodies ($\lambda_1 \approx 0.54$). Note that λ_1 and λ_3 coincide with those earlier obtained in the theory of three-dimensional stability and correspond to the critical shortening [55, 56, 61, 69, 70]. Thus, the three-dimensional linearized theory of waves allows, in both plane and spatial cases, determining the

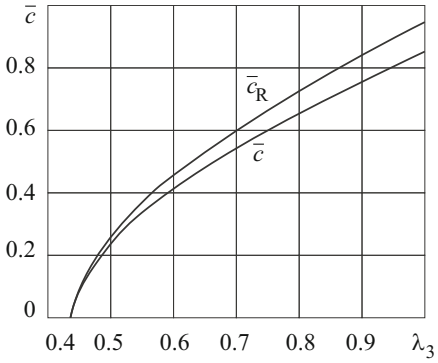

Fig. 2.45

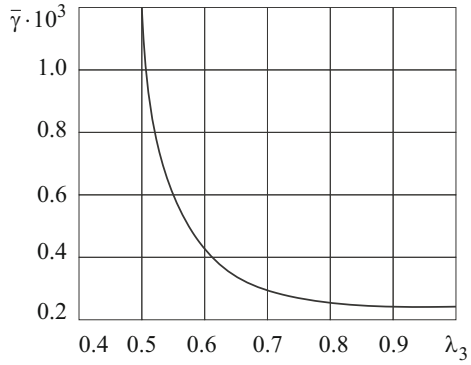

Fig. 2.46

critical compression parameters at which surface instability occurs in highly elastic incompressible elastic bodies and hydroelastic systems.

2.3.1.5. Waves in a Prestressed Solid Cylinder in a Compressible Viscous Fluid (Three-Dimensional Linearized Theory). An external wave problem was solved in [62, 63, 66, 72, 75] using general solutions of aerohydroelastic problems for prestressed bodies and the three-dimensional linearized theory.

2.3.1.5.1. Torsional Waves in a Circular Cylinder in a Compressible Viscous Fluid (Three-Dimensional Linearized Theory). The propagation of torsional modes in a solid circular cylinder in a compressible viscous fluid at rest was analyzed in [62, 63, 66, 72, 75].

Defining solutions in the class of traveling waves $\chi_1 = AZ_0(\eta_1 r)\exp[i(kz_3 - \omega t)]$, $\varphi = BJ_0(\xi_1 r)\exp[i(kz_3 - \omega t)]$, where J_0 is the zero-order Bessel function of the first kind; $H_0^{(1,2)}$ are the Hankel functions, $Z_0(\eta_1 r) \equiv H_0^{(1)}(\eta_1 r)$ for $\mathrm{Im}\,\eta_1 > 0$ and $Z_0(\eta_1 r) \equiv H_0^{(2)}(\eta_1 r)$ for $\mathrm{Im}\,\eta_1 < 0$, and performing some transformations, we obtain the dispersion equation

$$\alpha_1\beta_1[i\omega\mu^*\beta_1 Z_2(\beta_1)J_1(\alpha_1) + \lambda_3^{-1}\lambda_1^2\mu_{12}\alpha_1 J_2(\alpha_1)Z_1(\beta_1)] = 0, \tag{2.9}$$

where $\alpha_1 = \xi_1 R, \beta_1 = \eta_1 R$.

Special cases following from the general problem statement were considered in [62, 63, 72, 75]. The following special cases were detailed.

Cylinder in Vacuum. The dispersion equation for $\varepsilon << 1$ has the form

$$\lambda_3^{-1}\lambda_1^2\mu_{12}\alpha_1^* J_2(\alpha_1^*) = 0. \tag{2.10}$$

Denoting by α_m the mth root of the equation $J_2(\alpha_m) = 0$ and performing some transformations, we obtain the following analytic expression for the phase velocity of the mth torsional mode in a cylinder in vacuum: $c_m = c_s\omega R(R^2\omega^2 - \alpha_m^2\lambda_1^4\rho^{-1}\mu_{12})^{-1/2}$.

Cylinder in Fluid (Approximate Solution). Expanding the Bessel functions of the first kind into the series

$$J_n(\alpha_1^*) = (\alpha_1^*/2)^n \sum_{k=0}^{\infty} \frac{(-1)^k}{k!(n+k)!}(\alpha_1^*/2)^{2k},$$

we obtain the following analytic expressions for the phase velocity and damping factor:

$$c_1 \approx c_s(1 - (\rho_0/\rho)\sqrt{2}\varepsilon\lambda_3\lambda_1^2), \qquad \gamma_1 \approx \sqrt{2}\varepsilon\lambda_3\lambda_1^2 \frac{\omega\rho_0}{c_s\rho}. \tag{2.11}$$

Cylinder in Fluid (More Rigorous Solution). Solution (2.11) was obtained by expanding the Bessel functions appearing in (2.9) into series and retaining the first terms only. Only one value of velocity was obtained, though Eq. (2.9) allows

determining the velocities of all modes, which can be seen from the example of a wave process in a cylinder in vacuum (2.10). The following analytic expressions for the phase velocity and damping factor of the *m*th mode were derived in [63, 72, 75]:

$$c_m \approx c_s D\left(1-\frac{\varepsilon\rho_0\lambda_3\lambda_1^2}{\sqrt{2}\rho}\frac{J_1(\alpha_m)}{J_2(\alpha_m)}D\right), \qquad \gamma_m \approx \frac{\varepsilon\omega\rho_0\lambda_3\lambda_1^2}{\sqrt{2}c_s}\frac{J_1{}^*(\alpha_m)}{J_2(\alpha_m)}.$$

2.3.1.5.2. Longitudinal Waves in a Prestressed Solid Cylinder in an Ideal Fluid. The propagation of axisymmetric longitudinal modes in a prestressed incompressible solid cylinder in a compressible ideal fluid was studied in [32, 75]. For a cylinder loaded along the *oz*-axis, the following dispersion equation was derived:

$$\det||\varsigma_{ij}||=0 \qquad (i,j=\overline{1,3}). \tag{2.12}$$

Equation (2.12) was solved numerically for a highly elastic rubber-like incompressible material described by the Treloar potential function. The dimensionless phase velocity $\bar{c}$ was plotted against the dimensionless frequency $\bar{\omega}$ for precompressed ($\lambda_3 = 0.8$) and prestretched ($\lambda_3 = 1.5$) cylinders. The effect of large (finite) prerstrains on the phase velocities of waves of various length was studied as well. It was shown that the phase velocities of waves frequency close to the critical frequency increase in either compressed ($\lambda_3 < 1$) or stretched ($\lambda_3 > 1$) highly elastic cylinder. The phase velocities of modes whose frequencies differ considerably from the critical frequency depend differently on the prestrain: their velocities decrease in compression ($\lambda_3 < 1$) and increase in tension ($\lambda_3 > 1$). It was shown that the fluid decreases the phase velocities of the modes.

Studies of the propagation of various waves in prestrained elastic bodies without fluid performed using the linearized theory are reviewed in [3, 59, 71, 72, 79].

Numerous results in other research areas covering a wide range of theoretical and experimental studies of the influence of prestresses on the behavior of elastic bodies were analyzed and systemized in [3, 59, 168, 170, 173].

We have discussed only results on wave processes in hydroelastic systems. Those results are preferred that were obtained using the three-dimensional linearized theory and taking into account the prestresses in elastic bodies and the viscosity and compressibility of the fluid.

3. Acoustic Radiation Pressure on Solid Particles and Fluid Parcels. The study of the motion and interaction of solid particles and liquid drops during the propagation of an acoustic wave is of theoretical and applied importance. Three cases were examined: (i) a single particle in a fluid under acoustic pressure, (ii) interaction of two particles in a fluid in which a wave propagates, (iii) motion of a great number of particles in an oscillating medium. In case (iii), multiphase approaches were used [47]. Relevant studies, methods, and results are reviewed in [2, 40, 47, 147, 152, etc.].

Of certain technological interest is the study of the motion of solid particles and liquid drops under time-independent radiation pressure [147, 152], which is also called acoustic radiation pressure. It is more difficult to determine the acoustic radiation pressure if the obstacle is finite in size. Since the acoustic radiation pressure is determined by the acoustic field resulting from the interference of the incident and diffracted waves, it depends on the shape of the obstacle. To determine the wave reflected by the obstacle, it is necessary to solve the problem of the diffraction of an incident wave by an obstacle. To this end, it is necessary to take into account the displacements of an oscillating particle, its shape and size compared with the wavelength, the properties of the medium and the boundary of the space in which the wave propagates, and other factors. In this connection, the following simplified assumptions were made to solve the problem: the fluid is not heat-conductive, the particle is small compared with the wavelength and amplitude, the fluid is incompressible, etc.

These assumptions allow using various approaches to the study of the scattering of an incident acoustic wave by a particle and the calculation of the hydrodynamic force acting on it [139]. The constant component of the hydrodynamic force (radiation pressure) is calculated by averaging it over the wave period.

The results of one of the early studies on radiation force acting on a spherical particle in an ideal fluid were published in [180] where formulas were derived for the radiation forces acting on a sphere in the field of standing and traveling plane acoustic waves. It was established that the radiation force in the field of a standing acoustic wave has spatial periodicity with period equal to half-wavelength and greater than that in the field of a traveling wave. The expression for radiation force was used to deduce the equation for the drift of a small sphere in the field of a standing wave. Solving this equation made it possible to analyze the behavior of a particle.

To calculate the acoustic pressure up to second-order terms, the Bernoulli integral is used [1, 200]. The radiation force is represented by the integral of the period-average sound pressure over the surface of a spherical particle.

In [144, 199], it was proposed to determine the radiation force as time-average momentum flux through the closed surface of a particle. Selecting a surface surrounding a spherical particle and located at an arbitrarily long distance from its center (the fluid being assumed ideal) made it possible to avoid solving the scattering problem by using asymptotic expressions for the scattered wave. A similar approach to the calculation of the radiation force on a spherical particle in an ideal fluid was used in [136, 154, 195, etc.]. A more general problem statement (the particle is compressible and the acoustic field is arbitrary) was considered in [50, 184]. The potential of the wave scattered by a sphere was expanded into a multipole series with coefficients determined by solving the problem of a potential flow of an incompressible fluid past a sphere.

The method of determining the radiation force as time-average impulse was generalized to a viscous fluid in [104, 199, 165]. Radiation force is equal to the integral of the period-average momentum flux density tensor taken over an arbitrary surface around a particle. The average force was calculated in quadratic approximation for a fixed spherical solid particle small compared with the wavelength. It was established that the viscosity of the fluid substantially increases the radiation pressure force on a particle.

In [102], in calculating the radiation force acting on a fixed spherical particle, allowance was made for the acoustic flow developing around a particle in acoustic fields of high intensity and affecting the magnitude of the radiation force. In this connection, it was proposed to distinguish the concepts of time-average force and radiation force. Time-average force was determined by finding the total momentum flux through a quite distant closed surface around a spherical particle. The quadratic approximation was used and the radius of the particle was considered small compared with the wavelength.

We are aware of only one publication [141] that uses radiation forces to study the interaction of two particles that are closely spaced and smaller than the wavelength in an ideal fluid. To determine the perturbation of fluid pressure, the Bernoulli integral is used. It was assumed that the wave is scattered only once, and the wave field near the particle was represented as a superposition of the primary wave scattered by only one of the particles and a wave scattered by the other particle. The problem was reduced to finding this latter wave. The potential of the scattered wave field was expanded into a series of spherical wave functions in which the first three terms are retained. The constant coefficients in the series were determined from the boundary conditions on the spherical surfaces. The potentials on the spherical surfaces were expanded into Taylor series about their sphere centers.

The great number of publications on the subject [44, 103, 138, 156–158, 167, 178, 185–190, 196, etc.] are indicative of continued interest in it. Our goal is to review studies on radiation forces performed at the S. P. Timoshenko Institute of Mechanics using the piecewise-homogeneous material model, exactly satisfying all boundary conditions, incorporating inertial terms into the equations of motion of the medium, and assuming that the fluid is compressible and that the distances between and the dimensions of objects in the fluid are commensurable with the wavelength.

3.1. Viscous Fluid. Problem Statement and Basic Equations. Here we will present the basic equations used to analyze the acoustic radiation pressure acting on rigid and flexible particles in a compressible viscous fluid during the propagation of an acoustic wave. The approach used is to filter out the time-independent (radiation) force acting on an object in a fluid by averaging over time the resultant force exerted by the fluid on the object. In this connection, in calculating the stresses in a fluid, it is necessary to keep the second-order terms with respect to the parameters of the acoustic field, which do not vanish after averaging over time, i.e., to use the nonlinear relations of hydromechanics. In [85, 86, 108], it was proposed to determine the acoustic pressure in a compressible viscous fluid up to terms of the second order with respect to the Mach number from the velocity-field potential found from equations derived, to the same accuracy, from the nonlinear relations of hydrodynamics. The nonlinear relations for wave motions of the fluid were simplified by assuming that perturbations weakly decay at distances of the order of wavelength and that the dissipative coefficients are of the order of amplitudes of relative perturbations in pressure and density [150]. The resulting second-order formula for the pressure perturbations in a compressible viscous fluid caused by an acoustic wave is as follows [85]:

$$p = \rho_0 \left(\frac{\lambda^* + 2\mu^*}{\rho_0} \Delta - \frac{\partial}{\partial t} \right) \Phi + \frac{\rho_0}{2a_0^2} \left(\frac{\partial \Phi}{\partial t} \right)^2 - \frac{1}{2} \rho_0 (\nabla \Phi)^2 - \frac{\lambda^* + 2\mu^*}{a_0^2} \frac{\partial \Phi}{\partial t} \Delta \Phi, \tag{3.1}$$

where ρ_0 is the density of the fluid in equilibrium; μ^* and λ^* are the dynamic and kinematic viscosity coefficients; a_0 is the adiabatic speed of sound, and the second-order equation for the potential Φ is

$$\left[\left(1+\frac{\lambda^{*}+2\mu^{*}}{a_0^2\rho_0}\frac{\partial}{\partial t}\right)\Delta-\frac{1}{a_0^2}\frac{\partial^2}{\partial t^2}\right]\Phi=0. \tag{3.2}$$

Equation (3.2) coincides with Eq. (1.13) in the linearized theory of compressible viscous fluid. A solid body in a fluid through which an acoustic wave propagates causes an additional reflected wave field. It has potential and vortical components in a viscous fluid. The stress in the fluid is determined by the wave field resulting from the interference of the incident wave and the unknown scattered waves. The potentials of these waves are determined by solving the problem of scattering the incident wave by a body (particle). Since the potential Φ of the incident wave satisfies the linear equation (3.2), the potentials of the scattered waves can be found by solving the linear diffraction problem using the linearized theory of compressible viscous fluid [171]. In this theory, the potentials Φ and $\boldsymbol{\Psi}$ describing the motion of the fluid are the solutions of Eqs. (1.13) and (1.14). The potentials are used to calculate the velocity field $\mathbf{v}$ (1.10) and the stress tensor field $\hat{\sigma}$ (1.8).

Mathematically, the scattering problem is to solve Eqs. (1.13) and (1.14) satisfying the boundary conditions on the surface S of the object in the fluid

$$\mathbf{V}_S = \mathbf{v} \tag{3.3}$$

and the conditions at infinity. To calculate the velocity $\mathbf{V}_S$ of particles of the surface S of an object in a fluid, the equations of its motion (1.17) are derived using the center-of-mass theorem and the theorem of moments about the moving center. According to the linearized theory [64, 67, 75, 76], the pressure in the fluid in this case is calculated by formula (1.11), and the force acting on the object in the fluid is equal to the surface integral of internal product of the stress tensor (1.8) and the unit normal vector $\mathbf{N}$ to the surface S of the object:

$$\mathbf{F}=\iint_S \hat{\sigma}\cdot\mathbf{N}dS. \tag{3.4}$$

The first stage of the solution of the problem is to determine the velocity potentials using the linearized theory of compressible viscous fluid. The second stage is to calculate, up to second-order terms, the force (3.4) acting on the object in the fluid. The pressure p in the expression for the stress tensor $\hat{\sigma}$ (1.8) is now calculated by formula (3.1). The time-independent force $\mathbf{F}$ (radiation force) is determined by averaging it over period of the acoustic field.

In calculating the average force on a free object, it is necessary to take into account its displacements in oscillating fluid because if the position of the object in space changes, there appear terms in (3.1) that have the same order as that of the second, third, and fourth terms. This is because the partial derivative of the scalar potential Φ with respect to time should be evaluated in the fixed coordinate system in which the motion of the object is considered in determining the potential of the velocity field. In the coordinate system fixed (because of the necessity to satisfy the boundary conditions) to the moving object, this derivative should be evaluated by the following formula [108]:

$$\frac{\partial\Phi}{\partial t}=\frac{d\Phi}{dt}-\mathbf{V}_S\cdot\nabla\Phi. \tag{3.5}$$

The final stage is to analyze the motion of the object in the fluid under a constant (radiation) force.

In [118], it was established the problem of the small harmonic oscillations of a compressible viscous fluid described by the linearized theory is analogous to the problem of the stationary harmonic vibrations of a linear viscoelastic solid [42] (see [68] for another interesting analogy). Based on this analogy, the problem of the scattering of an incident wave in a compressible viscous fluid can be formulated as the problem of the scattering of an isothermal wave in a linear viscoelastic body. This circumstance made it possible to determine the velocity-field potentials in a compressible viscous fluid by using the approaches developed in solid mechanics [84] for solving problems of the scattering of elastic waves by multiply connected bodies.

Mathematically, the scattering problem is reduced to the solution of the equations

$$\Delta L+\alpha^2 L=0, \qquad \Delta\mathbf{X}+\beta^2\mathbf{X}=0, \tag{3.6}$$

satisfying the boundary conditions

$$\mathbf{u}=\mathbf{U} \tag{3.7}$$

and the conditions at infinity. The vector **u** of the displacement field in the body satisfies the equation

$$\mathbf{u} = \nabla L + \nabla \times \mathbf{X}, \qquad \nabla \cdot \mathbf{X} = \mathbf{0}, \tag{3.8}$$

and **U** is the displacement vector of particles of the surface S of the body (the object in the fluid). In (3.6), α and β are complex wave numbers,

$$\alpha = \omega\sqrt{\rho_0 / \left[\lambda^*(i\omega) + 2\mu^*(i\omega)\right]}, \qquad \operatorname{Im}\alpha^2 > 0, \qquad \beta = \omega\sqrt{\rho_0 / \mu^*(i\omega)}, \qquad \operatorname{Im}\beta^2 > 0,$$

where $\lambda^*(i\omega)$ and $\mu^*(i\omega)$ are complex moduli [42, 142].

In solving scattering problems, the components of the stress tensor are defined by

$$\sigma_{ij}(x_k, t) = \delta_{ij}\lambda^*(i\omega)\varepsilon_{nn}(x_k, t) + 2\mu^*(i\omega)\varepsilon_{ij}(x_k, t), \tag{3.9}$$

which are used to deduce the equations of motion of the body in the viscoelastic medium:

$$m\ddot{\mathbf{U}} = \iint_S \sigma_{ij} N_j \, dS. \tag{3.10}$$

The following formulas allow passing to velocity-field potentials in a compressible viscous fluid:

$$\Phi = \frac{\partial L}{\partial t}, \qquad \boldsymbol{\Psi} = \frac{\partial \mathbf{X}}{\partial t}. \tag{3.11}$$

The proposed approaches were used to solve specific problems [94, 95].

3.2. Radiation Force on a Single Object in a Viscous Fluid. Radiation forces acting on single objects in the field of a plane acoustic wave were mainly studied:

$$\Phi_0 = A\exp\left[i(\kappa x_3 - \omega t)\right], \tag{3.12}$$

that propagates along the ox_3-axis of the chosen coordinate system $ox_1x_2x_3$. These objects in a viscous fluid are a cylinder and a sphere, which are cylindrically and spherically isotropic, respectively, and a spherical drop with properties different from those of the surrounding fluid. In the case of a cylinder, the wave propagates at a right angle to its axis. In determining the velocity-field potentials, the problem of the scattering of the incident wave by a free object in a fluid was solved using either the linearized theory of compressible viscous fluid [87, 108, 109, 115, 175] or the theory of linear viscoelasticity [118, 121, 125]. To describe the damping of the wave, a complex wave number $\kappa = k + ik_1$ was introduced.

The case of a free spherical particle was examined in [87, 108, 109, 175]. The potentials of the waves reflected by the sphere, which are the solutions of the equations of motion of the viscous fluid, are expanded into generalized Fourier series of spherical wave functions. The coefficients of the series were determined from an infinite system of linear algebraic equations obtained by satisfying the boundary conditions on the surface of the free sphere. The radiation force was calculated using either the long-wave approximation [87, 108, 109, 175] or rigorous solutions [125] found on a computer. In the long-wave approximation ($\alpha = ka << 1$), asymptotic representations of spherical functions of small argument were used, and the fluid was assumed to have low viscosity ($\varepsilon = [\sqrt{\mu^* / (a^2\rho_0\omega)}] << 1$). As a result, the following formula for the radiation force acting on a sphere of radius a was derived:

$$\langle F_{\mathrm{w}} \rangle = \langle F_{\mathrm{id}} \rangle + \varepsilon \cdot 2\sqrt{2}\pi\rho_0 f(\eta)\alpha^3, \qquad f(\eta) = \frac{13\eta^2 - 14\eta + 1}{(2+\eta)^2}, \tag{3.13}$$

where the first term stands for the radiation force acting on the sphere in an ideal fluid [180]:

$$\langle F_{\mathrm{id}} \rangle = 2A^2\pi\rho_0 \frac{1 + \frac{2}{9}(1-\eta)^2}{(2+\eta)^2}\alpha^6. \tag{3.14}$$

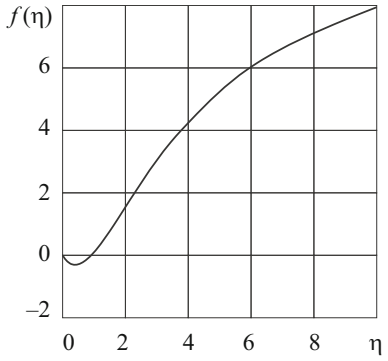

Fig. 3.1

The second term in (3.13) represents the effect of viscosity on the radiation force. In deriving expression (3.13), only the first term was retained in the series expansion in powers of ε; therefore, the effect of viscosity on the average force was characterized by η. The parameter η has critical value $\eta_{cr} = 5/11$ at which viscosity maximally reduces the radiation force (Fig. 3.1). There are values of η at which viscosity does not affect this force.

How an acoustic wave acts on a sphere in propanol ($\rho_0 = 785.4$ kg/m^3, $a_0 = 1247$ m/sec) is shown in Fig. 3.2 for $1-\mu^* = 0$ (curve *1*) and $2-\mu^* = 0.004$ kg/(m·sec) (curve *2*) and in Fig. 3.3 for $\mu^* = 0.0046$ kg/(m·sec) (curve *1*) and $\mu^* = 0.00239$ kg/(m·sec) (curve *2*). The energy flux density $I = 175.5$ W/m^2, which corresponds to moderate radiated power. The viscosity substantially increases the radiation force. Unlike the case of ideal fluid [180], the direction of its action on the sphere in a viscous fluid depends on the parameter $\eta = \rho_0 / \rho$ and can either coincide with the wave propagation direction ($\eta = 1.2$) or be opposite to it ($\eta = 0.8$). A similar phenomenon is observed when a sound beam is incident on the interface between two fluids. The direction of deflection of the interface caused by the radiation force does not depend on the beam propagation direction and is always toward the fluid, which has lower acoustic energy density [48].

The effect of the radiation force on a spherical drop of ideal fluid in a compressible viscous fluid was analyzed in [96]. The liquid drop with properties different from those of the surrounding viscous fluid causes an additional (reflected) wave field that has potential and vortical components. To determine the velocity potentials of the additional wave field, it is proposed, as a first stage, to solve the linear problem of the scattering of wave (3.12) by the liquid sphere.

In the axisymmetric case, the velocity potentials of the potential (Φ_d) and vortical (Ψ_d) components of the additional wave field satisfy Eqs. (1.13) and (1.14). The velocity potential $\overline{\Phi}$ in the drop satisfies the following equation (acoustic approximation):

$$\Delta\overline{\Phi} - \frac{1}{a_0^2}\frac{\partial^2\overline{\Phi}}{\partial t^2} = 0. \tag{3.15}$$

The incident wave causes periodic compression and expansion of the liquid sphere. In formulating the boundary conditions on the spherical surface, we assume that the amplitude of the surface of the drop is very low; therefore, it may be assumed that the drop radius $a = \text{const}$ (which is justified for a liquid sphere). We will neglect the effect of surface tension on the liquid sphere. Then the boundary conditions on the liquid sphere surface can be formulated as follows. The normal velocity and the normal stresses of the liquid are continuous and the tangential stresses are zero on the spherical surface. The velocity potentials of the scattered waves satisfy the Sommerfeld radiation conditions. The wave perturbations of the fluid inside the drop are bounded.

The velocity potentials in the surrounding viscous fluid, Φ_d, Ψ_d, and in the ideal fluid of the drop, $\overline{\Phi}$, are determined by solving a multiply connected problem for Eqs. (1.13), (1.14), (3.15) satisfying the boundary conditions on the surface of the liquid sphere, at infinity, and at the center of the sphere. The solutions of the equations were found as generalized Fourier series of spherical wave functions by the variable separation method in a spherical coordinate system. The coefficients of the series were determined by the reduction method from an infinite system of algebraic equations derived by satisfying the boundary conditions.

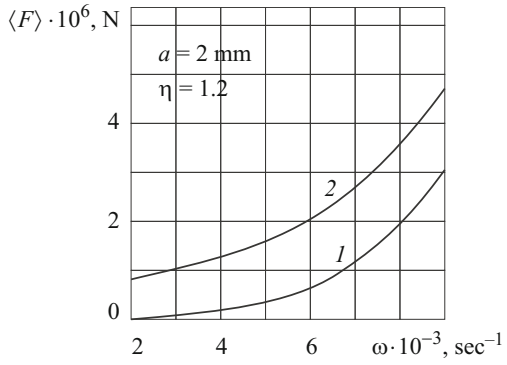

Fig. 3.2

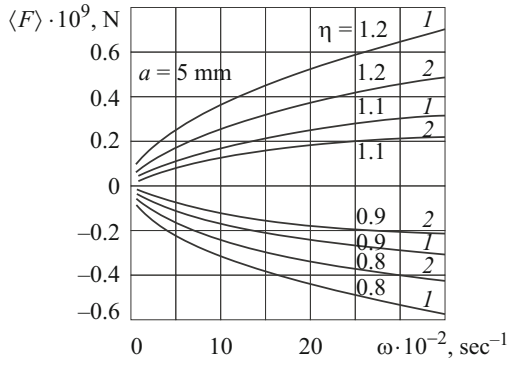

Fig. 3.3

At the second and third stages of problem solving, the case of a fluid of low viscosity was considered. The radiation force was calculated by averaging, over the period of the incident wave, the hydrodynamic force

$$F_{x_3} = \iint_S \mathbf{e}_3 \cdot \hat{\sigma} \cdot \mathbf{n} ds = 2\pi a^2 \int_0^\pi (\sigma_{rr} \cos\theta - \sigma_{\theta r} \sin\theta) \sin\theta d\theta, \tag{3.16}$$

exerted by the surrounding viscous fluid on the spherical drop of an ideal fluid and acting along the ox_3-axis. In (3.16), **n** is the unit normal to the surface S of the liquid sphere. The component $\sigma_{\theta r}$ of the stress tensor $\hat{\sigma}$ (3.16) is zero on the surface of the liquid sphere. The pressure p in (1.8) should be determined from (3.1) up to second-order terms.

The effect of radiation (average) force on a free solid cylinder was studied in [115, 121, 176]. The potentials of the waves reflected by the cylinder, which are the solutions of the equations of motion of the viscous fluid, are expanded into generalized Fourier series of cylindrical wave functions. The coefficients of the series were determined from an infinite system of linear algebraic equations obtained by satisfying the boundary conditions on the surface of the cylinder. The problem was solved using either the long-wave approximation for a low-viscosity fluid [115] or rigorous solutions [121] found with the help of a computer. Asymptotic representations of cylindrical functions for small values of the argument were used in the former case. The radiation force acting on a cylinder with length equal to its radius is expressed as

$$\langle F_w \rangle = \langle F_{id} \rangle + \varepsilon\pi\rho_0 A^2 \frac{\sqrt{2}}{4} \varphi(\eta) \alpha^3, \qquad \varphi(\eta) = \frac{1 - 8\eta + 7\eta^2}{(1+\eta)^2}, \tag{3.17}$$

where $\langle F_{id} \rangle$ is the radiation force acting on the cylinder in an ideal fluid. The function $\varphi(\eta)$ characterizes the effect of the parameter η on the average force. Its graph is shown in Fig. 3.4. As for the sphere, with increase in η, the viscosity increases the average force for a cylinder that is lighter than the fluid. For a cylinder that is heavier than the fluid, there exists a critical value of η equal to its critical value η_{cr} for the sphere. In the long-wave approximation, viscosity at $\eta = 1.0$ does not affect the radiation force acting on the sphere or the cylinder in an ideal fluid.

The numerical results on the radiation force exerted by an incident wave with energy flux density $I = 175.5$ W/m^2 on a cylinder in propanol are presented in Fig. 3.5 for $\mu^* = 0$ (curve *1*) and $\mu^* = 0.0046$ kg/(m·sec) (curve *2*) and in Fig. 3.6 for $\mu^* = 0.0046$ kg/(m·sec) (curve *1*) and $\mu^* = 0.00239$ kg/(m·sec) (curve *2*). It can be seen that the effect of viscosity on the radiation (time-average) force is similar to that in the case of sphere.

3.3. Radiation Force on a Two Objects in a Viscous Fluid. When an acoustic wave propagates through a fluid containing several solid objects, their flow fields distort each other because of the interference of the incident and reflected waves. Therefore, the forces exerted by the fluid on the objects, as well as their constant components (radiation forces) are different. The radiation forces cause the free objects to displace (drift) relative to each other, and the distance between them changes. If objects are arranged arbitrarily in a fluid, the interaction of two objects is of fundamental importance. Let these objects be two spherical and two cylindrical particles.

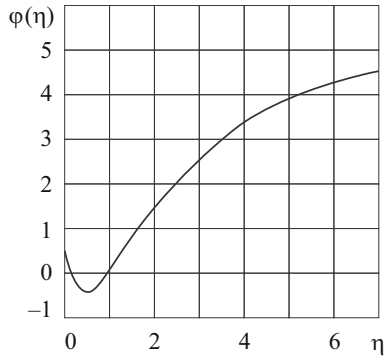

Fig. 3.4

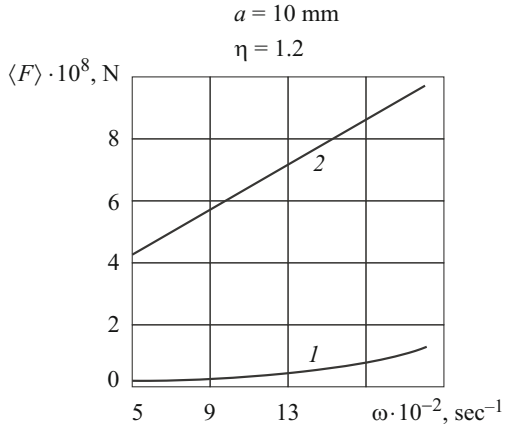

Fig. 3.5

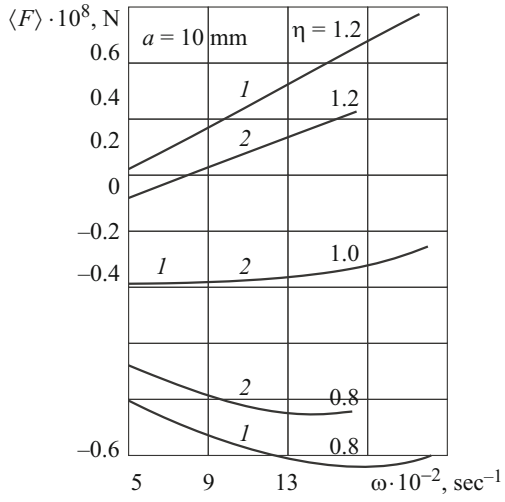

Fig. 3.6

The effect of a plane acoustic wave (3.12) on two spherical solid particles was studied in [127]. The wave propagates along a line coming through the centers of free spherically isotropic particles Nos. 1 and 2. At the first stage, the velocity potentials of the reflected waves were found by solving the problem of the scattering of the incident wave by two spherical particles using the theory of linear viscoelasticity [42, 142]. The equations of motion were solved by the variable separation method in a spherical coordinate system. A local spherical coordinate system was fixed to each particle. The velocity potentials of the reflected waves, which are the solutions of Eqs. (3.6) in the respective local coordinate systems, were expanded into generalized Fourier series of spherical wave functions. The coefficients of the series were determined from an infinite system of linear algebraic equations obtained by satisfying the boundary conditions on the surfaces of the particles by the reduction method. To derive expressions of the potentials in each of the local spherical coordinate systems, the summation theorems for spherical wave functions were used. The boundary conditions were the equality of the displacements of particles of the medium and particles of the surface of the solid sphere on this surface. Since the wave field is symmetric about the axis coming through the centers of the spheres, the forces acting on them are parallel to this axis. The displacements of the spheres were determined by integrating their equations of motion (1.17). The radiation forces were calculated by averaging over time the forces acting on the spherical particles and determined up to the second order.

Systems of two spheres of equal and different radii arranged differently relative to the wave propagation direction were studied.

Figures 3.7–3.9 show how spheres of radius $a = 0.001$ m interact in an acoustic field in propanol through which a wave with energy flux density $I = 175.5$ W/m^2 (measured at a point located on the line of sphere centers and equidistant from them) propagates. Curves *1* and *2* in Figs. 3.7 and 3.8 characterize the action of the time-average force on spheres *1* and *2*, respectively.

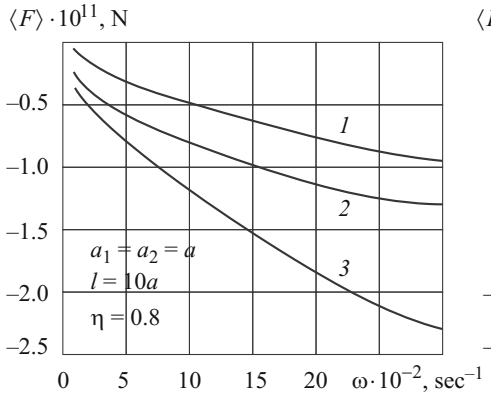

Fig. 3.7

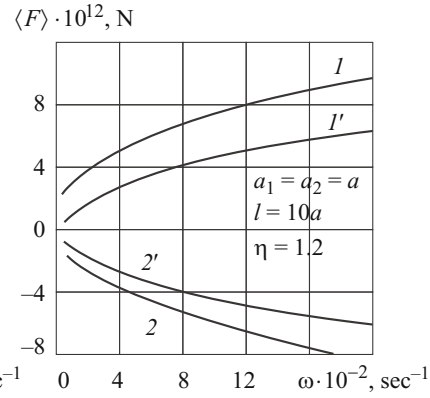

Fig. 3.8

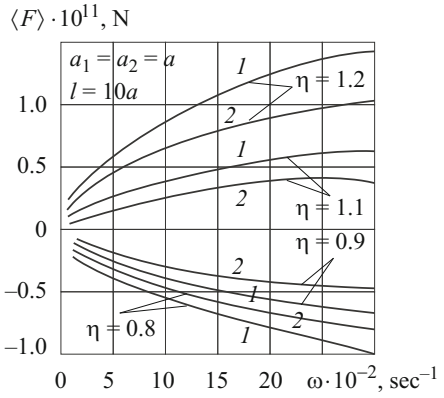

Fig. 3.9

Curve *3* represents a single sphere. The dynamic viscosity coefficient $\mu^* = 0.0046$ kg/(m·sec). With variation in η, the time-average force acting on each of the spheres changes in both magnitude and direction. In the frequency range being considered, the average forces increase with frequency. At $\eta = 1.2$, the effect of the second sphere on the first one (the deviation of curve *1* from curve *3*) is stronger than the effect of the first sphere on the second one (the deviation of curve *2* from curve *3*). At $\eta = 0.8$, the average forces change their direction. Sphere *1* repulses sphere 2 at $\eta = 1.2$ and attracts sphere 2 at $\eta = 0.8$.

Figure 3.9 shows the effect of the time-average force on sphere 2 depending on frequency, dynamic viscosity coefficient μ^*, and parameter $\eta = \rho_0 / \rho$ for $\mu^* = 0.0046$ kg/(m·sec) (curves *1*) and $\mu^* = 0.00239$ kg/(m·sec) (curves *2*). The higher the viscosity of the fluid, the stronger the average force exerted by the acoustic wave, the direction of the force depending on η. For $\eta = 1.2$ and $\eta = 1.1$, the average force is parallel to the wave propagation direction. For $\eta = 0.9$ and $\eta = 0.8$, the average force is opposite to the wave vector.

The effect of a plane acoustic wave (3.12) on two free parallel cylindrically isotropic circular cylinders 1 and 2 was studied in [89, 122, 126]. The cylinders were considered to be arranged in line parallel to the wave propagation direction. The cylinders were either of equal or different radii and were differently arranged relative to the wave vector. The potentials of scattered waves were determined using the linearized theory of compressible viscous fluid [89] or the theory of linear viscoelasticity [122, 126]. The problems posed were solved numerically.

At the first stage, the potentials of scattered waves were determined using the variable separation method in cylindrical coordinate systems. A local cylindrical coordinate system was fixed to each cylinder. The velocity potentials of the reflected waves, which are the solutions of the equations of motion of the medium in the respective local coordinate systems, were expanded into generalized Fourier series of cylindrical wave functions. The constant coefficients of the series were determined from infinite systems of algebraic equations obtained by satisfying the boundary conditions on the surfaces of the cylinders by the reduction method. To derive expressions of the potentials in each of the local cylindrical coordinate systems, the summation theorems for cylindrical wave functions were used. The boundary conditions were the equality of the displacements of particles of the medium and particles of the cylinder surface on this surface. The displacements of the cylinders in the medium were determined by integrating their equations of motion (1.17). The radiation forces were calculated by averaging over time the forces acting on the cylinders and determined up to the second order.

Systems of two cylindrical particles of equal and different radii arranged differently relative to the wave propagation direction were studied.

Figures 3.10 and 3.11 illustrate how cylinders of length equal to their radius $a = 0.001$ m interact depending on the frequency ω and parameter η under radiation forces in propanol through which a wave with energy flux density $I = 175.5$ W/m^2 propagates (measured in the midsurface of the system of cylinders perpendicular to the plane of their axes). Curves *1* and *2* correspond to cylinders 1 and 2, and curve *3* to a single cylinder. In all cases, $\mu^* = 0.0046$ kg/(m·sec). In the frequency range represented in Fig. 3.10, the effect of the first cylinder on the second one (the deviation of curve *2* from curve *3*) is stronger than the effect of the second cylinder on the first one (the deviation of curve *1* from curve *3*). As the parameter η is changed ($\eta = 1.2$ in Fig. 3.11), the interaction behavior of the cylinders changes substantially. The cylinders go away from each other at $\eta = 0.8$ (Fig.

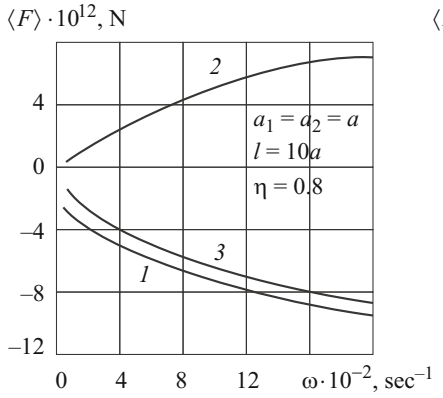

Fig. 3.10

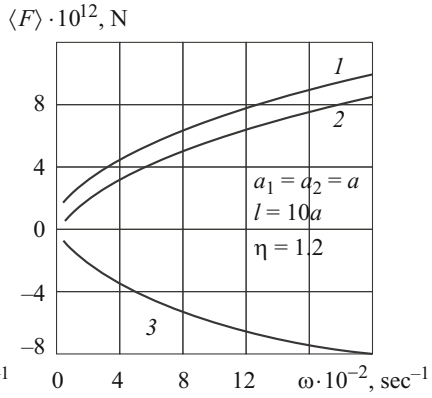

Fig. 3.11

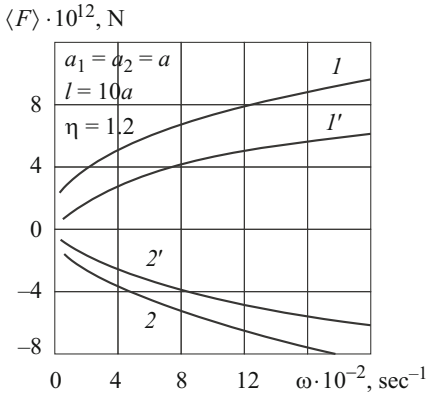

Fig. 3.12

3.10) and approach each other at $\eta = 1.2$ (Fig. 3.11). The first cylinder repulses the second one in the former case and attracts the second cylinder in the latter case. With variation in η, the average force acting on the first cylinder changes in both magnitude and direction.

Figure 3.12 shows how the viscosity of the fluid affects the average force for $\mu^* = 0.0046$ kg/(m·sec) (curves *1* and *2*) and $\mu^* = 0.00239$ kg/(m·sec) (curves *1′* and *2′*). The curve number corresponds to the cylinder number. It can be seen that the higher the viscosity of the fluid, the stronger the time-average (radiation) force exerted by the acoustic wave.

3.4. Ideal Fluid. Basic Equations and Problem Statement. The method proposed in [85, 86, 108] to determine the average forces in a compressible viscous fluid can be applied to the equations for an ideal fluid after passing to the limit ($\lambda^* \to 0, \mu^* \to 0$) [88, 110–114, 116, 119, 120, 123, 124, etc.]. After passing to the limit, formula (3.1) takes the form

$$p = -\rho_0 \frac{\partial \Phi}{\partial t} + \frac{\rho_0}{2a_0^2}\left(\frac{\partial \Phi}{\partial t}\right)^2 - \frac{1}{2}\rho_0 (\nabla \Phi)^2, \tag{3.18}$$

which corresponds to the formula obtained earlier, with the same accuracy, for the perturbations of pressure in an ideal fluid in [180].

At the first stage, the scattering problem is formulated in acoustic approximation in which the potentials Φ of the incident and scattered waves are the solutions of the equation

$$\Delta \Phi - \frac{1}{a_0^2}\frac{\partial^2 \Phi}{\partial t^2} = 0. \tag{3.19}$$

Formula (3.4) for the hydrodynamic force becomes

$$\mathbf{F} = -\int_S p\mathbf{N}dS, \tag{3.20}$$

where the pressure p in the acoustic wave is calculated by the following formula in determining the displacement of the object:

$$p = -\rho_0 \frac{\partial \Phi}{\partial t}. \tag{3.21}$$

To formulate the boundary conditions on the surface of the free object, the velocities of particles of its surface are determined by solving the equation of motion of the object in a fluid under force (3.20):

$$m\dot{\mathbf{V}} = -\int_S p\mathbf{N}dS, \tag{3.22}$$

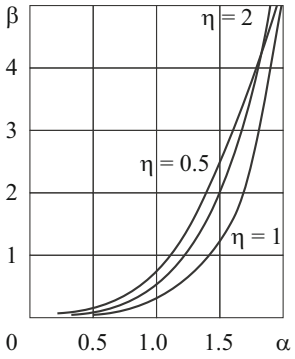

Fig. 3.13

where m is the mass of the object; **V** is the velocity of the object; p is the pressure in the fluid (3.21); **N** is the unit normal vector to the surface S of the object.

At the second stage, the hydrodynamic force (3.20) is calculated up to the second order (3.18). At the third stage, the constant component of the hydrodynamic force (radiation force) is determined by averaging (3.20) over time.

3.5. Radiation Force on a Single Object in an Ideal Fluid. Objects in a fluid that were examined are a circular cylinder, a sphere, and a spherical drop. The radiation force exerted by an acoustic wave on a free circular cylinder was studied in [112]:

$$\Phi_0 = A\exp\left[i(kx_3 - \omega t)\right]. \tag{3.23}$$

It is perpendicular to the cylinder axis. The potential of the wave reflected by the cylinder, which is the solution of Eq. (3.19), is expanded into a generalized Fourier series of cylindrical wave functions. The coefficients of the series were determined from an infinite system of linear algebraic equations obtained by satisfying the boundary conditions on the surface of the free cylinder. The system of algebraic equations is regular and has a unique solution, which can be found numerically, by the reduction method. The radiation force was calculated by averaging expressions (3.20) over time, provided that the pressure p is defined by (3.18), where Φ is the total potential of the incident and scattered waves. The radiation force per unit length of the cylinder is expressed as

$$\langle F\rangle = \frac{8A^2\rho_0}{\pi^2 a}\left\{\frac{\alpha^7}{\Omega_0^2\Omega_1^2} + \frac{\alpha^3\left[\alpha^2 - 2(1-\eta)\right]^2}{\Omega_1^2\Omega_2^2} + \sum_{n=2}^{\infty}\frac{\alpha^3[\alpha - n(n+1)]^2}{\Omega_n^2\Omega_{n+1}^2}\right\}, \tag{3.24}$$

where a is the radius of the cylinder; $\eta = \rho_0/\rho$ is the ratio of the density of the fluid to the density of the cylinder; k is the wave number of the incident wave; A is its amplitude. Expression (3.24) is based on the assumption that the body is cylindrically isotropic. Using the asymptotic representations of cylindrical functions of a small argument in the long-wave approximation ($\alpha = ka << 1$), formula (3.24) was transformed to

$$\langle F\rangle = \frac{A^2\pi^2\rho_0}{8a}\cdot\frac{4+(1-\eta)^2}{(1+\eta)^2}\alpha^5 + O(\alpha^7), \tag{3.25}$$

whence it follows that the radiation force is strongly dependent on the parameter η. For small values of α, the radiation force is minimum when $\eta = 3.0$. Figure 3.13 shows graphs of $\beta = \langle F\rangle / A^2\cdot 10^{-3}$ versus α plotted using formula (3.24) for a cylinder in water ($\rho_0 = 10^3$ kg/m^3). The radiation force acting on the cylinder increases with the frequency and strongly depends on the parameter η. At $\alpha = 0.2$, the radiation force can be calculated with adequate accuracy by formula (3.25).

A free cylinder in the field of a plane standing acoustic wave with the following potential was studied in [116]:

$$\Phi_0 = \frac{1}{2}A\exp\{i[k(l+x) - \omega t]\} + \exp\{-i[k(l+x) + \omega t]\}. \tag{3.26}$$

The origin of the coordinate system *oxyz* is on the cylinder axis at a distance *l* from the chosen fixed reference plane. The radiation force per unit length of a cylindrically isotropic cylinder is defined by the expression

$$\langle F\rangle = A^2\pi\rho_0\,\frac{3-\eta}{4a(1+\eta)}\sin(2kl)\,\alpha^3 + O(\alpha^5), \tag{3.27}$$

which was derived in long-wave approximation in [40]. The radiation force (3.27) has spatial period equal to half-wavelength and acts on the lighter cylinder ($\eta > 3$) toward the nodes of the velocity field and on the denser cylinder ($\eta < 3$) toward the antinodes of the velocity field. In (3.27), *l* is the distance from the fixed reference plane.

The equation of motion of the cylinder under the radiation force (3.27) is reduced to the nonlinear oscillator equation

$$\ddot{\theta} + n^2 \sin\theta = 0, \qquad \theta = \pi - 2kl, \qquad n^2 = A^2k^4\,\frac{\eta(3-\eta)}{2(1+\eta)^2}. \tag{3.28}$$

It is significant that the radius of the cylinder does not influence the oscillatory process. For the denser cylinder $n^2 > 0$, the positions of stable equilibrium in its time-average motion are the antinodes of the velocity field. The period of oscillation of the cylinder about them is

$$T = \frac{2\tilde{\lambda}}{\pi v_0}\left[\frac{2(1+\eta)^2}{\eta(3-\eta)}\right]^{1/2} K(\kappa). \tag{3.29}$$

For the lighter cylinder $n^2 < 0$, the positions of stable equilibrium in its time-average motion are the nodes of the velocity field. The period of oscillation of the cylinder about them is

$$T = \frac{2\tilde{\lambda}}{\pi v_0}\left[\frac{2(1+\eta)^2}{\eta(\eta-3)}\right]^{1/2} K(\kappa). \tag{3.30}$$

In (3.29) and (3.30), $\tilde{\lambda}$ is the wavelength; v_0 is the amplitude of the velocity field; $K(\kappa)$ is a complete elliptic integral of the first kind; $\kappa = \sin(kx_0)$; x_0 is the maximum distance of the cylinder from a node or an antinode of the velocity field (amplitude in its time-average oscillative motion). The period *T* of oscillation (3.29) has a minimum.

The acoustic radiation pressure on a small scatterer moving in a homogeneous isotropic field was studied in [105]. The problem of determining the radiation force acting on a solid sphere in a fluid flow was formulated in [128]. It was assumed that the compressible ideal fluid is barotropic with pressure function P_0. The flow is along the $o\varsigma_3$-axis of a fixed Cartesian coordinate system $o\varsigma_1\varsigma_2\varsigma_3$, and $\mathbf{V}_\infty$, ρ_∞, and p_∞ are, respectively, the velocity, density, and pressure of the fluid at infinity. In the fluid, there is a spherical particle of radius *R* that also moves along the $o\varsigma_3$-axis with velocity **U**. The sphere makes the flow nonuniform. If a coordinate system $o_1x_1x_2x_3$ (the axes $o\varsigma_3$ and o_1x_3 coinciding) is fixed to the sphere, then the parameters of the nonuniform flow (velocity **u**, density ρ', and pressure p') in the moving coordinate system are determined in solving the problem of a stationary flow with velocity $\mathbf{u}_\infty = \mathbf{V} - \mathbf{U}$ at infinity past a sphere. The quantities p' and ρ' are related by the Tait equation.

When an acoustic wave propagates, the quantities **u**, ρ', and p' are subject to small increments **v**, ρ, and *p*, respectively, which characterize the oscillations of fluid parcels about the stable state of the perturbed flow. If the motion of the fluid caused by the acoustic field is also potential

$$\mathbf{v} = \nabla\Phi, \tag{3.31}$$

the potential Φ of the acoustic field in the flow past the moving solid sphere is described by the equation

$$\frac{d^2\Phi}{dt^2} - a^2\Delta\Phi - (\nabla P_0\cdot\nabla\Phi) - \frac{d\Phi}{dt}(\mathbf{u}\cdot\nabla\ln c^2) = 0, \tag{3.32}$$

where *a* is the local velocity of small perturbations relative to the fluid flow. For a stationary barotropic flow, we have

$$a^2 = -\frac{\mathbf{u}\cdot\nabla P_0}{\nabla\cdot\mathbf{u}}. \tag{3.33}$$

To determine the pressure p up to the second order, we have the equation

$$p = -\rho'\left(\frac{\partial}{\partial t} + \mathbf{u}\cdot\nabla\right)\Phi - \frac{1}{2}\rho'(\nabla\Phi)^2 + \frac{1}{2}\frac{\rho'}{c^2}\left(\left(\frac{\partial\Phi}{\partial t}\right)^2 + u^2\,\frac{\partial\Phi}{\partial t}\right.$$

$$\left. + \left(2\frac{\partial\Phi}{\partial t} + u^2\right)(\mathbf{u}\cdot\nabla\Phi) + \frac{3}{2}u^2(\nabla\Phi)^2\right), \tag{3.34}$$

where the terms vanishing after averaging over time have been omitted. If there is no flow and the sphere is fixed ($\mathbf{u} = 0$, $p' = p_0$, $\rho' = \rho_0$), formula (3.34) transforms into (3.18).

The parameters of the perturbed flow appearing in Eqs. (3.32) and (3.34) are determined by solving the problem of a potential fluid flow with velocity $\mathbf{u}_\infty$ at infinity past a sphere. The potentials of both incident Φ_0 and reflected (from the sphere) waves must satisfy Eq. (3.32). The potential Φ_d of the reflected wave is determined by solving the problem of the scattering of the incident wave by a sphere, provided that the velocity v_r on its surfaces and the potential Φ_d at infinity are equal to zero. The radiation pressure force on the sphere is filtered out by averaging the hydrodynamic force (3.20) over time, provided that the pressure p is defined by formula (3.34) where the potential $\Phi = \Phi_0 + \Phi_d$ results from the interference of the incident and scattered waves.

In [130, 131], the approach developed for solid particles was used to study the effect of acoustic radiation on a spherical drop of radius a different in mechanical characteristics from the surrounding fluid in which the acoustic wave (3.23) propagates. It is assumed that both fluids are ideal. At the first stage, the problem of the diffraction of wave (3.23) by a spherical drop is formulated. The potentials Φ_d and $\overline{\Phi}_d$ of the wave reflected from the drop and the wave inside the drop are the solutions of Eq. (3.19) found by the variable separation method in the spherical coordinate system fixed to the drop. They are represented by generalized Fourier series of spherical wave functions. The coefficients of the series are determined by the reduction method from an infinite system of linear algebraic equations obtained by satisfying the boundary conditions on the surface of the drop: continuity of the normal velocity and pressure on the surface. The case where the radius of the sphere is small compared with the length of the acoustic wave was analyzed in detail. Asymptotic representations of the functions $j_n(w)$ and $h_n(w)$ with a small argument were used. At the third stage, an expression for the radiation force exerted by the acoustic wave on the liquid sphere is derived:

$$\langle F_x\rangle = \frac{2}{27}A^2\pi\rho_0\,\frac{1}{2+\eta}[k^*(\eta-10)+4(1-\eta)]\alpha^6 + O(\alpha^8), \tag{3.35}$$

where $\langle F_x\rangle$ is the projection of the radiation force onto the wave vector $\mathbf{k}$ (parallel to the *ox*-axis); ρ_0 is the density of the surrounding fluid in equilibrium; $\eta = \rho_0/\overline{\rho}_0$; $\overline{\rho}_0$ is the density of the drop; $\alpha = ka << 1$; $k^* = 3(\kappa - \overline{\kappa})/(3\overline{\kappa} - \kappa\alpha^2)$; κ and $\overline{\kappa}$ are the adiabatic bulk moduli of the surrounding fluid and the drop, respectively.

In [96], numerical results for the following two cases were analyzed in detail: (i) the density of the ethyl-spirit drop is lower than the density of the surrounding water ($\eta > 1$); (ii) the density of the water drop is higher than the density of the surrounding ethyl spirit ($\eta < 1$). Figures 3.14 and 3.15 show the radiation force acting on the drop versus the parameter ka (curves *1–1*). Curve *2* represents a solid spherical particle. The value $ka = \sqrt{3\overline{\kappa}/\kappa}$ corresponds to the pulsation resonance of the spherical liquid drop. The expression for radiation force (3.35) has been derived assuming that ka is different from $\sqrt{3\overline{\kappa}/\kappa}$. In this case, the drop mainly oscillates rather than pulsates. An analysis of the figures reveals the following qualitative phenomena:

(i) when the parameter ka reaches the resonant value, the radiation force acting on the drop reverses its direction (curves *1–1* in Figs. 3.14 and 3.15);

(ii) the direction of the radiation force on the drop depends on $\eta = \rho_0/\overline{\rho}_0$.

The effect of the radiation force on a spherical drop has the following features.

1. As the value of ka tends to the pulsation resonance ($ka = 1.21$ in the former case (Fig. 3.14) and $ka = 2.48$ in the latter case (Fig. 3.15)), the radiation force increases (curves *1–1* in Figs. 3.14 and 3.15).

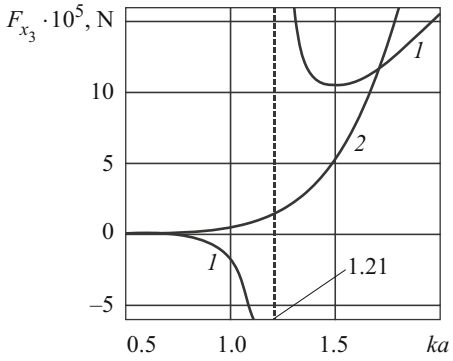

Fig. 3.14

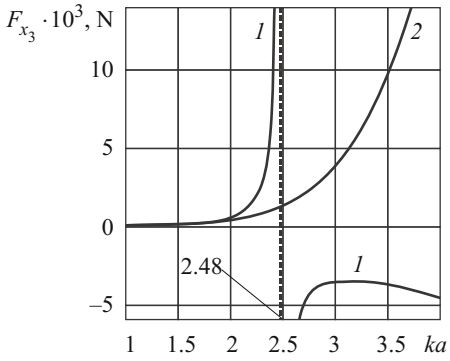

Fig. 3.15

2. If the mechanical properties of the drop are similar to those of the surrounding fluid ($\eta = 1, k^* = 0$), the radiation force is zero.

3. The direction of the radiation force acting on a solid spherical particle does not depend on η and coincides with the direction of propagation of the acoustic wave (curve *2* in Figs. 3.14 and 3.15). It monotonically increases with the frequency of the wave.

The effect of the radiation force on a solid spherical particle fixed on the axis of a cylindrical cavity filled with a compressible ideal fluid was studied in [134, 202]. A plane acoustic wave described by the following potential function was considered to propagate along the cavity:

$$\Phi_0 = A \exp\left[i(kz - \omega t)\right]. \tag{3.36}$$

This potential function satisfies the linear wave equation (3.19). The *oz*-axis of a rectangular coordinate system with the origin at the center of the sphere is aligned with the axis of the cylindrical cavity.

The approach applied above to a free particle was used. The wave field in the cylindrical cavity is formed by the incident wave (3.36) and the waves reflected from the sphere, Φ_{sph}, and the cavity, Φ_{cyl}. At the first stage, the method proposed in [181] was used to solve the linear multiply connected problem of the scattering of wave (3.36) by the sphere and the cylindrical cavity. The problem was solved by the variable separation method in a spherical coordinate system. The potential Φ_{sph} of the wave scattered by the sphere is expanded into a generalized Fourier series of spherical wave functions:

$$\Phi_{\text{sph}}(r, \theta) = \sum_{n=0}^{\infty} A_n h_n^{(1)}(\omega r) P_n(\cos\theta), \tag{3.37}$$

and the potential of the wave reflected by the cylindrical cavity is represented by the integral

$$\Phi_{\text{cyl}}(\rho, z) = \int_{-\infty}^{\infty} B(\xi) J_0\left(\sqrt{\omega^2 - \xi^2}\,\rho\right) e^{i\xi z} d\xi, \tag{3.38}$$

where $J_0(x)$ is the cylindrical Bessel function of zero order; ω is the angular frequency; ρ is the radial coordinate of the cylindrical coordinate system; $B(\xi)$ is unknown density; ξ is the separation constant. In expressions (3.37) and (3.38), the factor $\exp(-i\omega t)$ is omitted, and the quantities are dimensionless.

To satisfy the boundary conditions on the cylindrical and spherical surfaces, the spherical wave functions in the expressions for the potentials of the waves were expanded into series of cylindrical functions and vice versa [181]. The coefficients of the series were determined by the reduction method from an infinite system of algebraic equations derived by satisfying the boundary conditions. The potentials found at the first stage were used to determine the pressure in the fluid up to the second order (3.18) and the hydrodynamic force (3.20) acting on the spherical particle. Its constant component (radiation force) was found by averaging over time.

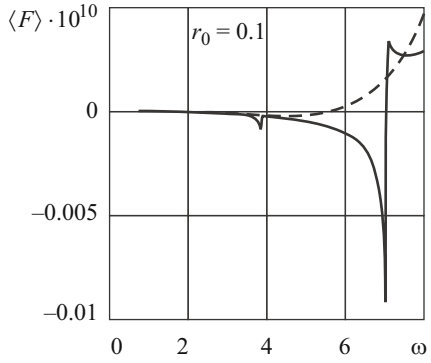

Fig. 3.16

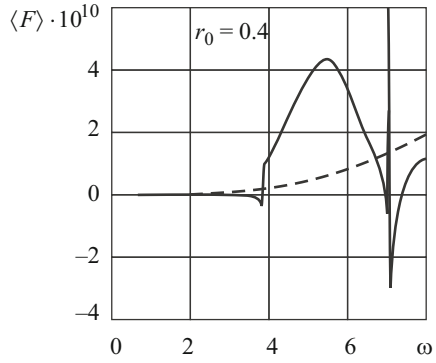

Fig. 3.17

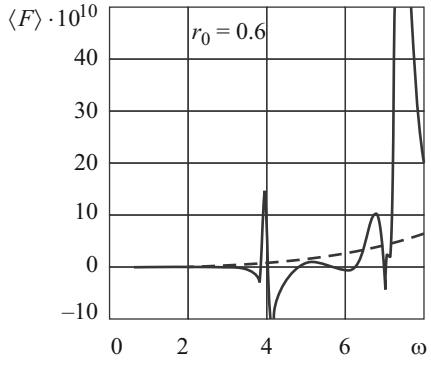

Fig. 3.18

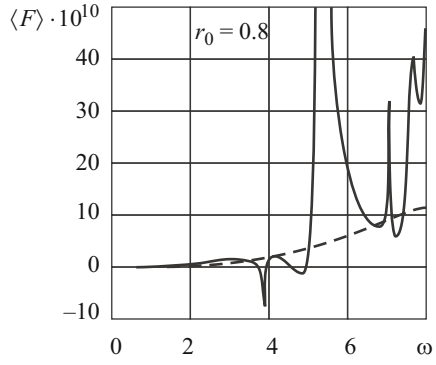

Fig. 3.19

The effect of the radiation force on a solid spherical particle in a circular cylinder filled with a fluid was analyzed numerically, using dimensionless quantities. The scaling parameters were the parameters of the compressible fluid (water): speed of sound $a_0 = 1500$ m/sec, density $\gamma = 1000$ kg/m^3. The plane acoustic wave (3.36) was assumed to have energy flux density $I = 175.5$ W/m^2, which corresponds to moderate radiative power at which the wavelength $\tilde{\lambda} = 0.038$ m and the velocity of fluid parcels is 0.015 m/sec. Figures 3.16–3.19 show the variation in the dimensionless radiation force calculated at the second stage of problem solving. The solid and dashed lines represent the dependence on the dimensionless frequency $\omega\rho_0 / a_0$ (ρ_0 is the radius of the cylindrical cavity) of the radiation force (at dimensionless pressure $p / (\gamma a_0^2)$) acting on the spherical particle in the cylindrical cavity and in an unbounded fluid, respectively. The figures indicate that the radiation force varies nonmonotonically with the frequency. The radiation force changes abruptly at certain frequencies ω ($\omega \to 4, \omega \to 7$), which is observed for all sizes of the spherical particle.

The following features in the effect of the radiation force on the spherical particle revealed by an analysis of the figures are noteworthy:

(i) if a particle in an unbounded fluid is subject to radiation force that acts in the direction of wave propagation and monotonically increases with frequency, then the frequency dependence of this force acting on the particle in the cylindrical cavity becomes very complicated because of the complication of the diffraction field inside the cylinder;

(ii) depending on the frequency, the radiation force acting on the particle in the cavity (unlike the unbounded fluid) is directed either along wave propagation or in the opposite direction;

(iii) at some frequencies, the radiation force displays nearly resonant behavior: there are peaks on the curves at these frequencies. It is obvious that the resonant frequencies are the natural frequencies of the mechanical system consisting of a rigid cylinder filled with a fluid and a solid spherical particle inside it [181].

The problem of the effect of the radiation force on a spherical drop in a cylindrical cavity filled with a fluid with dissimilar mechanical properties was solved [135]. Unlike the case of a solid spherical particle, the boundary conditions on the surface of the spherical drop are the continuity of the normal velocities of fluid parcels in the drop and surrounding fluid, and the continuity of the pressure in the fluids. The potential $\Phi_1(r, \theta)$ that describes the wave motion in the drop is expressed as

$$\Phi_1(r,\theta)=\sum_{n=0}^{\infty}C_n j_n(\eta\omega r)P_n(\cos\theta), \tag{3.39}$$

where $\eta = c_0 / c_1$ is the ratio of the speed of sound in the surrounding fluid to the speed of sound in the drop. Expression (3.39) is dimensionless. The problem was solved using the approach applied to a solid spherical particle in a cylindrical cavity filled with a fluid [202].

3.6. Radiation Force on Two Objects in an Ideal Fluid. When there are many particles in a fluid, it is a challenge to analyze their interaction caused by the radiation force exerted by an acoustic wave. If the particles are randomly arranged in the fluid and the average distance between the nearest particles is large compared with the size of the particles, then the most important interaction is between two particles appeared close to each other. Groups of three and more closely spaced particles are less frequent. In this connection, studying the interaction of two particles in a large volume of fluid is of fundamental importance. Therefore, there are many theoretical and experimental studies on the interaction of two particles in the field of an acoustic wave. In these studies, particles were assumed small compared with the amplitude of oscillation of the medium and the wave length. Therefore, it is assumed that the flow of incompressible fluid past the particles is unidirectional and steady-state (quasistationary), which gives rise to hydrodynamic forces. These forces explain the interaction of the particles. These are Bernoulli forces if the Reynolds number is great. If the Reynolds number is small, Stokes and Oseen forces are considered, and the equations of motion of the fluid include no or some of the inertial terms. In [139], the interaction of particles in an acoustic field of low frequency is attributed to Bjerknes forces acting between particles oscillating with different velocities in an incompressible ideal fluid.

In the sited publications, systems of two free spherical bodies and of two free cylindrical bodies were considered. Their interaction caused by radiation forces was studied. To solve the problems posed, the approach outlined above was used. At the first stage of problem solving, the potentials of the waves scattered by the objects were determined using the linear theory of wave propagation (3.19). To determine the velocity potentials, the superposition principle was used. The scattering problem was solved by the variable separation method in a cylindrical (spherical) coordinate system [149]. A local cylindrical (spherical) coordinate system in which the velocity potentials of waves are represented by generalized Fourier series of cylindrical (spherical) wave functions was fixed to each object. The coefficients of the series were determined from infinite systems of linear algebraic equations obtained by satisfying the boundary conditions on the surface of each object. The velocities of surface particles of the objects were determined by solving the equations of their motion (3.22) under forces (3.20) where the pressure is defined by (3.21). To formulate the boundary conditions for each object in the local coordinate system, the summation theorems for the corresponding wave functions were used [84, 149]. The resulting systems of equations are regular and, thus, have a unique solution, which can be found numerically, by the reduction method. The prescribed accuracy is achieved by increasing the number of equations. Such an approach was used to solve many problems of the interaction of objects with a fluid [166, 174, 181]. The potentials of the waves found at the first stage were used to determine the pressure in the fluid up to the second order (3.18), to calculate, at the second stage, the forces (3.20) acting on the bodies in the fluid and, at the third stage, their constant components (radiation forces), and to study the motion of the bodies under the radiation forces.

The effect of radiation forces on two free spherically isotropic solid spheres was studied in [88, 110, 111, 117, 123, 129].

Wave (3.23) propagates along the line of the centers of the spheres (the wave vector is assumed directed from sphere 1 to sphere 2) that can be differently arranged relative to each other and have equal [88, 110, 117] or different [123] radii. Since the wave field is symmetric, the radiation forces acting on the spheres are parallel to the line of their centers. Closed-form expressions for these forces were derived for the case $\alpha = ka << 1$, $kl >> 1$ (l is the distance between the centers of the spheres of radius a) using asymptotic representations of spherical functions of small and large arguments:

$$\langle F^{(2)}\rangle = 2A^2\pi\rho_0\,\frac{1+\frac{2}{9}(1-\eta)^2}{(2+\eta)^2}\,\alpha^6, \tag{3.40}$$

$$\langle F^{(1)}\rangle = \langle F^{(2)}\rangle + 2A^2\pi\rho_0\,\frac{(5-4\eta)}{9(2+\eta)}\,\frac{\sin(2kl)}{kl}\,\alpha^6, \tag{3.41}$$

where $\eta = \rho_0 / \rho_s$; ρ_0 is the density of the fluid; ρ_s is the density of the sth sphere (s = 1, 2).

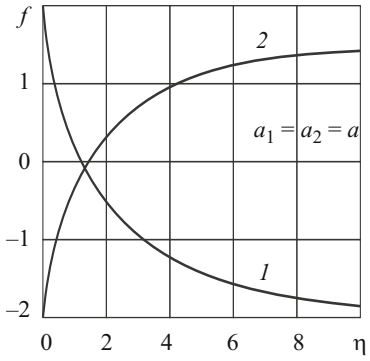

Fig. 3.20

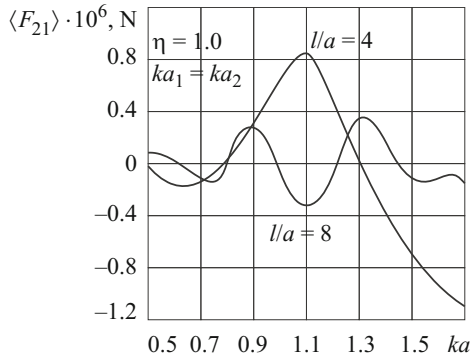

Fig. 3.21

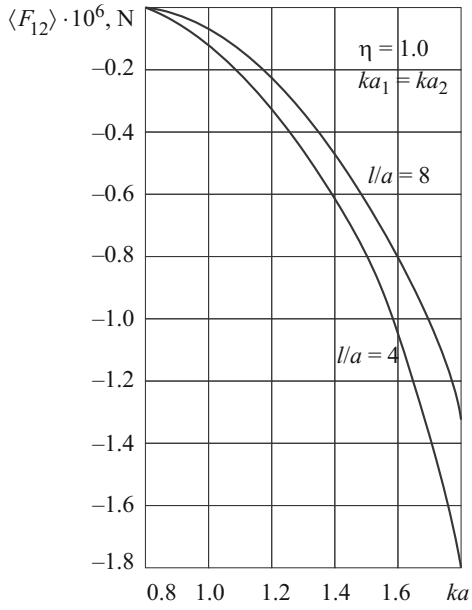

Fig. 3.22

If $kl \to \infty$, then formulas (3.40) and (3.41) coincide with formula (3.14) for a single sphere derived in [180]. The second term in (3.41) represents the time-averaged force exerted by the second sphere on the first one due to the wave reflected by the second sphere. The first sphere does not affect the second sphere because in the long-wave approximation, the energy scattered by the sphere is directed toward the incident wave. If the second term in (3.41) is positive (negative), then the second sphere attracts (repulses) the first one.

Figure 3.20 shows graphs of $f = (\langle F^{(1)}\rangle - \langle F^{(2)}\rangle) \cdot 10^4$ N versus η for two identical spheres of radius a in water (ka = 0.1, $kl = 10$ (curve *1*) and $ka = 0.112$, $kl = 11.2$ (curve *2*)) through which a plane wave of unit amplitude (3.23) propagates. As the frequency or the density of the spheres changes, their interaction behavior changes substantially.

Figures 3.21–3.24 show the radiation forces for a system of two spheres in propanol (for $\mu^* = 0$) numerically calculated without constraints on the wavelength and the radii of and the distance between the spheres. The incident wave has amplitude $A = 0.918 \cdot 10^{-4}$ m^2/sec. The force F_{ij} $\{i, j = 1, 2\}$ exerted by the ith sphere on the jth sphere was determined as the difference of the radiation force acting in the acoustic field on the jth sphere in a system of two spheres and the radiation force acting in the acoustic field on the single jth sphere. Interacting, the spheres either approach each other or move apart (Figs. 3.21 and 3.22). Figure 3.23 shows $\langle \Delta F\rangle = \langle F^{(1)}\rangle - \langle F^{(2)}\rangle$ versus ka_1 for a systems of two spheres of radii a_1 and a_2 ($a_1, a_2 = 0.8a_1$ (curve *1*); $a_1, a_2 = a_1$ (curve *2*); $a_1, a_2 = 1.2a_1$ (curve *3*)) for $l = 4a_1$. The forces of interaction are strongly dependent on the size of the spheres and on their position relative to the wave propagation direction.

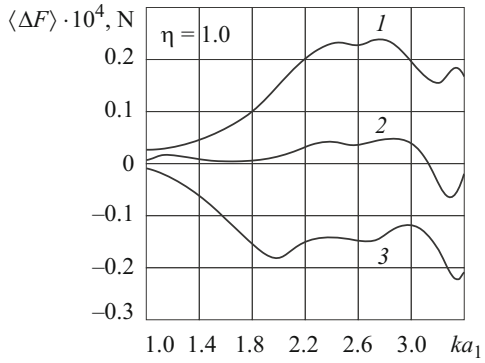

Fig. 3.23

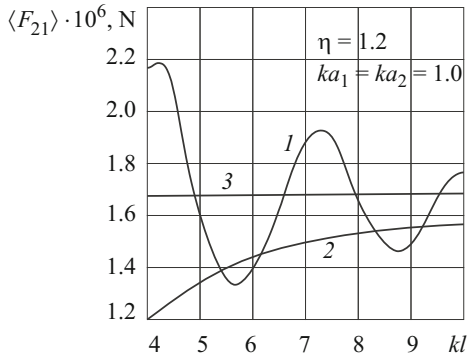

Fig. 3.24

Figure 3.24 shows the radiation force versus the distance between the centers of the spherical particles. Curves *1* and *2* represent the first and second spheres, respectively. Curve *3* represents a single sphere. It can be seen that the acoustic field has zones of attraction and repulsion of the particles and stable and unstable interfaces between these zones.

The propagation of a plane wave at a right angle to the line of the centers of two spheres of equal radii *a* spaced by a distance *l* was studied in [111, 129]. The problem was solved in long-wave approximation ($ka << 1$) for spheres spaced far apart ($kl >> 1$). Expressions for the radiation forces were derived in closed form. Their projections onto the line between the centers of the spheres are expressed as

$$\langle F^{(1)} \rangle = \frac{2}{9} A^2 \pi \rho_0 \frac{\sin(kl)}{kl} \alpha^6, \qquad \langle F^{(2)} \rangle = -\langle F^{(1)} \rangle. \tag{3.42}$$

The radiation forces (3.42) do not depend on the parameter $\eta = \rho_0 / \rho$. This is because the displacements of the spheres along the center-to-center line are negligible. The radiation forces decrease with increase in the distance between the spheres. They are zero at distances multiple of the half-wavelength. The behavior of the radiation forces suggests the existence of zones in the wave field in which the spheres are attracted or repulsed in the direction perpendicular to the wave vector. At the boundaries of the zones, the spheres form a stable or unstable pair. The motion of the spheres under radiation forces (3.42) was studied in [129]. Figure 3.25 shows a phase portrait of a specific system of two spherical particles. Depending on the distance of the spheres to the stable equilibrium position, they are either move apart in opposite directions (phase paths *1* and *2*) or oscillate about the equilibrium positions (phase paths *4*). The zones of oscillation and divergence are separated by separatrix *3*.

The effect of radiation forces on a system of two parallel cylindrically isotropic circular cylinders separated by a distance *l* and located along the propagation of a plane acoustic wave (3.23) was studied in [113, 119, 124]. An approach similar to that applied to the case of two spherical bodies was used. A system of two free solid cylinders of equal radii *a* and systems of two cylinders of different radii differently arranged relative to each other were considered. The cases of variable distance *l* between the cylinders at constant frequency and fixed distance *l* between them at variable frequency were examined.

Closed-form expressions for the radiation forces were derived for the case of $ka << 1$ and $kl >> 1$ using asymptotic representations of cylindrical functions of small and large arguments:

$$\langle F^{(1)} \rangle = \langle F \rangle + f, \qquad f = \frac{1}{\sqrt{kl}} \frac{A^2 \pi^{3/2} \rho_0}{4(1+\eta)} (\sin(2kl) + \cos(2kl)) \alpha^5, \tag{3.43}$$

$$\langle F^{(2)} \rangle = \langle F \rangle - A^2 \pi^{3/2} \rho_0 \frac{1}{4(1+\pi)} \frac{\alpha^5}{\sqrt{kl}}, \tag{3.44}$$

where $\langle F \rangle$ is the radiation force acting on a single cylinder (3.25). The forces of interaction are represented by the second terms. Figure 3.26 shows how the second cylinder acts on the first cylinder in water in which a wave of unit amplitude $\tilde{\lambda} = 0.1$ m propagates provided that $a / \tilde{\lambda} = 0.016$. The force is oscillating and strongly dependent on the parameter η, frequency, and distance *l* between the cylinders. It changes in both magnitude and direction with variation in frequency (wavelength).

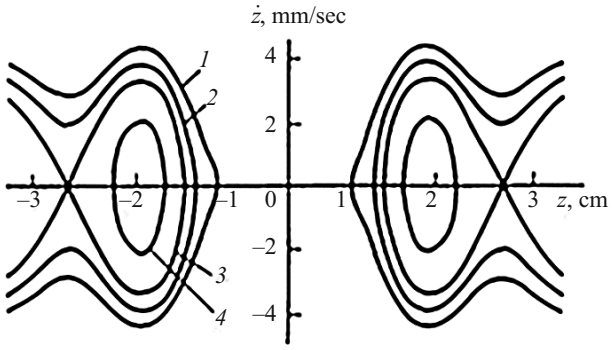

Fig. 3.25

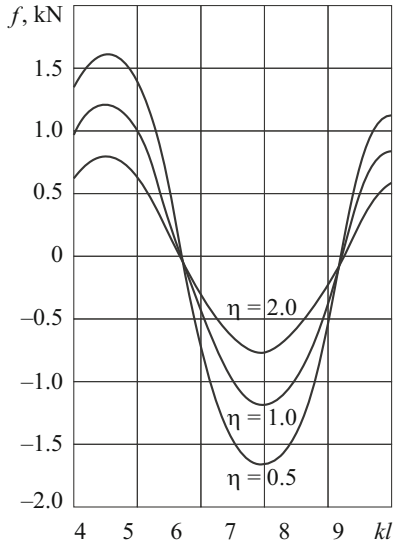

Fig. 3.26

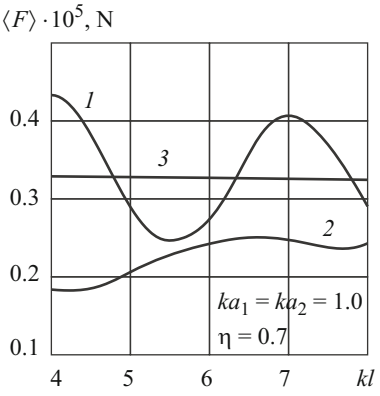

Fig. 3.27

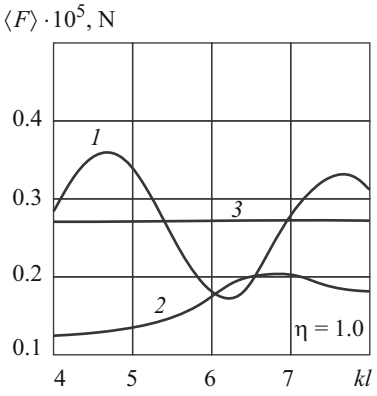

Fig. 3.28

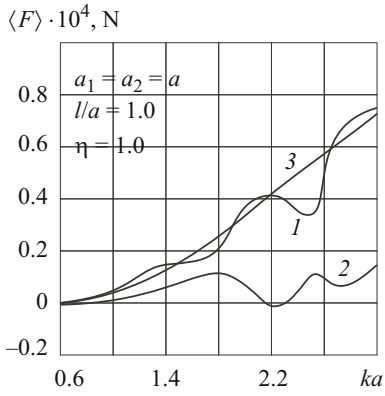

Fig. 3.29

Figures 3.27–3.29 show the radiation forces for cylinders in propanol (for $\mu^* = 0$) numerically calculated without constraints on the ratios of the wavelength to the radii of the cylinders and to the distance between them. The acoustic wave has amplitude $A = 0.9 \cdot 10^{-4}$ m^2/sec (Figs. 3.27 and 3.28) or energy flux density $I = 175.5$ W/m^2 and frequency (Fig. 3.29).

Curves *1* and *2* correspond to the first and second cylinders of equal radii, and curve *3* to a single cylinder. The second cylinder attracts the first one. The force of attraction depends on the distance *l* between the cylinders. Figure 3.28 shows more complex interaction of two systems of parallel cylinders of different radii (a_1 and a_2). Curve *1* corresponds to the first cylinder of system 1 ($ka_1 = 1.0$, $ka_2 = 1.3$), and curve *2* to the second cylinder of system 2 ($ka_1 = 1.3$, $ka_2 = 1.0$). Curve *3* represents a single cylinder ($ka = 1.0$). The interaction of the cylinders has a strong effect on the radiation forces acting on each of the cylinders (the deviation of curves *1* and *2* from curve *3*). The cylinders of different radii complicate the way the radiation forces depend on the distance: the cylinders can not only approach, but also move apart. As the frequency changes, the cylinders either rapidly or slowly approach each other (Fig. 3.29). This tendency is characterized by the deviation of curves *1* and *2*, which represent the first and second cylinders, respectively. Curve *3* represents a single cylinder. The deviation of curves *1* and *2* from curve *3* indicates how the cylinders interact. The higher the frequency, the stronger the interaction of the cylinders.

The propagation of a plane acoustic wave at a right angle to the plane of the axial lines of two free parallel cylinders of equal radii *a* spaced by a distance *l* was studied in [113]. An approach similar to that applied to the case of two spheres was used. The following expressions for the radiation forces were derived in long-wave approximation for cylinders spaced far apart:

$$\langle F_x^{(1)} \rangle = \frac{A^2}{8} \pi^{3/2} \rho_0 [\sin(kl) + \cos(kl)] \frac{\alpha^5}{\sqrt{kl}}, \tag{3.45}$$

$$\langle F_y^{(1)} \rangle = \langle F \rangle + \frac{A^2}{8} \pi^{3/2} \rho_0 [\sin(kl) + \cos(kl)] \frac{\alpha^5}{\sqrt{kl}}, \tag{3.46}$$

$$\langle F_x^{(2)} \rangle = -\langle F_x^{(1)} \rangle, \quad \langle F_y^{(2)} \rangle = \langle F_y^{(1)} \rangle, \tag{3.47}$$

where $\langle F_x^{(s)} \rangle$ ($s = 1, 2$) is the projection of the radiation force acting on the sth cylinder onto the ox-axis (the ox-axis is located in the plane of the cylinder axes and is perpendicular to the axis of cylinder 2); $\langle F_y^{(s)} \rangle$ is the projection of the radiation force onto the oy-axis parallel to the wave vector. In (3.46), $\langle F \rangle$ is the radiation force acting on a single cylinder in the same conditions (3.25).

It follows from (3.45)–(3.47) that the cylinders do not interact when they are far from each other ($kl \to \infty$) and when the wavelength $\tilde{\lambda}$ and distance l between the cylinder axes are related by $2l / \tilde{\lambda} = n + 3/4$. If $2l / \tilde{\lambda} = n + 1/4$, then the interaction of the cylinders is the most intensive. In this case, the radiation forces draw the cylinders together when n is even and diverge them when n is odd. It was assumed that n is large. As with two spheres, the forces of interaction do not depend on the parameter $\eta = \rho_0 / \rho$.

The methods proposed to solve problems of the effect of radiation forces in an acoustic field on a system of two objects were also used to solve the problem of the effect of radiation force on a body near a flat liquid surface [92, 93]. The effect of the radiation force caused by an acoustic wave (3.36) propagating at a right angle to a flat wall on a free spherical particle of radius a located at a distance l from the wall was studied in [132, 133, 177]. The wave field results from the interference of the incident wave and the waves reflected from the wall and scattered by the sphere. In determining the potentials of the acoustic field at the first stage, boundary conditions on the surface of the sphere and on the flat liquid surface are formulated. To solve the linear problem of the scattering of the acoustic wave by the spherical particle and the reflection of the wave scattered by the sphere from the flat liquid surface, the method of virtual images was used. This problem was reduced to the problem of the scattering of the wave by two spherical particles solved by determining the potentials of the reflected waves in a spherical coordinate system. The potentials of the waves were represented by generalized Fourier series of spherical wave functions with unknown constant coefficients. The case where $\alpha = ka << 1$ and $\beta = kl >> 1$ was examined. In this case, the infinite system of linear algebraic equations for the unknown coefficients obtained by satisfying the boundary conditions was solved using asymptotic representations of spherical functions and their derivatives of small and large arguments. At the second stage, certain potentials of the acoustic field are used to calculate the acoustic pressure in the fluid and the hydrodynamic force acting on the sphere. Its constant term (the radiation force obtained by averaging the hydrodynamic force over time) is given by

$$\langle F_{z_1} \rangle = -\frac{8}{3} A^2 \pi \rho_0 \frac{1-\eta}{2+\eta} \sin \beta \alpha^3 + O(\alpha^5). \tag{3.48}$$

The motion of a spherical particle, which is at the point z at time t, under the radiation force (3.48) was studied. The equation of its motion is

$$(m + m') \frac{d^2 z}{dt^2} = -\frac{8}{3} A^2 \pi \rho_0 \frac{1-\eta}{2+\eta} \alpha^3 \sin(2\kappa z), \tag{3.49}$$

where $m = 4/3\pi R^3 \rho_1$ is the mass of the spherical particle; $m' = 2/3\pi R^3 \rho_0$ is its added mass; $\eta = \rho_0 / \rho_1$. It was established that the radiation force (3.49) does not act on the spherical particle suspended in the fluid ($\eta = 1$). The radiation force is also zero at certain distances z_n from the flat boundary (equilibrium positions). The stable equilibrium positions for $\eta < 1$ are unstable equilibrium positions for $\eta > 1$. The particles oscillate about the stable equilibrium positions. Heavy particles ($\eta < 1$) have longer period T of oscillation than light particles ($\eta > 1$), their amplitudes being equal.

The effect of the radiation force on a solid cylinder located in parallel to and at a distance δ from a flat wall was studied in [97, 83]. The problem was solved using the approach applied to a solid spherical particle near flat liquid boundary. It was assumed that a plane acoustic wave is incident at an arbitrary angle θ on the wall. To solve the linear problem of the scattering of the acoustic wave by the solid cylinder and the reflection of the wave scattered by the cylinder from the flat liquid surface, the

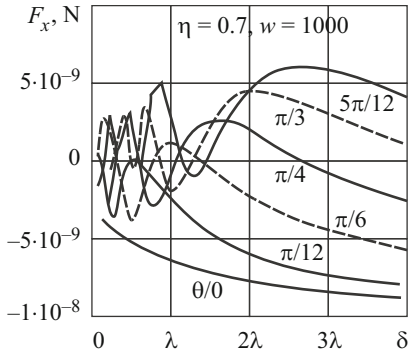

Fig. 3.30

method of virtual images was used. This problem was reduced to the problem of the scattering of the wave by two cylindrical bodies solved by determining the potentials of the reflected waves in a cylindrical coordinate system. The potentials of the waves were represented by generalized Fourier series of cylindrical wave functions with unknown constant coefficients. The long-wave case where $\alpha = ka << 1$ and $\beta = k\delta >> 1$ was examined. Expressions for the projections of the radiation force onto an axis perpendicular to and an axis parallel to the flat boundary were derived in [97]. The component of the radiation force perpendicular to the flat boundary

$$\langle F_x \rangle = A^2 \frac{\pi\rho_0}{a(1+\eta)} \sin(2k\delta\cos\theta)[(1-\eta)\cos 3\theta + 2\cos\theta] + O((ka)^5) \tag{3.50}$$

causes the cylinder to undergo motion described by a nonlinear oscillator equation. Its period of oscillations increases with the angle of incidence θ and strongly depends on the parameter η, wavelength, and the velocity amplitude of fluid parcels. In [83], the problem was solved numerically for a cylinder of radius $a = 0.005$ m in propanol through which a wave with energy flux density $I = 175.5$ W/m^2 propagates. The components of the force δ are most strongly dependent on the distance from the cylinder to the liquid boundary and the angle of incidence θ of the acoustic wave. Figure 3.30 shows how the component of the radiation force perpendicular to the boundary depends on these parameters. This dependence is complex for small values of δ.

Conclusions. In the publications reviewed, mathematical models and methods to study the dynamics of elastic bodies, solid particles, and fluid parcels in a viscous fluid were developed based on the linearized theories of a compressible viscous fluid and prestressed elastic bodies.

The basic results of these studies are the following.

1. Linearized equations for a compressible viscous fluid either at rest or undergoing nonstationary small harmonic motions (oscillations) were derived.

2. The general solutions of the three-dimensional equations of the linearized theory for a compressible viscous liquid were expressed in terms of scalar and vector potentials. The equations from which these potentials are derived were presented as well.

3. Representations of the general solutions in rectangular, circular cylindrical, and spherical coordinate systems were obtained, which made it possible to analyze the dynamic interaction of liquid and elastic bodies of such shapes with a compressible viscous fluid.

4. It was shown that by passing to the limit, these general solutions can be reduced to general solutions for simpler fluid models (incompressible viscous fluid; compressible or incompressible ideal fluid).

5. A problem statement was formulated and a method was proposed for studying the motion of solid bodies in a compressible fluid under the action of acoustic waves, the propagation of perturbations in elastic cylindrical shells filled with a compressible viscous fluid, and wave processes in prestressed elastic bodies interacting with a compressible viscous fluid.

6. A problem statement was formulated and the basic classes of elastokinetic problems for Rayleigh, Stoneley, Lamb waves and quasisurface, longitudinal, and torsional modes propagating in various hydroelastic systems (liquid and elastic half-spaces, a liquid layer and an elastic half-space, an elastic layer and a liquid half-space, elastic and liquid layers, a shell and a

hollow cylinder containing a fluid, an infinite body with a cylindrical cavity filled with a compressible viscous fluid, a solid cylinder in a fluid) were solved taking into account prestresses and the viscosity and compressibility of the fluid.

7. Dispersion equations in a general form invariant to the elastic potential function and valid for arbitrary compressible and incompressible materials were derived using general solutions of linearized problems of aerohydroelasticity for bodies with homogeneous prestrains and a compressible viscous fluid at rest. The basic classes of problems were solved numerically which made it possible to discover new properties, laws, and mechanical effects caused by the interaction of prestresses and dynamic stresses and the interaction of an elastic body and a viscous fluid.

The basic results are the following:

(a) in hydroelastic waveguides consisting of elastic bodies and a compressible viscous fluid, unlike ideal systems, damped waves propagate, these waves in a hydroelastic system with a compressible ideal fluid tending to become normal as the coefficient of viscosity tends to zero;

(b) the propagation of torsional modes in shell-like hydroelastic waveguides can only be studied using viscous fluid models, the viscous fluid having a strong effect on the wave process and generating damped waves;

(c) the viscosity of the fluid and the prestresses have a strong effect on the critical frequencies of waves and the phase velocities of modes at these frequencies;

(d) with increase in the compressibility of the fluid interacting with compressible elastic bodies, the number of propagating modes increases and their phase velocities and damping factors change substantially. Using an incompressible fluid model can lead to rather inaccurate quantitative and qualitative results;

(e) there are certain lengths of normal waves at which the prestresses do not affect their phase velocities and damping factors;

(f) there are certain numbers and frequencies of modes at which the viscosity of the fluid does not affect their phase velocities;

(g) the presence of a liquid layer gives rise to new quasi-Lamp waves with zero cutoff frequencies. The fluid changes the critical frequencies and the configuration of the dispersion curves and shifts them to the long-wave part of the spectrum;

(h) the localization of the low-order modes in the liquid layer–elastic layer system depends on the mechanical parameters of the hydroelastic system. The basic criterion of distribution of the normal low-order waves between the media is the ratio between the acoustic velocity in the fluid and the velocity of the quasi-Rayleigh wave propagating in the elastic layer near its free surface;

(i) the effect of the viscosity of the fluid is due to its interaction with the displacements occurring in the hydroelastic system during the propagation of waves. At those points of the modes where the shear displacements at the interface between the media are predominant, the effect of viscosity is the strongest and the damping factors and relative changes in the velocities are maximum;

(j) the effect of the viscosity of the liquid layer on the phase velocities and damping factors of all (except for the first) quasi-Lamb modes weakens with increase in the thickness of the elastic layer in the short-wave part of the spectrum of the hydroelastic waveguide;

(k) the three-dimensional linearized theory of waves allows, in both plane and spatial cases, determining the critical compression parameters at which surface instability occurs in highly elastic incompressible elastic bodies and hydroelastic systems.

8. The quantitative and qualitative data obtained made it possible to determine the errors introduced by simplified theories and simplified models of elastic and liquid media and the limits of applicability of results obtained with approximate applied two-dimensional theories, the linear classical theory of elasticity, and incompressible viscous or ideal fluid models.

9. The interaction of an acoustic wave with objects in a compressible (viscous or ideal) fluid by means of radiation (time average) forces was studied, including:

(a) statement of general problems to be solved to find the time-average force and the force of interaction between objects (without constraints on the wavelength and the size of the objects) and development of methods to solve them;

(b) solution of some classes of problems for solid and flexible particles of specific shape (a spherical particle, a cylindrical particle, two spherical particles, two cylindrical particles) in a fluid through which a plane acoustic wave propagates in various directions;

(c) analysis of new mechanical effects due to the interaction of objects in an acoustic field and the viscosity of the fluid.

10. A method to calculate the stresses in an acoustic wave in a compressible viscous fluid was developed based on a simplified system of nonlinear hydroelastic equations that include both nonlinear and dissipative terms. An expression for the stresses in a compressible viscous fluid up to second-order terms with respect to the Mach number was derived from the potentials of the velocity field of the fluid determined with the same accuracy from the linearized hydroelastic equations. The radiation (the constant component of the hydrodynamic force) force acting on the body is the period-average surface integral of internal product of the stress tensor in the fluid and the unit normal vector to the surface of the elastic body.

11. An analogy was established between a compressible viscous fluid whose flow is described by the system of linearized hydroelastic equations and a linear viscoelastic body that behaves as a Voigt body upon change in volume and as a Newton body upon change in shape. This analogy allowed reducing the problem of the small harmonic oscillations of a compressible viscous fluid to the problem of the stationary harmonic vibrations of a viscoelastic body. This made it possible to reduce the problem of the scattering of an acoustic wave by free solid particles in a compressible viscous fluid, which is solved to determine the velocity potentials of the fluid, to the problem of diffraction of an isothermal harmonic expansion wave by perfectly rigid bodies in a viscoelastic medium, which is solved using methods used in solid mechanics to solve problems of the diffraction of elastic waves in multiply connected domains.

12. The approach developed in the reviewed studies allows studying the behavior of systems of solid particles in a compressible viscous fluid without constraints on the ratio of the wavelength to the size of and the distances between the particles.

13. Passing to the limit in the expressions for viscous fluid as the coefficients of viscosity tend to zero made it possible to apply the approach to the case of a compressible ideal fluid.

14. Analytic closed-form solutions were found for a solid particle much smaller than the length of the acoustic wave. Such a solution was also obtained for a system of two solid particles in an ideal fluid in the case where they are smaller than the wavelength, which, in turn, is shorter than the distance between the particles. Comparing the results obtained numerically and by approximate formulas allowed identifying the ranges of the parameters of the fluid, solid particles, and acoustic wave in which the approximate formulas can be used to calculate the time-average forces with adequate accuracy.

15. The effect of the time-average forces acting on single solid particles and systems of two particles in either ideal or viscous fluid through which an acoustic wave propagates was analyzed numerically and with approximate formulas. New mechanical effects were discovered, of which the most important are the following:

(a) the time-average force acting on a solid particle in a fluid is strongly dependent on the ratio of the density of the fluid to the density of the particle and increases with frequency;

(b) at the same frequency, the time-average force acting on a solid particle in a compressible viscous fluid is strongly dependent on the dynamic coefficient of viscosity. The higher the viscosity of the fluid, the stronger the time-average force exerted by the acoustic wave. This force is several orders of magnitude higher than the radiation force acting on the particle in an ideal fluid;

(c) unlike ideal fluid, the direction of the time-average force acting on the particle in a compressible viscous fluid depends on the ratio of the density of the fluid to the density of the particle;

(d) free particles located in a fluid along the propagation direction of the acoustic wave are under time-average forces which change in both magnitude and direction with the distance between the particles, the frequency being constant. In this connection, there are zones of attraction in the acoustic field in which the time-average force draws the particles together and zones of repulsion in which particles go away from each other. At the interfaces between these zones, the pair of particles is either stable or unstable;

(e) a system of two free particles perpendicular to the wave propagation direction in a fluid is subject to the time-average force acting both in parallel to the wave propagation direction and in perpendicular direction. The forces that are perpendicular to the wave propagation direction decrease with increase in the distance between the particles. They are not monotonic functions of the distance, but change in both magnitude and direction. As a result, the zones of attraction and repulsion of the particles occur;

(f) the direction of the radiation force acting on a liquid drop depends on the ratio of the density of the drop to the density of the surrounding fluid. The radiation force increases as the frequency of the acoustic wave tends to the resonant frequency of pulsations of the drop and changes its direction at the resonant frequency;

(g) depending on the frequency, the radiation force acting on the particle in the cavity (unlike the unbounded fluid) is directed either along wave propagation or in the opposite direction. At some frequencies, the radiation force changes resonantly.

In the reviewed studies, the general problem of the action of the time-average force on solid particles was formulated and a method to solve it was developed, which makes it possible to analyze the behavior of particles in an acoustic field irrespective of the ratio of the wavelength to the size of and the distance between the particles. In this connection, the results obtained can be used to validate results produced by using simplified approaches.

Note that we have reviewed only some results on the dynamics of elastic bodies, solid particles, and fluid parcels in a compressible viscous fluid. Those results were preferred that were obtained using the three-dimensional linearized theory and taking into account the prestresses in elastic bodies and the viscosity and compressibility of the fluid. The results obtained at the S. P. Timoshenko Institute of Mechanics in recent years have been discussed in more detail.

REFERENCES

1. V. N. Alekseev, "The radiation pressure force on a sphere revisited," *Akust. Zh.*, **29**, No. 2, 129–136 (1983).
2. W. Altberg, "Uber die Druckkrafte der Schallwellen und die absolute Messung der Schallintensitat (On the force due to sound waves and the absolute measurement of sound intensity)," *Annalen der Physik*, **11**, 405–420 (1903).
3. S. Yu. Babich, A. N. Guz, and A. P. Zhuk, "Elastic waves in bodies with initial stresses," *Int. Appl. Mech.*, **15**, No. 4, 277–291 (1979).
4. S. Yu. Babich and A. P. Zhuk, "Revisiting the theory of Stoneley waves at the cylindrical interface between a fluid and a prestrained body," *Dokl. AN USSR*, *Ser. A*, No. 7, 36–39 (1981).
5. A. M. Bagno, "Small-perturbation propagation in a system consisting of a preliminarily stressed incompressible cylinder and fluid," *Int. Appl. Mech.*, **16**, No. 6, 487–491 (1980).
6. A. M. Bagno, "Propagation of longitudinal waves in a prestressed compressible cylinder containing a liquid," *Int. Appl. Mech.*, **16**, No. 8, 672–676 (1980).
7. A. M. Bagno, "The question of the influence of initial stresses on the "backward wave" in a prestressed compressible cylinder–fluid system," *Int. Appl. Mech.*, **19**, No. 3, 245–248 (1983).
8. A. M. Bagno, "Effect of initial stresses on wave propagation through compressible cylinder containing viscous compressible fluid," *Int. Appl. Mech.*, **20**, No. 4, 387–392 (1984).
9. A. M. Bagno, "Influence of a viscous compressible fluid on stoneley wave propagation on the interface of solid and liquid media," *Int. Appl. Mech.*, **20**, No. 6, 557–560 (1984).
10. A. M. Bagno, "Influence of a fluid on the velocities of axisymmetric waves in a prestrained compressible cylinder," *Gidromekh.*, **50**, 34–36 (1984).
11. A. M. Bagno, "Effect of finite strains on the velocities of Stoneley waves in highly elastic incompressible half-space interacting with an ideal fluid," *Prikl. Mekh.*, **21**, No. 6, 116–119 (1985).
12. A. M. Bagno, "Influence of initial stress on surface waves in a system consisting of a preliminarily deformed compressible body and a viscous compressible liquid," *Int. Appl. Mech.*, **22**, No. 6, 523–526 (1986).
13. A. M. Bagno, "Effect of initial stresses on the velocity of surface waves in a compressible half-space interacting with an ideal liquid layer," *Int. Appl. Mech.*, **25**, No. 1, 95–99 (1989).
14. A. M. Bagno, "Effect of the initial stresses on the wave process in a compressible elastic half-space interacting with a viscous liquid layer," *Dokl. AN USSR*, *Ser. A*, No. 8, 22–25 (1989).
15. A. M. Bagno, "Waves in a prestrained elastic half-space interacting with a compressible viscous liquid layer," in: *Proc. All-Union Symp. on Interaction of Acoustic Waves with Elastic Bodies* (Tallinn, October 26–27, 1989) [in Russian], Tallinn (1989), pp. 22–25.
16. A. M. Bagno, "Effect of finite strains on the wave process in an incompressible half-space under a viscous liquid layer," *Dokl. AN USSR*, *Ser. A*, No. 7, 36–40 (1990).
17. O. M. Bagno, "Propagation of waves in a prestrained incompressible elastic layer interacting with a compressible ideal liquid layer," *Visn. Kyiv. Nats. Univ. im. T. Shevchenka*, *Ser.: Fiz.-Mat. Nauky*, No. 3, 22–27 (2014).
18. O. M. Bagno, "A wave process in a compressible elastic layer interacting with a viscous liquid layer," in: *Problems of Computational Mechanics and Structural Strength* [in Ukrainian], Issue 23, Lira, Dnipropetrovsk (2014), pp. 27–39.
19. O. M. Bagno, "Waves in a prestrained compressible elastic layer interacting with a compressible viscous liquid layer," *Visn. Kyiv. Nats. Univ. im. T. Shevchenka*, *Ser.: Fiz.-Mat. Nauky*, No. 4, 63–68 (2014).

20. O. M. Bagno, “Dispersion of waves in an elastic layer under a viscous liquid layer,” *Dop. NAN Ukrainy*, No. 5, 40–46 (2015).
21. A. M. Bagno, “Frequency spectrum of normal waves in a prestressed compressible layer interacting with an idela liquid layer,” *Dop. NAN Ukrainy*, No. 6, 30–36 (2015).
22. A. M. Bagno, “Lamb waves in an elastic layer–ideal liquid layer system,” *Dop. NAN Ukrainy*, No. 7, 39–46 (2015).
23. A. M. Bagno, “Localization of quasi-Lamb waves in an elastic layer–ideal liquid layer system,” *Dop. NAN Ukrainy*, No. 2, 38–46 (2016).
24. A. M. Bagno, “Quasi-Lamb waves in a prestressed compressible elastic layer–ideal liquid layer system,” *Dop. NAN Ukrainy*, No. 3, 38–47 (2016).
25. A. M. Bagno, “Effect of a viscous fluid on quasi-Lamb waves in an elastic layer interacting with a liquid layer,” *Dop. NAN Ukrainy*, No. 4, 41–48 (2016).
26. A. M. Bagno and A. N. Guz, “Effect of a fluid on the propagation of longitudinal waves in a prestressed incompressible cylinder,” *Dokl. AN USSR*, *Ser. A*, No. 9, 39–42 (1980).
27. A. M. Bagno and A. N. Guz, “Wave propagation in a previously stressed, incompressible cylinder containing a viscous compressible liquid,” *Mech. Comp. Mater.*, **18**, No. 2, 250–254 (1982).
28. A. M. Bagno and A. N. Guz, “Propagation of small perturbations in a prestressed compressible body–compressible viscous fluid system,” *Izv. AN SSSR*, *Mekh. Tverd. Tela*, No. 1, 167–170 (1983).
29. A. M. Bagno and A. N. Guz, “Effect of initial stresses on the speed of waves in a hollow cylinder with a fluid,” *Int. Appl. Mech.*, **22**, No. 3, 211–215 (1986).
30. A. M. Bagno and A. N. Guz, “Stoneley waves at the interface between a prestressed incompressible half-space and a compressible viscous fluid,” *Izv. AN SSSR*, *Mekh. Tverd. Tela*, No. 3, 107–110 (1987).
31. A. M. Bagno and A. N. Guz, “Elastic waves in prestressed bodies interacting with a fluid (survey),” *Int. Appl. Mech.*, **33**, No. 6, 435–463 (1997).
32. A. M. Bagno, A. N. Guz, and V. I. Efremov, “Effect of initial strains on the propagation of waves in an incompressible cylinder located in an ideal fluid,” *Int. Appl. Mech.*, **30**, No. 8, 582–585 (1994).
33. A. M. Bagno, A. N. Guz, and G. I. Shchuruk, “Influence of initial strains on the wave velocity in a prestressed incompressible half-space interacting with an ideal fluid layer,” *Int. Appl. Mech.*, **24**, No. 6, 593–597 (1988).
34. A. M. Bagno, A. N. Guz, and G. I. Shchuruk, “Waves in a viscous layer of fluid on an elastic half-space,” *Int. Appl. Mech.*, **26**, No. 4, 317–320 (1990).
35. A. M. Bagno, A. N. Guz, and G. I. Shchuruk, “Nonaxisymmetric waves in an orthotropic timoshenko shell containing a viscous fluid,” *Int. Appl. Mech.*, **26**, No. 12, 1132–1138 (1990).
36. A. M. Bagno, A. N. Guz, and G. I. Shchuruk, “Waves in a prestressed elastic layer in compression interacting with an ideal fluid,” *Int. Appl. Mech.*, **30**, No. 2, 85–90 (1994).
37. A. M. Bagno, A. N. Guz, and G. I. Shchuruk, “Influence of fluid viscosity on waves in an initially deformed, compressible, elastic layer interacting with a fluid medium,” *Int. Appl. Mech.*, **30**, No. 9, 643–649 (1994).
38. A. M. Bagno and V. P. Koshman, “Effect of finite prestrains on the velocities of Rayleigh waves in an incompressible half-space,” *Dokl. AN USSR*, *Ser. A*, No. 9, 18–20 (1983).
39. O. M. Bagno and G. I. Shchuruk, “Features of the wave process in an elastic layer–viscous fluid system,” *Dop. AN Ukrainy*, *Mat.*, *Pryrodozn.*, *Tekhn. Nauky*, No. 9, 52–56 (1993).
40. A. S. Basmat, A. N. Guz, and A. P. Zhuk, “Wave and nonstationary motions of rigid bodies in a compressible viscous fluid,” in: A. N. Guz (ed.), *Dynamics of Bodies Interacting with a Medium* [in Russian], Naukova Dumka, Kyiv (1991), pp. 6–52.
41. T. I. Belyankova and V. V. Kalinchuk, “On the problem of analyzing the dynamic properties of a layered half-space,” *Acoust. Phys.*, **60**, No. 5, 530–542 (2014).
42. D. R. Bland, *The Theory of Linear Viscoelasticity*, Pergamon Press, Oxford (1960).
43. L. M. Brekhovskikh and O. A. Godin, *Acoustics of Layered Media*, Springer-Verlag, Berlin (1998–1999).
44. A. I. Vesnitskii and G. A. Utkin, “Motion of a body along a string under wave pressure forces,” *Dokl. AN SSSR*, **302**, No. 2, 278–280 (1988).
45. I. A. Viktorov, *Surface Acoustic Waves in Solids* [in Russian], Nauka, Moscow (1981).

46. M. M. Vol'kenshtein and V. M. Levin, "Structure of a Stoneley wave at the interface between a viscous fluid and a solid," *Akust. Zh.*, **34**, No. 4, 608–615 (1988).
47. R. F. Ganiev and L. E. Ukrainskii, *Dynamics of Particles Subject to Vibrations* [in Russian], Naukova Dumka, Kyiv (1975).
48. Z. A. Gol'dberg, "Sound pressure," in: L. D. Rosenberg (ed.), *High-Power Ultrasonic Fields* [in Russian], Nauka, Moscow (1968), pp. 49–86.
49. Z. A. Gol'dberg and K. A. Naugol'nykh, "Rayleigh sound pressure," *Akust. Zh.*, **9**, No. 1, 28–31 (1963).
50. L. P. Gor'kov, "The forces acting on a small particle in an acoustic field in an ideal fluid," *Dokl. AN SSSR*, **140**, No. 1, 88–91 (1961).
51. V. T. Grinchenko and G. L. Komissarova, "Wave propagation in a hollow elastic cylinder with a fluid," *Int. Appl. Mech.*, **20**, No. 1, 18–23 (1984).
52. V. T. Grinchenko and G. L. Komissarova, "Properties of normal nonaxisymmetric waves in a hollow fluid-filled cylinder," *Int. Appl. Mech.*, **24**, No. 10, 950–954 (1988).
53. V. T. Grinchenko and G. L. Komissarova, "Surface waves in an elastic layer on a liquid half-space system," *Akust. Visn.*, **8**, No. 4, 38–45 (2005).
54. V. T. Grinchenko and V. V. Meleshko, *Harmonic Vibrations and Waves in Elastic Bodies* [in Russian], Naukova Dumka, Kyiv (1981).
55. A. N. Guz, *Stability of Three-Dimensional Deformable Bodies* [in Russian], Naukova Dumka, Kyiv (1971).
56. A. N. Guz, *Stability of Elastic Bodies Subject to Finite Deformations* [in Russian], Naukova Dumka, Kyiv (1973).
57. A. N. Guz, "Representation of general solutions in the linearized theory of elasticity of compressible bodies," *Dokl. AN USSR*, *Ser. A*, No. 8, 700–703 (1975).
58. A. N. Guz, "Representation of general solutions in the linearized theory of elasticity of incompressible bodies," *Dokl. AN USSR*, *Ser. A*, No. 12, 1092–1095 (1975).
59. A. N. Guz, "Linearized theory of propagation of elastic waves in bodies with initial stresses," *Int. Appl. Mech.*, **14**, No. 4, 339–362 (1978).
60. A. N. Guz, "Love waves in prestressed bodies," *Dokl. AN USSR*, *Ser. A*, No. 12, 1092–1095 (1978).
61. A. N. Guz, *Stability of Elastic Bodies under Triaxial Compression* [in Russian], Naukova Dumka, Kyiv (1979).
62. A. N. Guz, "Hydroelastic problems for a viscous fluid and prestressed elastic bodies," *Dokl. AN SSSR*, **251**, No. 2, 305–308 (1980).
63. A. N. Guz, "Aerohydroelasticity problems for bodies with initial stresses," *Int. Appl. Mech.*, **16**, No. 3, 175–190 (1980).
64. A. N. Guz, "Representation of solutions to the linearized Navier–Stokes equations," *Dokl. AN SSSR*, **253**, No. 4, 825–827 (1980).
65. A. N. Guz, "Representation of solutions to the linearized Navier–Stokes equations for a moving fluid," *Dokl. AN SSSR*, **255**, No. 5, 1066–1068 (1980).
66. A. N. Guz, "Wave propagation in a cylindrical shell containing a viscous compressible liquid," *Int. Appl. Mech.*, **16**, No. 10, 842–850 (1980).
67. A. N. Guz, "Dynamics of rigid bodies in an incompressible viscous fluid (quiescent liquid)," *Int. Appl. Mech.*, **17**, No. 3, 207–223 (1981).
68. A. N. Guz, "An analogy in continuum mechanics," *Dokl. AN SSSR*, **263**, No. 3, 563–565 (1982).
69. A. N. Guz, *Brittle Fracture Mechanics of Prestressed Materials* [in Russian], Naukova Dumka, Kyiv (1983).
70. A. N. Guz, *Fundamentals of the Three-Dimensional Theory of Stability of Deformable Bodies* [in Russian], Vyshcha Shkola, Kyiv (1986).
71. A. N. Guz, *General Issues*, Vol. 1 of the two-volume series *Elastic Waves in Prestressed Bodies* [in Russian], Naukova Dumka, Kyiv (1986).
72. A. N. Guz, *Propagation Laws*, Vol. 2 of the two-volume series *Elastic Waves in Prestressed Bodies* [in Russian], Naukova Dumka, Kyiv (1986).
73. A. N. Guz, "Problems of hydroelasticity for compressible viscous fluids," *Int. Appl. Mech.*, **27**, No. 1, 1–12 (1991).
74. A. N. Guz, "Elastic waves in compressible materials with initial stresses and a nondestructive ultrasonic method for the determination of biaxial residual stresses," *Int. Appl. Mech.*, **30**, No. 1, 1–14 (1994).
75. A. N. Guz, *Dynamics of Compressible Viscous Fluid* [in Russian], A.S.K., Kyiv (1998).

76. A. N. Guz, "Compressible, viscous fluid dynamics (review). Part I," *Int. Appl. Mech.*, **36**, No. 1, 14–39 (2000).
77. A. N. Guz, "Necessary and sufficient conditions for fescription of the motion of objects in a viscous fluid under ultrasonic actions," *Int. Appl. Mech.*, **36**, No. 2, 197–202 (2000).
78. A. N. Guz, "The dynamics of a compressible viscous liquid (review). II," *Int. Appl. Mech.*, **36**, No. 3, 281–302 (2000).
79. A. N. Guz, *Elastic Waves in Bodies with Initial* (*Residual*) *Stresses* [in Russian], A.S.K., Kyiv (2004).
80. A. N. Guz and A. M. Bagno, "Stoneley waves on the interface of an elastic half-space with initial stresses and a viscous compressible fluid," *Int. Appl. Mech.*, **20**, No. 12, 1089–1092 (1984).
81. A. N. Guz and A. M. Bagno, "Effect of the prestresses on the velocities of waves in a prestrained compressible layer contacting with a liquid half-space," *Dokl. AN SSSR*, **329**, No. 6, 715–717 (1993).
82. A. N. Guz, A. M. Bagno, and G. I. Shchuruk, "Axisymmetric elastic waves in an orthotropic cylindrical shell containing a compressible viscous fluid," *Dokl. AN USSR*, *Ser. A*, No. 9, 41–46 (1989).
83. O. M. Guz, N. V. Gerashchenko, and O. P. Zhuk, "Effect of an acoustic wave on a cylindrical particle near a flat solid boundary," *Dop. NAN Ukrainy*, No. 2, 52–56 (1996).
84. A. N. Guz and V. T. Golovchan, *Diffraction of Elastic Waves in Multiply Connected Bodies* [in Russian], Naukova Dumka, Kyiv (1972).
85. A. N. Guz and A. P. Zhuk, "Hydrodynamic forces acting in an acoustic field in a viscous fluid," *Dokl. AN SSSR*, **266**, No. 1, 32–35 (1982).
86. A. N. Guz and A. P. Zhuk, "Nonlinear problems in the theory of small vibrations of particles in a compressible viscous fluid," in: *Proc. 9th Int. Conf. on Nonlinear Vibrations: Application of Methods of Nonlinear Vibration Theory in Mechanics*, *Physics*, *Electronics*, *and Biology* [in Russian], 3, Naukova Dumka, Kyiv (1984), pp. 85–88.
87. A. N. Guz and A. P. Zhuk, "Forces acting on a spherical particle in an acoustic field in a viscous fluid," *Sov. Phys. Dokl.*, **29**, 98 (1984).
88. A. N. Guz and A. P. Zhuk, "Hydrodynamic interaction of two spherical particles in an acoustic wave field in an ideal fluid," *Dokl. AN SSSR*, **279**, No. 3, 566–570 (1984).
89. A. N. Guz and A. P. Zhuk, "Motion of two parallel cylinders in an acoustic wave field in a viscous fluid," *Izv. AN SSSR*, *Mekh. Tverd. Tela*, No. 6, 158–164 (1990).
90. A. N. Guz and A. P. Zhuk, "Effect of an acoustic wave on solid particles in a fluid," in: *Nonlinear Dynamic Problems for Machines* [in Russian], Inst. Mashinovedeniya, Moscow (1992), pp. 43–52.
91. A. N. Guz and A. P. Zhuk, "Dynamics of solid particles in a fluid under the action of an acoustic field. Model of a piecewise-homogeneous medium (review)," *Int. Appl. Mech.*, **29**, No. 5, 329–344 (1993).
92. A. N. Guz and A. P. Zhuk, "Dynamics of particles near a plane boundary in the radiation field of an acoustic wave," *Int. Appl. Mech.*, **35**, No. 10, 1040–1045 (1999).
93. A. N. Guz and A. P. Zhuk, "Motion of a solid particle near a flat liquid boundary in the field of average forces of an acoustic wave," in: *Problems of Mechanics* [in Russian], Fizmatlit, Moscow (2003), pp. 342–349.
94. A. N. Guz and A. P. Zhuk, "Motion of solid particles in a liquid under the action of an acoustic field: The mechanism of radiation pressure," *Int. Appl. Mech.*, **40**, No. 3, 246–265 (2004).
95. A. N. Guz and A. P. Zhuk, "Motion of solid particles under the action of an acoustic field in a fluid," Vol. 5 of the six-volume series A. N. Guz (ed.), *Advances in Mechanics* [in Russian], Litera, Kyiv (2009), pp. 144–166.
96. A. N. Guz and A. P. Zhuk, "Effect of acoustic radiation in a viscous liquid on a spherical drop of ideal liquid," *Int. Appl. Mech.*, **50**, No. 6, 605–614 (2014).
97. O. M. Guz, O. P. Zhuk, and N. V. Gerashchenko, "Motion of a cylinder near a flat solid surface in the radiation field of an acoustic wave," *Dop. NAN Ukrainy*, No. 11, 61–65 (1994).
98. A. N. Guz, A. P. Zhuk, and F. G. Makhort, *Waves in a Prestressed Layer* [in Russian], Naukova Dumka, Kyiv (1976).
99. A. N. Guz (ed.), S. Markus, L. Pust, et al., *Dynamics of Bodies Interacting with a Medium* [in Russian], Naukova Dumka, Kyiv (1991).
100. A. N. Guz, F. G. Makhort, and O. I. Gushcha, *An Introduction to Acoustoelasticity* [in Russian], Naukova Dumka, Kyiv (1977).
101. A. N. Guz, F. G. Makhort, O. I. Gushcha, and V. K. Lebedev, *Fundamentals of the Ultrasonic Nondestructive Stress Analysis of Solids* [in Russian], Naukova Dumka, Kyiv (1974).

102. S. D. Danilov, "Average force acting on a small sphere in a traveling wave field in a viscous fluid," *Akust. Zh.*, **31**, No. 1, 45–49 (1985).
103. S. D. Danilov and M. A. Mironov, "One-dimensional modeling of average forces in acoustics," *Akust. Zh.*, **30**, No. 3, 306–309 (1984).
104. S. D. Danilov and M. A. Mironov, "Radiation pressure force acting on a small particle in an acoustic field," *Akust. Zh.*, **30**, No. 6, 467–473 (1984).
105. S. D. Danilov and M. A. Mironov, "Radiation pressure force acting on a small scatterer moving in a uniform isotropic field," *Akust. Zh.*, **36**, No. 1, 21–24 (1990).
106. A. P. Zhuk, "Stoneley waves in a prestressed medium," *Prikl. Mekh.*, **16**, No. 1, 113–116 (1980).
107. O. P. Zhuk, "Stoneley waves at the interface between a fluid and a prestressed body," *Dop. AN URSR*, *Ser. A*, No. 4, 36–40 (1980).
108. A. P. Zhuk, "Interaction of a sound wave with solid particles in a viscous fluid," *Int. Appl. Mech.*, **19**, No. 11, 1013–1020 (1983).
109. A. P. Zhuk, "Average hydrodynamic force acting on a spherical particle in an acoustic field in a viscous fluid," *Prikl. Mekh.*, **20**, No. 1, 126–127 (1984).
110. A. P. Zhuk, "Hydrodynamic interaction of two spherical particles from sound waves," *Int. Appl. Mech.*, **20**, No. 9, 875–880 (1984).
111. A. P. Zhuk, "Hydrodynamic interaction of two spherical particles due to sound waves propagating perpendicularly to the center line," *Int. Appl. Mech.*, **21**, No. 3, 307–312 (1985).
112. A. P. Zhuk, "Radiation force acting on a cylindrical particle in a sound field," *Int. Appl. Mech.*, **22**, No. 7, 689–693 (1986).
113. A. P. Zhuk, "Interaction of two parallel cylinders located in tandem along the direction of sound wave propagation," *Int. Appl. Mech.*, **23**, No. 8, 782–788 (1987).
114. A. P. Zhuk, "Interaction of two parallel cylinders in the propagation of a sound wave perpendicular to the plane of the axial lines," *Int. Appl. Mech.*, **23**, No. 11, 1101–1106 (1987).
115. A. P. Zhuk, "Interaction of a solid cylinder with a sound wave in a viscous fluid," *Int. Appl. Mech.*, **24**, No. 1, 94–99 (1988).
116. A. P. Zhuk, "Motion of a cylinder in the radiation field of a standing acoustic wave," *Prikl. Mekh.*, **25**, No. 3, 123–126 (1989).
117. A. P. Zhuk, "Interaction of two spherical bodies in an ideal fluid through which an acoustic wave propagates," *Dokl. AN USSR*, *Ser. A*, No. 5, 30–33 (1989).
118. A. P. Zhuk, "Applicability of the theory of viscoelasticity to problems of the interaction between an acoustic wave and rigid bodies in a viscous fluid," *Dokl. AN USSR*, *Ser. A*, No. 6, 35–38 (1989).
119. A. P. Zhuk, "Interaction of two parallel circular cylinders in an ideal fluid through which an acoustic wave propagates," *Dokl. AN USSR*, *Ser. A*, No. 8, 28–32 (1989).
120. A. P. Zhuk, "Interaction of two bodies in an ideal fluid through which a plane acoustic wave propagates," in: *Proc. All-Union Symp. on Interaction of Acoustic Waves with Elastic Bodies* (Tallinn, October 26–27, 1989) [in Russian], Tallinn (1989), pp. 92–95.
121. A. P. Zhuk, "Using the theory of viscoelasticity to study the interaction of an acoustic wave with a cylinder in a viscous fluid," *Dokl. AN USSR*, *Ser. A*, No. 3, 49–52 (1990).
122. A. P. Zhuk, "Using the theory of viscoelasticity to study the interaction of two parallel cylinders in a viscous fluid through which an acoustic wave propagates," *Dokl. AN USSR*, *Ser. A*, No. 4, 42–45 (1990).
123. A. P. Zhuk, "Action of an acoustic wave on a system of two spherical bodies in an ideal fluid," *Int. Appl. Mech.*, **26**, No. 5, 510–514 (1990).
124. A. P. Zhuk, "Action of an acoustic wave on a system of two parallel circular cylinders in an ideal fluid," *Int. Appl. Mech.*, **27**, No. 1, 101–106 (1991).
125. A. P. Zhuk, "Using the theory of viscoelasticity to study the interaction of an acoustic wave with a spherical particle in a viscous fluid," *Dokl. AN USSR*, *Ser. A*, No. 2, 30–34 (1991).
126. A. P. Zhuk, "A study of the interaction of an acoustic wave in a viscous liquid with two cylinders placed in parallel," *Int. Appl. Mech.*, **27**, No. 3, 321–327 (1991).

127. A. P. Zhuk, "Effect of an acoustic wave on a system of two spheres in a viscous fluid," *Prikl. Mekh.*, **29**, No. 2, 110–116 (1993).
128. O. P. Zhuk, "Effect of the radiation force on a solid sphere in a fluid flow," *Dop. NAN Ukrainy*, No. 7, 50–54 (2000).
129. O. P. Zhuk, "Motion of a system of solid particles in the radiation field of an acoustic wave," *Visn. Kyiv. Nats. Univ. im. T. Shevchenka*, *Ser. Fiz.-Mat. Nauky*, No. 5, 275–279 (2001).
130. A. P. Zhuk, "Effect of acoustic radiation on a spherical drop of liquid," *Int. Appl. Mech.*, **43**, No. 7, 726–733 (2007).
131. O. P. Zhuk, "Motion of a spherical liquid drop under the radiation force of an acoustic field," *Dop. NAN Ukrainy*, No. 7, 55–59 (2007).
132. O. P. Zhuk, "Effect of acoustic radiation forces on a spherical particle near a flat liquid surface," *Dop. NAN Ukrainy*, No. 7, 71–76 (2008).
133. A. P. Zhuk, "Dynamics of a spherical particle near a flat liquid boundary under acoustic radiation forces," *Int. Appl. Mech.*, **44**, No. 11, 1223–1232 (2008).
134. O. P. Zhuk, V. D. Kubenko, and Ya. O. Zhuk, "The radiation force of a plane acoustic wave acting on a spherical body in a cylindrical cavity filled with a fluid," *Dop. NAN Ukrainy*, No. 9, 48–54 (2012).
135. A. P. Zhuk, V. D. Kubenko, and Ya. A. Zhuk, "Acoustic radiation acting on a liquid sphere in a circular cylinder filled with a fluid," *Int. Appl. Mech.*, **49**, No. 5, 501–511 (2013).
136. L. K. Zarembo and V. A. Krasil'nikov, *Introduction to Nonlinear Acoustics* [in Russian], Nauka, Moscow (1966).
137. L. K. Zarembo and V. I. Timoshenko, *Nonlinear Acoustics* [in Russian], Izd. MGU, Moscow (1984).
138. P. V. Zinin, V. M. Levin, O. I. Lobkis, and R. G. Maev, "Radiation pressure forces in the focal region of an acoustic microscope," *Akust. Zh.*, **32**, No. 6, 785–790 (1986).
139. I. N. Kanevskii, "Constant forces in an acoustic field (review), *Akust. Zh.*, **7**, No. 1, 3–17 (1961).
140. G. L. Komissarova, "Solution of a problem concerning propagation of elastic waves in a fluid-containing cylinder," *Int. Appl. Mech.*, **26**, No. 8, 735–738 (1990).
141. V. A. Krasil'nikov and V. V. Krylov, *Introduction to Physical Acoustics* [in Russian], Nauka, Moscow (1984).
142. R. M. Christensen, *Theory of Viscoelasticity. An Introduction*, Academic Press, New York (1971).
143. S. V. Kuznetsov, "Lamb waves in anisotropic plates (review)," *Acoust. Phys.*, **60**, No. 1, 95–103 (2014).
144. L. D. Landau and V. M. Livshitz, *Fluid Mechanics*, Vol. 6 of *Course of Theoretical Physics*, Pergamon Press, New York (1987).
145. M. E. McIntyre, "On the 'wave momentum' myth," *J. Fluid Mech.*, **106**, 331–347 (1981).
146. L. Mandel'shtam, "Group velocity in a crystal lattice," *Zh. Eksp. Teor. Fiz.*, **15**, No. 9, 475–478 (1945).
147. E. P. Mednikov, *Acoustic Coagulation and Precipitation of Aerosols*, Consultants Bureau, New York (1965).
148. T. R. Meeker and A. H. Meitzler, "Guided wave propagation in elongated cylinders and plates," in W. P. Mason (ed.), *Physical Acoustics: Principles and Methods*, Vol. 1A, Academic, New York (1964), pp. 111–167.
149. P. M. Morse and H. Feshbach, *Methods of Theoretical Physics*, McGraw–Hill, New York (1953).
150. O. V. Rudenko and S. I. Soluyan, *Theoretical Fundamentals of Nonlinear Acoustics* [in Russian], Nauka, Moscow (1975).
151. J. W. Strutt (Baron Rayleigh), *The Theory of Sound*, Vol. II, Macmillan, London (1896).
152. N. L. Shirokova, "Coagulation of aerosols," in: *Physical Fundamentals of Ultrasonic Technology* [in Russian], Vol. 3, Nauka, Moscow (1970).
153. G. I. Shchuruk, "Torsional waves in a cylindrical shell containing a compressible viscous fluid," *Int. Appl. Mech.*, **19**, No. 4, 117–121 (1983).
154. J. Avatani, "Studies on acoustic radiation pressure," *J. Acoust. Soc. America*, **27**, No. 2, 278–286 (1955).
155. A. Bagno, "Propagation of waves in pre-stressed elastic cylinders, containing liquid," in: *Proc. Int. Conf. EAHE. Engineering Aerohydroelasticity*, **2**, Prague, December 5–8, (1989), pp. 180–184.
156. R. T. Bayer, "Radiation pressure—the history of mislabeled fluid," *J. Acoust. Soc. America*, **63**, 1025–1030 (1978).
157. R. T. Bayer, "Radiation pressure in a sound wave," *Amer. J. Phys.*, **18**, 25 (1950).
158. K. Beissner, "Acoustic radiation pressure in the near field," *J. Sound Vibr.*, **93**, No. 4, 537–548 (1984).
159. M. A. Biot, "Propagation of elastic waves in a cylindrical bare containing a fluid," *J. Appl. Phys.*, **23**, No. 9, 997–1005 (1952).
160. G. Brankov, A. Rachev, and V. Petrov, "Propagation of pulse waves in prestressed arteries," *Biomekh.*, **1**, 17–26 (1974).

161. F. E. Borgnis, “Theory of acoustic radiation pressure,” *Rev. Mod. Phys.*, **25**, No. 3, 653–664 (1953).
162. L. Brillouin, “Sur les tensions de radiation,” *Ann. de Physique*, **10**, No. 4, 528–586 (1925).
163. L. Brillouin, “Les pressions de radiation et leur aspect tensorial,” *J. Phys. et radium*, **17**, No. 5, 370 (1956).
164. F. Cai, L. Meng, Y. Pan, and H. Zheng, “Computation of the acoustic radiation force using the finite-difference time-domain method,” *J. Acoust. Soc. Am.*, **128**, 1617–1622 (2010).
165. A. Doinnikov, “Radiation force due to a spherical sound field on a rigid sphere in a viscous fluid,” *J. Acoust. Soc. America*, **96**, No. 5, 3100–3105 (1994).
166. V. V. Dzyuba and V. D. Kubenko, “Axisymmetric interaction problem for a sphere pulsating inside an elastic cylindrical shell filled with and immersed into a liquid,” *Int. Appl. Mech.*, **38**, No. 10, 1210–1219 (2002).
167. K.A. Fisher and R. Miles, “Modeling the acoustic radiation force in microfluidic chambers,” *J. Acoust. Soc. Am.*, **123**, 1862–1865 (2008).
168. A. N. Guz, “On linearized problems of elasticity theory,” *Int. Appl. Mech.*, **6**, No. 2, 109–116 (1970).
169. A. N. Guz, “Analogies between linearized and linear elasticity theory problems for homogeneous initial states,” *Int. Appl. Mech.*, **8**, No. 5, 549–552 (1972).
170. A. N. Guz, “Elastic waves in bodies with initial (residual) stresses,” *Int. Appl. Mech.*, **38**, No. 1, 23–59 (2002).
171. A. N. Guz, *Dynamics of Compressible Viscous Fluid*, Cambridge Scientific Publishers, Cambridge (2009).
172. A. N. Guz, “On the foundations of the ultrasonic non-destructive determination of stresses in near-the-surface layers of materials. Review,” *J. Phys. Sci. Appl.*, **1**, No. 1, June, 1–15 (2011).
173. A. N. Guz, “Ultrasonic nondestructive method for stress analysis of structural members and near-surface layers of materials: Focus on Ukrainian research (review),” *Int. Appl. Mech.*, **50**, No. 3, 231–252 (2014).
174. A. N. Guz, V. D. Kubenko, and A. E. Babaev, “Dynamics of shell systems interacting with a liquid,” *Int. Appl. Mech.*, **38**, No. 3, 260–301 (2002).
175. A. N. Guz and A. P. Zhuk, “On nonlinear interaction of solid particles with a sound wave in viscous liquid,” *IUTAM Symp.*, Tallin, ESSR, 1982, Springer Verlag, Berlin (1983), pp. 365–378.
176. A. N. Guz and A. P. Zhuk, “The dynamics of rigid bodies near the wall in a compressible viscous fluid under the action of acoustic waves,” in: A. N. Guz (ed.), *Dynamics of Compressible Viscous Fluid*, An International Series of Scientific Monographs, Textbooks and Lecture Notes “Stability, Oscillations and Optimization of System,” Appendix II, Cambridge Scientific Publishers (2009), pp. 367–395.
177. A. N. Guz and A. P. Zhuk, “Dynamics of a rigid cylinder near a plane boundary in the radiation field of an acoustic wave,” *J. Fluids Struct.*, **25**, 1206–1212 (2009).
178. T. Hazegava, M. Ochi, and K. Matsuzava, “Acoustic radiation force on a solid elastic sphere in a spherical wave field,” *J. Acoust. Soc. America*, **69**, 937–943 (1981).
179. E. M. J. Herray, “Experimental studies on acoustic radiation pressure,” *J. Acoust. Soc. America*, **25**, No. 5, 981–896 (1955).
180. L. V. King, “On the acoustic radiation pressure on sphere,” *Proc. Roy. Soc.*, *Ser. A*, **147**, No. 861, 212–240 (1934).
181. V. D. Kubenko and V. V. Dzyuba, “Diffraction of a plane acoustic wave by a rigid sphere in a cylindrical cavity: An axisymmetric problem,” *Int. Appl. Mech.*, **45**, No. 4, 424–437 (2009).
182. H. Lamb, “On waves in an elastic plate,” *Proc. Roy. Soc. London*, *A*, **93**, No. 648, 114–128 (1917).
183. G. Maidanik, “Acoustical radiation pressure due to incident plane progressive waves on spherical objects,” *J. Acoust. Soc. America*, **29**, No. 6, 738–742 (1957).
184. G. Maidanik, “Torques due to acoustical radiation pressure,” *J. Acoust. Soc. America*, **30**, No. 7, 620 (1958).
185. P. L. Marston, “Radiation force of a belicoidal Bessel beam on a sphere,” *J. Acoust. Soc. Am.*, **125**, 3539–3547 (2009).
186. A. H. Meitzler, “Backward-wave transmission of stress pulses in elastic cylinders and plates,” *J. Acoust. Soc. Amer.*, **38**, No. 5, 835–842 (1965).
187. H. Olsen, W. Romberg, and H. Wergeland, “Radiation force on bodies in a sound field,” *J. Acoust. Soc. America*, **30**, No. 1, 69–76 (1958).
188. H. Olsen, H. Wergeland, and P. J. Westervelt, “Acoustic radiation force,” *J. Acoust. Soc. America*, **30**, No. 7, 633–638 (1958).
189. H. T. O’Neyl, “Theory of focusing radiation,” *J. Acoust. Soc. America*, **21**, 516–526 (1949).

190. M. Ottenio, M. Destrade, and R. W. Ogden, "Acoustic waves at the interface of a pre-stressed incompressible elastic solid and a viscous fluid," *Int. J. Non-Linear Mech.*, **42**, No. 2, 310–320 (2007).
191. L. Pochhammer, "Uber die Fortpflanzungeschwindigkeiten Schwingungen in einem unbergrawzten isotropen Kreiscylinder," *J. Reine und Angew. Math.*, **81**, No. 4, 324–336 (1876).
192. J. W. Rayleigh, "On waves propagated along the plane surface of an elastic solid," *Proc. Lond. Math. Soc.*, **17**, No. 253, 4–11 (1885/1886).
193. Rayleigh (J. W. Strutt), "On the momentum and pressure of gaseous vibrations and on the connexion with virial theorem," *Phil. Mag.*, **10**, No. 47, 364–374 (1905).
194. G. T. Silva, "An expression for the radiation force exerted by an acoustic beam with arbitrary wavefront," *J. Acoust. Soc. America*, **130**, 3541–3544 (2011).
195. W. E. Smith, "Average radiation-pressure forces produced by sound fields," *Austral. J. Phys.*, **17**, No. 3, 389 (1964).
196. W. E. Smith, "Radiation pressure forces in terms of impedance, admittance and scattering matrices," *J. Acoust. Soc. America*, **37**, No. 5, 932 (1965).
197. R. Stoneley, "The elastic waves at the interface of separation of two solids," *Proc. Roy. Soc. London*, *A*, **106**, No. 732, 416–429 (1924).
198. I. Tolstoy and E. Usdin, "Wave propagation in elastic plates: low and high mode dispersion," *J. Acoust. Soc. America*, **29**, No. 1, 37–42 (1957).
199. P. J. Westervelt, "Acoustic radiation pressure," *J. Acoust. Soc. America*, **29**, No. 1, 26–29 (1957).
200. K. Yosioka and Y. Kawasima, "Acoustic radiation pressure on compressible sphere," *Acoustic*, **5**, No. 3, 167–173 (1955).
201. A. P. Zhuk, "Interaction of solid bodies immersed in liquid in the acoustic wave field," in: *Proc. Int. Conf. EANE on Engineering Aero-hydroelasticity*, **2**, Prague (1989), pp. 310–315.
202. A. P. Zhuk, V. D. Kubenko, and Ya. A. Zhuk, "Acoustic radiation force on a spherical particle in a fluid-filled cavity," *J. Acoust. Soc. America*, **132** (4), 2189–2197 (2012).